Targeting Cancer Vulnerabilities

From molecular targets to antitumor immunity

Catarina Pinto

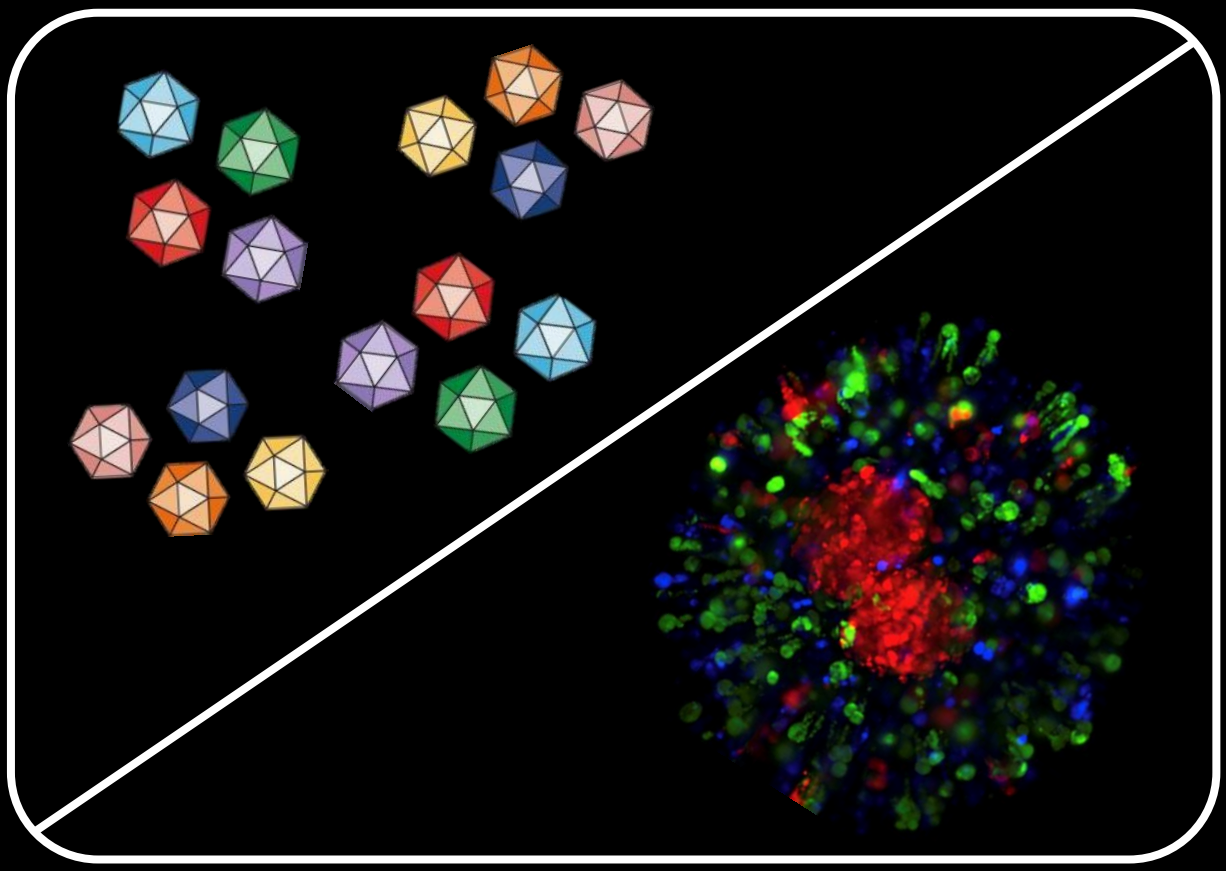

Dissertation presented to obtain the Ph.D degree in Engineering and Technology Sciences – Biomedical Engineering

Instituto de Tecnologia Química e Biológica António Xavier | Universidade Nova de Lisboa

Oeiras,
July, 2018

Targeting Cancer Vulnerabilities

From molecular targets to antitumor immunity

Ana Catarina Pereira Pinto

Dissertation presented to obtain the Ph.D degree in Engineering and Technology Sciences – Biomedical Engineering

Instituto de Tecnologia Química e Biológica António Xavier | Universidade Nova de Lisboa

Oeiras, July, 2018

Targeting Cancer Vulnerabilities

From molecular targets to antitumor immunity

Ana Catarina Pereira Pinto

The work developed in this thesis was supervised by:

- **Doctor Paula Alves**, Instituto de Biologia Experimental e Technológica (iBET) e Instituto de Tecnologia Química e Biológica António Xavier, Universidade Nova de Lisboa (ITQB-NOVA)

- **Doctor Catarina Brito**, Instituto de Biologia Experimental e Technológica (iBET) e Instituto de Tecnologia Química e Biológica António Xavier, Universidade Nova de Lisboa (ITQB-NOVA)

Financial support from:

Fundação para a Ciência e Tecnologia (FCT)

Ph.D grant PD/BD/52202/2013

FCT grant PTDC/BBB-BIO/1240/2012

iNOVA4Health (UID/Multi/04462/2013), financially supported by FCT/MEC, through national funds and co-funded by FEDER under the PT2020 Partnership Agreement

IMI Joint Undertaking (grant agreement no. 115188)

Targeting Cancer Vulnerabilities: from molecular targets to antitumor immunity

Instituto de Tecnologia Química e Biológica António Xavier, Universidade Nova de Lisboa

Instituto de Biologia Experimental e Tecnológica

From left to right: Dr. Carlos M. Farinha, Dr. Luís Pereira de Almeida, Dr. Emmy Verschuren, Catarina Pinto, Dr. Paula Alves, Dr. Catarina Brito and Prof. Maria Arménia Carrondo.

SUPERVISORS

Doctor Paula Alves, Instituto de Biologia Experimental e Tecnológica (iBET) e Instituto de Tecnologia Química e Biológica António Xavier, Universidade Nova de Lisboa (ITQB-NOVA), Portugal;

Doctor Catarina Brito, Instituto de Biologia Experimental e Tecnológica (iBET) e Instituto de Tecnologia Química e Biológica António Xavier, Universidade Nova de Lisboa (ITQB-NOVA), Portugal.

JURY

Emmy Verschuren, Principal Investigator at Institute for Molecular Medicine Finland (FIMM), University of Helsink;

Luís Pereira de Almeida, Principal Investigator and Assistant professor at Center for Neuroscience and Cell Biology (CNC), University of Coimbra, Faculty of Pharmacy;

Carlos M Farinha, Assistant Professor at Faculty of Sciences, University of Lisboa;

Maria Arménia Carrondo, Cathedratic Professor at Instituto de Tecnologia Química e Biológica António Xavier, Universidade Nova de Lisboa (ITQB-NOVA), Coordinator of the Macromolecular Crystallography Unit and Leader of the Structural Genomics Laboratory at ITQB.

ACKNOWLEDGEMENTS

I would like to express my gratitude to all of those who helped me during these years and contributed to the present thesis. Also, to the hosting institutions, IBET and ITQB, for the excellent working conditions.

To my supervisor, Dr. Paula Alves, for the support, knowledge and experience shared with me throughout these years. Thank you for the professional advices and for sharing with me the vision of an experienced team leader, which contributed to my development as a scientist.

To my co-supervisor, Dr. Catarina Brito, for taking me into her lab with no reservations. The constant support and confidence you shared with me were a critical driving force for finishing this journey successfully. Thank you for always promoting my independence, while still being there when I needed guidance and motivation. The numerous scientific discussions throughout the years helped shape the researcher I am today, which will help me tackle the upcoming challenges with confidence and enthusiasm.

A special acknowledgment to Dr. Gabriela Silva and Dr. Sofia Rebelo. This work is truly shared with you both and I want to thank you for all the help, support and encouragement over the years.

To Dr. Liliane Tenenbaum and Dr. Carlos Miguel Farinha, for the discussions at key points during the work.

To Dr. Joana Paredes, Dr. Ana Ribeiro and Mónica Oliveira, for the support and many discussions along the development of the project. Thank you for the hard work and for performing the *in vivo* experiments.

To Dr. José Cabeçadas, Dr. Wolfgang Sommergruber and Dr. Nathalie Harrer, for all the support during our collaboration and for all the helpful discussions.

I would also like to thank my colleagues at the Animal Cell Technology Unit, for creating a great working environment, where we continuously learn from each other in such different fields.

To the Virus lab team: Dr. Ana Sofia Coroadinha, Dr. Manuel Garrido, Vanessa Bandeira, Ana Oliveira, Hélio Tomás, Miguel Guerreiro, Ana Isabel and Hugo Soares. Thank you for welcoming me into such a fun and challenging work environment, and for sharing with me all your knowledge and experience, both at the virus and molecular biology labs.

To the Downstream Processing team: Dr. Cristina Peixoto and André Nascimento. Thank you for making my entry into the DSP world so smooth and simple. This would not have been possible without all your hard work.

To the Phage display team: Dr. Ana Barbas and Inês Barbosa. Thank you for all your help and discussions.

To the 3D team (and friends): Dr. Sofia Rebelo, Marta Estrada, Dr. Daniel Simão, Ana Paula, Tatiana Martins, Francisca Arez, Marta Silva, João Sá, Rita Costa, Dr. Vítor Espirito-Santo, Daniel Pais, Ana Luísa, Dr. Dusica Rados, Nuno Lopes, Sofia Abreu, Teresa Mendes Maria João Sebastião and Bernardo Abecassis. Thank you for all the encouragement and support, for all the discussions, ideas and suggestions shared throughout the years, and for all your help.

E porque fizeram muito mais do que contribuir para um bom *working environment*, um *shout out* especial para Sofia, Marta E., Ana Paula, Ana Oliveira, Marta S, Daniel, João V., Mafalda, João S. e Francisca! São amizades que ficam e que bom que foi partilhar esta aventura convosco!

Por fim, quero fazer um agradecimento especial:

À Joana, por todos os momentos que vão deixar tantas saudades e pela amizade que nunca deixa sentir a distância.

Ao João, pela partilha das frustrações a alegrias desta viagem, que tornou tudo mais fácil. Obrigada pela confiança e motivação constantes.

À minha família, em especial aos meus pais e irmão, porque são o meu principal apoio. Obrigada pela força, incentivo e confiança que me enchem de coragem a cada novo desafio.

ABSTRACT

This thesis aimed at the development of strategies that could contribute to the evaluation of the clinical potential of new anticancer therapies. The work was divided into two main sections comprising the development of a therapeutic approach to target cancer genetic vulnerabilities and the development of 3D tumor models incorporating cues from the stromal and immune microenvironments.

In the first part of the work, we evaluated the feasibility of a therapeutic strategy based on gene therapy to target tumor genetic vulnerabilities. Basal-like Breast Cancer (BLBC) usually manifests as high grade aggressive tumors with poor prognosis. Since there are no validated molecular targets for this subtype, current therapeutic options are based on cytotoxic chemotherapy. This results in high toxicity due to side effects, and most patients relapse after a few years. Thus, there is a need to develop targeted therapies that can improve prognosis for BLBC patients. For this, in ***Chapter II***, we generated small-hairpin RNA (shRNA) sequences targeting genetic vulnerabilities previously identified for this subtype.

Adeno-associated viral (AAV) vectors have been increasingly used in clinical trials. These present low toxicity *in vivo* and support long-term transgene expression. Thus, AAV-based viral vectors were chosen as the delivery agent for the generated shRNA sequences. Using this strategy, we were able to confirm BLBC cells´ increased dependency on the proteasome machinery, as previously reported. AAV-mediated delivery of shRNA targeting *PSMA2*, a proteasome machinery subunit, induced significant target gene knockdown, which resulted in a 2-fold apoptosis induction in BLBC cell lines. Moreover, intratumoral injection of the developed AAV vectors led to a reduction of tumor growth over time, in a mouse BLBC xenograft model. These results suggest that the developed strategy could be used to target cancer-intrinsic genetic vulnerabilities and interrogate their clinical potential. Nevertheless, the AAV serotype used in this work – AAV2 - presents a very broad tropism. Thus, in ***Chapter III***, we took advantage of AAV´s amenability for capsid engineering to restrict its tropism towards BLBC. This would lower the off-target effects, as it would reduce infection of non-

relevant tissues. For this, and since there are no known receptors specific for BLBC, we applied a directed evolution approach using an AAV2 random peptide library to restrict its tropism towards BLBC. After multiple rounds of infection on BLBC cell lines, a 15% enrichment was achieved for a single peptide motif. However, analysis of its transduction properties reveled that it was not specific for BLBC. Furthermore, it presented increased transduction efficiency for normal breast epithelial cells and human dermal fibroblasts. These findings limit its potential for BLBC targeted therapy and, since this was our main goal, the studies were concluded.

In the second part of the work, we aimed at the development of 3D heterotypic tumor models that could better represent the crosstalk between different players within the tumor microenvironment (TME) and be used to screen novel drug candidates.

The increasing understanding that TME cues play a decisive role in the outcome of cancer drug response urges its integration in preclinical tumor models. Several anticancer therapies require the presence of an engaged immune system to enhance their efficacy. These include untargeted approaches, namely chemo- and radiotherapy, as well as targeted molecular approaches aiming at inducing tumor cell death. Therefore, in ***Chapter IV***, we developed a 3D co-culture model that incorporated three cellular compartments: tumor - non-small cell lung cancer (NSCLC) spheroids, stromal – cancer-associated fibroblasts (CAF), and immune – monocytes. The tumoral compartment was composed of proliferative cells and presented phenotypic features characteristic of aggressive stages of NSCLC, such as cells positive for vimentin and cadherin 2. The monocytes in culture differentiated into macrophages which presented phenotypic characteristics of M2-like polarization, such as expression of CD163 and MRC1. These markers have been described for tumor-associated macrophages (TAM), also present in human NSCLC tumors. Moreover, the cytokine secretory profile evidenced an immunosuppressive TME, with accumulation of cytokines such as IL4, IL10, IL13, CCL22, CCL24 and CXCL1. Specific increase in matrix metalloproteases MMP1 and 9 and extensive accumulation of extracellular matrix (ECM) components, such as collagen I and IV and fibronectin, suggested progression into an aggressive and invasive tumoral state. The spatial distribution of the different cells was altered along culture

time, with extravasation of tumor cells into the surrounding stroma, accompanied by an infiltration of the macrophages into the tumoral mass, as evidenced by light-sheet fluorescence microscopy and histology. Although probably supported by the MMP expression and ECM accumulation, this indicated that the alginate microcapsules were amenable to cell migration, enabling cell-cell contacts and supporting myeloid cell infiltration, thus mimicking several aspects of the aggressive and immunosuppressive TME of NSCLC.

Finally, this model allowed the interrogation of both tumor and myeloid targeting drugs, and depiction of their effect on tumor cell viability. Upon challenge with two standard-of-care chemotherapeutics – paclitaxel and cisplatin – we were able to identify a lower susceptibility of the tumor compartment to paclitaxel, when in triple co-culture with CAF and TAM. This suggests that the TME may be responsible for acquired resistance to taxane chemotherapies. Moreover, upon challenge with a macrophage receptor (CSF1R) inhibitor, the macrophage phenotype was modulated, resulting in a decrease of the M2-like macrophages in culture and concomitant increase in the expression of M1-like macrophage markers, namely *CCR7*. Thus, the model developed constitutes a novel tool to study macrophage plasticity and repolarization in response to chemotherapeutic and immunomodulatory drugs. Moreover, it is compatible with continuous monitoring and high-throughput platforms, facilitating its integration in drug screening and disease modeling studies.

Finally, we hope that the experimental approach and data gathered during this thesis, that could potentially also be applied to different cancer pathologies, can contribute to the identification of novel actionable molecular targets and to the dissection of the immunomodulatory action of antitumoral agents.

RESUMO

Esta tese de doutoramento teve como objectivo o desenvolvimento de estratégias *in vitro* que pudessem contribuir para avaliar o potencial clínico de novas terapias contra o cancro. O trabalho foi dividido em duas partes: A) o desenvolvimento de uma abordagem terapêutica que permitisse explorar vulnerabilidades genéticas tumorais e B) o desenvolvimento de modelos tumorais 3D que incorporassem componentes do estroma e sistema imunitário presentes no microambiente tumoral.

Na primeira parte deste trabalho (A), procedeu-se à avaliação do potencial de uma estratégia terapêutica baseada em terapia génica, direccionada a vulnerabilidades genéticas tumorais. O cancro de mama do subtipo basal (BLBC) é um dos subtipos mais agressivos e com pior prognóstico, uma vez que não pode beneficiar das terapias direccionadas existentes contra os restantes subtipos de cancro de mama por não expressar os respectivos receptores membranares. BLBC tem então como única opção terapêutica a quimioterapia citotóxica. Embora apresente elevada taxa de resposta à terapia, esta resulta em consideráveis efeitos secundários e a maioria dos doentes sofre de recaída passado poucos anos. Assim, torna-se necessário o desenvolvimento de terapias direccionadas que possam melhorar o prognóstico de doentes com BLBC. Para isso, no ***Capítulo II***, tomámos partido de vulnerabilidades genéticas que tinham sido previamente identificadas para este subtipo por Petrocca *et al.* (2013). Assim, foram geradas sequências de small-hairpin RNA (shRNA) que pudessem mediar a diminuição da expressão dos genes alvos.

Os biofármacos derivados de vírus recombinantes são frequentemente utilizados como vectores de terapia génica. Os vectores baseados em vírus adeno-associados (AAV) ocupam um segmento importante deste mercado, sendo hoje em dia o vector viral mais utilizado em ensaios clínicos. Estes apresentam um perfil clínico seguro e eficaz, assim como uma capacidade de mediar expressão prolongada do transgene. Como tal, vectores virais baseados em AAV foram escolhidos como veículo para a terapia genética desenvolvida. Procedeu-se à produção e purificação de AAV expressando como transgene as sequências de shRNA previamente identificadas. Usando esta estratégia,

foi possível confirmar a dependência que BLBC apresenta para com o proteassoma. Knockdown de uma das subunidades do proteassoma - *PSMA2* - induziu morte celular por apoptose em células de BLBC. Mais, injecções intratumorais dos AAV a expressar sequências de shRNA contra *PSMA2* resultaram na diminuição do crescimento tumoral ao longo do tempo, quando comparado com ratinhos injectados com PBS ou com um vector controlo. Estes resultados sugerem que esta estratégia poderá apresentar potencial para ser usada como terapia direccionada para alvos moleculares com potencial terapêutico. No entanto, o serotipo de AAV utilizado – AAV2 – apresenta um tropismo que abrange múltiplos tecidos. Visto isto, no ***Capítulo III*** procedemos à alteração proteica da cápside com o objectivo de restringir o tropismo deste vector para BLBC. Assim, seria possível reduzir os efeitos secundários resultantes da terapia, mediados pela infecção inespecífica de células que não as alvo. Para isso, usámos uma biblioteca de péptidos apresentada em cápsides de AAV para, numa abordagem baseada em evolução dirigida, isolar uma variante com tropismo específico para este subtipo de cancro de mama. No entanto, após múltiplos rounds de infecções da referida biblioteca em linhas celulares derivadas de BLBC, foi apenas possível enriquecer a biblioteca numa única sequência peptídica, que representava 15% da preparação final. Após análise do tropismo desta variante em linhas celulares derivadas de vários tecidos, verificou-se que a sua capacidade de transdução não era restricta a células de BLBC. Além disso, a eficiência de transdução para células primárias derivadas do epitélio mamário e para fibroblastos humanos apresentava-se aumentada, diminuindo assim o potencial desta variante para ser usada com agente de terapia génica para este subtipo tumoral.

A segunda parte do trabalho (B) teve como objectivo o desenvolvimento de modelos celulares heterotípicos com possam ser usados como modelo de doença e para a avaliação de novas terapêuticas contra o cancro.

O microambiente tumoral (TME) influencia directamente a resposta a drogas por parte do tumor. A incorporação dos elementos presentes neste TME em modelos celulares pré-clínicos poderá permitir uma melhor avaliação da sua eficácia e modo de acção. Assim, no ***Capítulo IV***, desenvolvemos um modelo celular de co-cultura de três tipos

celulares presentes no TME: esferoides tumorais derivados de cancro do pulmão de não-pequenas células (NSCLC), fibroblastos associados a tumor (CAF) e monócitos. O compartimento tumoral neste modelo apresentava células proliferativas e características fenotípicas de estágios tardios de NSCLC, nomeadamente a presença de células positivas para vimentina e n-caderina. Por outro lado, os monócitos em cultura diferenciaram para macrófagos com expressão de CD163 e MRC1. Estes marcadores membranares sugerem um estado de polarização M2, característicos dos macrófagos associados a tumor (TAM) presentes neste subtipo tumoral. Além disso, o perfil de secreção de citocinas nas culturas triplas apresentava uma acumulação de citocinas características do TME imunossupressor encontrado neste tipo tumoral, nomeadamente IL4, IL10, IL13, CCL22, CCL24 e CXCL1. Acumulação de componentes da matrix extracelular nas cápsulas de alginato suportou uma remodelação extensa dos compartimentos celulares durante a cultura. Foi possível observar infiltração de macrófagos na massa tumoral, algo que é visível em amostras derivadas de pacientes de NSCLC.

Como prova de conceito este modelo foi sujeito a drogas quimioterapêuticas usadas na clínica. Assim, foi possível diferenciar o efeito na viabilidade tumoral destas drogas na presença ou ausência dos restantes componentes do TME. O compartimento tumoral apresentou uma susceptibilidade reduzida a paclitaxel quando em co-cultura com CAF e TAM. Isto poderá sugerir que o TME tem um efeito na aquisição de resistência a quimioterapia mediada por taxanos, e realça a importância da incorporação desta componente nos modelos tumorais pré-clínicos. Por fim, o modelo foi sujeito a um composto imunomodulatório que tem como alvo os macrófagos. O tratamento com um inibidor do receptor de macrófagos CSF1R resultou na diminuição da percentagem de células positivas para os marcadores de macrófagos M2 – CD163 e MRC1 – e aumento da expressão de um marcador de macrófagos M1 – CCR7. Este efeito tinha sido previamente descrito para o inibidor utilizado, comprovando assim o potencial do modelo desenvolvido para a avaliação do efeito imunomodulatório na população mieloide de novos compostos com potencial terapêutico.

Por fim, esperamos que a abordagem experimental e dados recolhidos ao longo deste trabalho, que podem potencialmente ser aplicados a diferentes patologias oncológicas, possam contribuir para a identificação de novos alvos moleculares terapêuticos e para a elucidação de mecanismos de acção, nomeadamente imunomodulatória, de novas terapias anti-tumorais.

THESIS PUBLICATIONS

Pinto C, Silva G, Garrido M, Bandeira VS, Nascimentos A, Ribeiro AS, Oliveira M, Paredes J, Coroadinha AS, Peixoto C, Barbas A, Brito C, Alves PM. *Evaluation of AAV-mediated delivery of shRNA to target basal-like breast cancer genetic vulnerabilities* (submitted)

Rebelo SP*, **Pinto C***, Martins TR, Harrer N, Estrada MF, Loza-Alvarez P, Cabeçadas J, Alves PM, Gualda EJ, Sommergruber W, Brito C. (*equal contribution) *3D-3-culture: A tool to unveil macrophage plasticity in the tumour microenvironment.* Biomaterials 163, 185–197 (2018).

OTHER PUBLICATIONS

Santo VE, Estrada MF, Rebelo SP, Abreu SA, Silva I, **Pinto C**, Veloso SC, Serra AT, Boghaert E, Alves PM, Brito C. *Adaptable stirred-tank culture strategies for large scale production of multicellular spheroid-based tumor cell models*. J. Biotechnol. 221, 118-129 (2016).

*equal contribution

TABLE OF CONTENTS

LIST OF FIGURES

LIST OF TABLES

ABBREVIATIONS

2D	Two-dimensional
3D	Three-dimensional
AAV	Adeno-associated virus
ACTA2	Aactin, alpha 2, smooth muscle, aorta
AKT	AKT Serine-Threonine Kinase
ARG1	Arginase 1
ASO	Antisense oligonucleotide
BC	Breast cancer
BCL2	BCL2, apoptosis regulator
BCL2L2	BCL2 like 1
BIK	BCL2 interacting killer
BLBC	Basal-like breast cancer
CAF	Cancer-associated fibroblast
CAV1	Caveolin 1
CCL	C-C motif chemokine ligand
CDH1	Cadherin 1
CNS	Central nervous system
CSC	Cancer stem cell
CSF1	Colony stimulating factor 1
CSF1R	Colony stimulating factor 1
CTC	Circulating tumor cells
CTNNB1	Catenin beta 1
CXCL	C-X-C motif chemokine ligand
CXCR	C-X-C motif chemokine receptor
ECM	Extracellular matrix
EGF	Epidermal growth factor
EGFR	Epidermal growth factor receptor
EMT	Epithelial to mesenchymal transition
EMT-TF	EMT-associated transcription factors
ER	Estrogen receptor 1

ERBB2	Erb-b2 receptor tyrosine kinase 2
FAP	Fibroblast activation protein alpha
FASLG	Fas ligand
FGF2	Fibroblast growth factor 2
GEMM	Genetically engineered mouse models
HGF	Hepatocyte growth factor
HPRT1	Hypoxanthine phosphoribosyltransferase 1
Hpt	Hours post transfection
ICAM1	Intercellular adhesion molecule 1
IC-BEVS	Insect cells / baculovirus expression vector system
IDH1/2	Isocitrate dehydrogenase (NADP(+)) 1 / 2
IGF1R	Insulin-like growth factor 1 receptor
IGFBP3	Insulin like growth factor binding protein 3
IL	Interleukin
ip	Infectious particles
ITGB2	Integrin subunit beta 2
JAK	Janus kinase
MAPK	Mitogen-activated protein kinase
MCL1	MCL1, BCL2 family apoptosis regulator
MET	MET proto-oncogene, receptor tyrosine kinase
MET	Mesenchymal to epithelial transition
Mj	Macrophage
MMP	Matrix metalloprotease
MOI	Multiplicity of infection
MRC1	Mannose receptor C-Type 1
MSDC	Myeloid derived suppressor cells
MTOR	Mechanistic target of rapamycin kinase
NFKB	Nuclear factor kappa B
NK	Natural killer
NSCLC	Non-small cell lung cancer
PBM	Peripheral blood derived monocytes

PDCD1LG2	Programmed cell death 1 ligand 2
PDX/CDX	Patient- or cell line-derived xenografts
PI3K	Phosphoinositide 3-kinase
PLK1	Polo like kinase 1
PR	Progestrone receptor
PSMA2	Proteasome subunit alpha 2
PSMB4	Proteasome subunit beta 4
PTGS2	Prostaglandin-endoperoxide synthase 2
RB1	RB transcriptional corepressor 1
RPL22	Ribosomal protein L22
RTK	Receptor tyrosine kinase
shRNA	Short hairpin RNA
siRNA	Small interfering RNA
SNAI1/2	Snail family transcriptional repressor 1/2
SRC	SRC proto-oncogene, non-receptor tyrosine kinase
STAT	Signal transducers and activators of transcription
STC1	Stanniocalcin 1
TAM	Tumor-associated macrophage
TCA	Tricarboxylic acid
TCR	T cell receptor
TGFB1	Transforming growth factor beta 1
Th	T helper
TJP1	Tight junction protein 1
TME	Tumor microenvironment
TNBC	Triple negative breast cancer
TOH	Time of harvest
TP53	Tumor protein p53
Treg	Regulatory T cells
TSLP	Thymic stromal lymphopoietin
TWIST1	Twist family bHLH transcription factor 1
VEGF	Vascular endothelial growth factor

vg	Viral genomes
vp	Viral particles
Wt	Wild-type
ZEB1/2	Zinc finger E-box binding homeobox ½

CHAPTER I

INTRODUCTION

TABLE OF CONTENTS

1. CANCER

Cancer progression has been compared to the development of multicellular organisms where mechanisms controlling cell division, cell-fate determination and tissue organization are deregulated[1]. Understanding which physiological processes are being co-opted by tumors to thrive in harsh physicochemical conditions and avoid cell death, acquire unrestricted growth capacity and the propensity to invade adjacent tissues and disseminate throughout the host, will be crucial for rational design of efficacious therapies. These properties emerge in different tumor types through distinct mechanisms and are enabled by both tumor cell intrinsic and extrinsic properties (Fig. 1.1)[2].

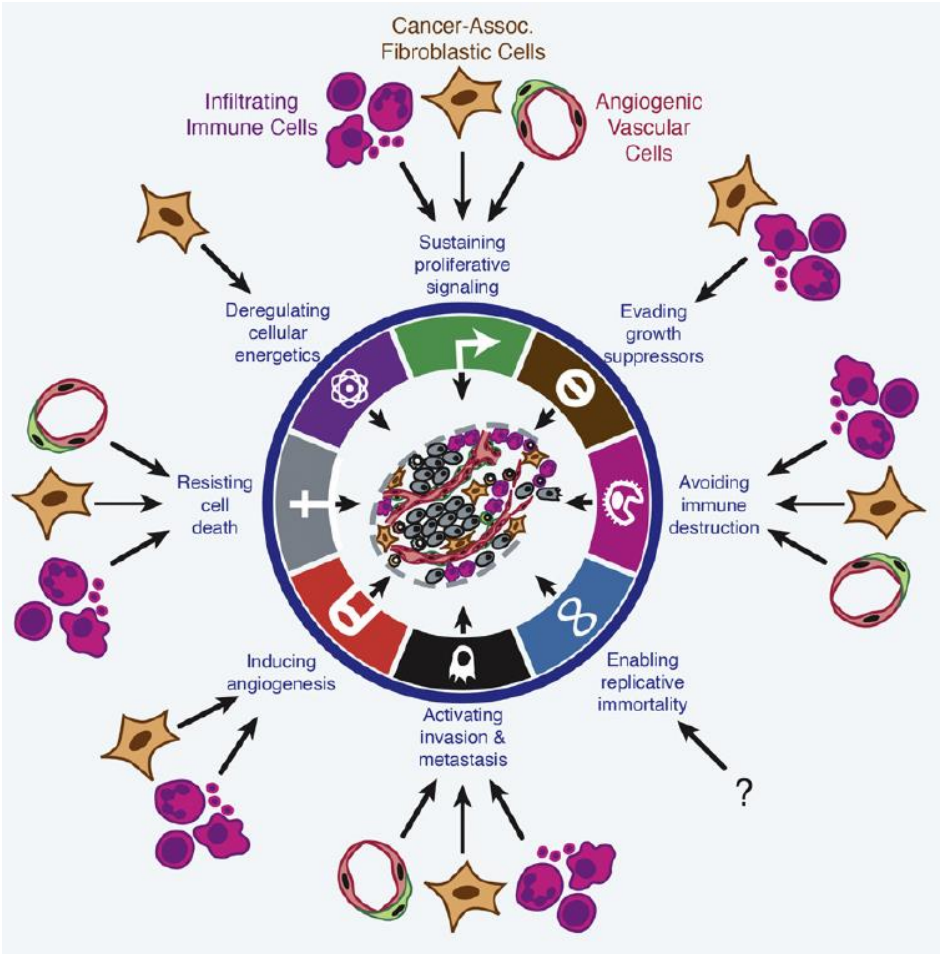

Figure 1.1: Tumor cell intrinsic and extrinsic properties influencing the different hallmarks of tumor biology. Adapted from Hanahan *et al.*, Cancer Cell (2012)[2].

2. INTRINSIC CHARACTERISTICS – THE QUEST FOR CANCER-SPECIFIC VULNERABILITIES

A fundamental feature of cancer is genomic instability. The progression from normal into malignant cells accompanies an accumulation of mutations or altered expression in specific genes, that confers them tumorigenic potential. These genes, termed either tumor suppressors or oncogenic drivers, generate tissue or cancer subtype-specific genetic vulnerabilities, and constitute prime candidates for targeted therapies. The discovery and exploitation of such targets over the years has drastically improved cancer treatment.

2.1 Chronic Proliferation and Survival

Normal tissues depend on controlled growth signaling and cell cycle to maintain homeostasis, which is disrupted in cancer. Oncogenic signaling through receptor tyrosine kinases (RTK), either by upregulation of receptor expression or by aberrant activation of the downstream signaling pathways in the absence of growth factors, drives tumor initiation and progression across several solid tumors[3]. RTK constitute cell surface receptors for many growth factors that regulate several biological processes including the maintenance of chronic proliferation in tumor cells (Fig. 1.2)[4]. In fact, the first reports linking a genetic alteration to the development of cancer involved the erb-b2 receptor tyrosine kinase 2 (*ERBB2)* gene[5]. This gene, commonly referred to as *HER2*, was shown to be amplified in up to 20% of invasive breast cancers, and it correlated with decreased overall survival and reduced time of relapse[6]. This potentiated the development of the first therapies targeting cancer molecular aberrations, namely monoclonal antibodies (trastuzumab and pertuzumab), tyrosine kinase inhibitors (lapatinib), and antibody–drug conjugates, which improved the outcome for $HER2^{+}$ breast cancer patients[7].

ERBB2 belongs to the ERBB family of RTK, which entails another prototypical example - epidermal growth factor receptor (EGFR). Activating mutations in this receptor can be found in high proportion in different tumor types, including glioblastoma,

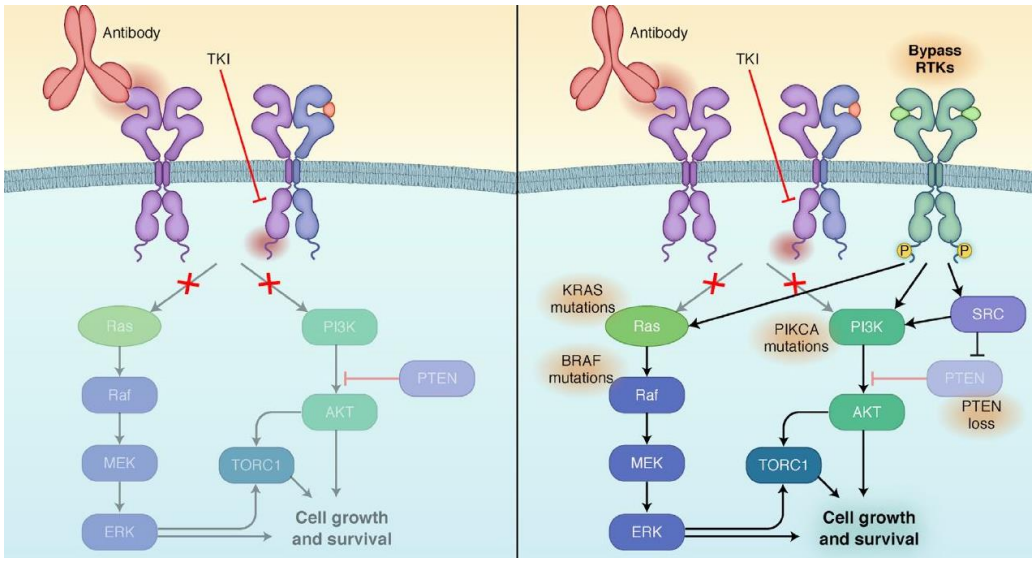

Figure 1.2: Main downstream pathways of ERBB2 and EGFR. A) Model depicting the action of small-molecule inhibitor or antibody and consequent downstream signaling suppression. **B)** Model depicting an ERBB2-amplified or EGFR mutant cancer, where the maintenance of downstream signaling in the presence of inhibitors is achieved by i) activation of additional RTK or ii) constitutive mutational activation of downstream signaling. Adapted from Arteaga *et al.*, Cancer Cell (2014)[3].

medulloblastoma, breast, head and neck, ovarian, lung and prostate[8]. In transgenic mouse models, mutant *EGFR* expression induces lung adenocarcinomas, and inhibition of EGFR signaling by small molecule inhibitors, such as erlotinib, or monoclonal antibodies, such as cetuximab, leads to tumor regression[9], thus confirming both its role as an oncogenic driver and as an oncogenic addiction that can be targeted for clinical benefit. The development of EGFR blockers has drastically improved the outcome of patients with tumors bearing activating mutations of this receptor, especially in non-small cell lung cancer (NSCLC) metastatic setting[10]. Still, single agent strategies fall short in clinical trials; constant exposure to RTK inhibitors often induces resistance through secondary mutations in downstream pathways or through compensatory activation of alternative RTK, such as MET proto-oncogene, receptor tyrosine kinase (MET) or insulin-like growth factor 1 receptor (IGF1R), maintaining overall survival signaling (Fig. 1.2 – B)[3]. Large-scale high-throughput approaches for

mapping cellular signaling networks showed that cancer cells also activate several RTK simultaneously[11]. Such RTK co-activation influences tumor response to targeted therapies[12] and is a frequent mechanism of acquired resistance in tumor cells[13,14].

Downstream mediators of these receptors include mitogen-activated protein kinase (MAPK), phosphoinositide 3-kinase/AKT Serine-Threonine Kinase (PI3K/AKT), mechanistic target of rapamycin kinase (MTOR) and Janus kinase/signal transducers and activators of transcription (JAK/STAT) pathways, as well as, SRC proto-oncogene, non-receptor tyrosine kinase (SRC)[3]. DNA sequencing analysis has shown that somatic mutations in protein regulators of these pathways constitute common oncogenic drivers and result in constitutive signaling that is usually attributed to activated growth factor receptors[2]. This confers the necessary plasticity for tumor cells to retain proliferative signaling even when one of these elements is disrupted[11]. To overcome these mechanisms, combinatorial strategies have been developed and often attain higher decrease in tumor cell viability than any of the monotherapies tested[12,15].

2.2 Cell Death Evasion

Hyperproliferation and overexpression of oncogenes often results in DNA damage that is a potent trigger of apoptosis[2]. However, malignant transformation often entails deregulation of apoptotic signaling or activation of antiapoptotic systems, rendering tumor cells resistant to apoptosis stimuli, which further supports uncontrolled proliferation and survival signaling[16]. This escape from normal control of cell death networks aids proliferative cells and contributes to survival, leading to the development of higher grade malignancy, and contributing directly to therapeutic resistance and disease recurrence[16].

Various mechanisms culminate in apoptosis evasion; key examples include mutations in regulatory proteins such as tumor protein p53 (TP53) and RB transcriptional corepressor 1 (RB1)[2]. The former is a tumor suppressor gene that was identified as the most often mutated in cancer and leads to detrimental phenotypes across several cancer types[17,18]. It acts as a stress detector with a prominent role in determining how the cell responds to DNA damage, nutrient deprivation and hypoxia, by either promoting

cell survival or arresting cell proliferation and inducing apoptosis[19]. Alternative mechanisms include upregulation of survival signaling and of antiapoptotic regulators, such as members of the BCL2 family[2]. The latter regulate the intrinsic apoptosis pathway (Fig. 1.3)[20]. Overexpression of these proteins confers chemotherapy resistance to pancreatic, ovarian, lymphoma, multiple myeloma, lung adenocarcinoma, prostate adenocarcinoma, among others[16].

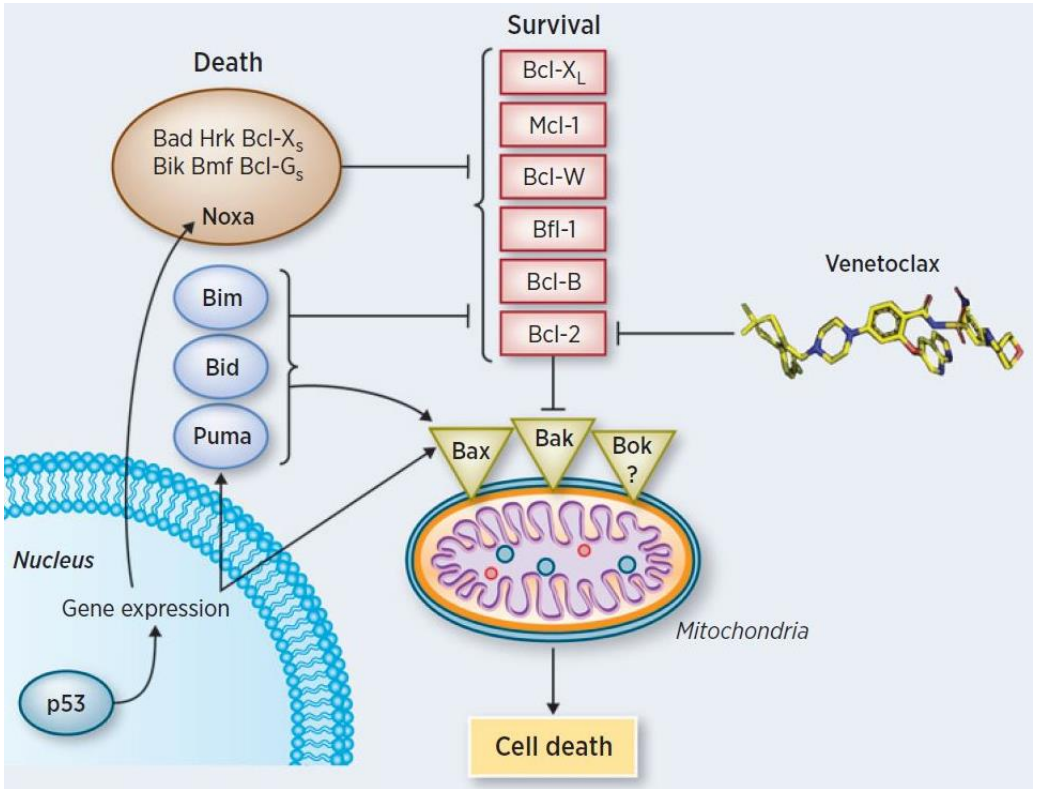

Figure 1.3: Different categories of the BCL2 family. In red: antiapoptotic proteins; in yellow: proapoptotic multidomain that permeabilizes the outer mitochondrial membrane (intrinsic apoptosis pathway); in blue: BH3-only proteins agonists for the proapoptotic multidomain and antagonists of antiapoptotic BCL2 members; and in brown: BH3-containing proapoptotic members that serve as antagonists of antiapoptotic BCL2 members. Also illustrated is TP53's role in regulating proapoptotic stimuli after stress, such as chemotherapeutic challenge. Finally, the actions of venetoclax, an BCL2 antagonist, is also depicted. Adapted from Croce *et al.*, Cancer Res (2016)[21].

Several small molecule inhibitors have been developed that target mediators of this

pathway and, recently, FDA approval of venetoclax, a BCL2, apoptosis regulator (BCL2) inhibitor, constituted the first apoptosis-targeting drug available for cancer patients (Fig. 1.3)[21]. Possible resistance mechanisms to BCL2 inhibition include the upregulation of MCL1, BCL2 family apoptosis regulator (*MCL1*) and BCL2 like 1 (*BCL2L2*) genes (Fig. 1.3)[22]. Functional studies into MCL1 function, have shown that it blocks apoptosis induced by many chemo- or radiotherapeutic stimuli[16]. MCL1 is overexpressed in many different tumors[23] and, contrary to other BCL2 family proteins, has a very short half-life[24] due to proteasome degradation[25]. Therefore, targeting *MCL1* expression can be a promising approach[26–28]. Although several reports studied the effect of antisense oligonucleotide (ASO) therapy targeting *MCL1*, these have yet to be successfully translated into the clinic, possibly due to the low stability of ASO in circulation[29].

The proteasome machinery has also been implicated in evading apoptosis, since some of its substrates are protein regulators of cell survival and apoptotic pathways[30]. A compromised proteasome regulation can induce tumorigenesis by altering the turnover of key oncogene or tumor suppressor gene protein products[31]. In fact, while functional in healthy tissue, bortezomib, a 20S proteasome inhibitor, is only toxic for cancer cells, indicating a selective dependency of cancer cells[31]. The proteasome machinery controls TP53 protein levels and activity[32,33], as well as protein regulators of the BCL2 family, including BCL2 interacting killer (BIK), phorbol-12-myristate-13-acetate-induced protein 1 (PMAIP1, also known as NOXA) and BCL2 like 11 (BCL2L11, also known as BIM) proteins (Fig. 1.3)[34]. Proteasome can also regulate cell cycle progression by controlling the turnover of cyclins and cyclin-dependent kinase inhibitors[35], as well as of transcription factors implicated in cell survival pathways, such as nuclear factor kappa B (NFKB)[36].

Targeted inhibition of proteasome pathway mediators may switch the balance towards tumor cell death by inducing the accumulation of proapoptotic proteins[16]. The development of inhibitors of the proteasome machinery has led to significant improvements in cancer care, mainly in hematological malignancies[31]. On the other hand, for solid cancers, the translation of the promising preclinical results has been

challenging. Primary and acquired resistance does occur, and it has been linked to mutations or overexpression of proteasomal subunits, among others[31]. Thus, more predictive preclinical models are needed, along with further investigation into the mechanisms of resistance in order to optimize combinatorial regimens and broaden the applicability and efficacy of proteasome inhibitor therapy[31].

2.3 Reprograming of cell energy metabolism

Oncogenic growth signaling needs support from cell-autonomous nutrient uptake and from metabolic regulation to accommodate proliferation[37]. Therefore, cancer cells undergo metabolic reprogramming in order to fuel the biological processes behind biomass formation, tumor growth and energy generation, and to survive the stresses associated, namely oxidative stress[38]. While glucose metabolism in normal differentiated cells is mainly dependent on oxidative phosphorylation, cancer cells undergo a metabolic switch, termed Warburg effect, thus relying mostly on aerobic glycolysis[37]. Although it generates less ATP per glucose molecule, it allows fast ATP production even at low oxygen tension, which occurs at later stages of tumor development. Plus, ATP requirements for proliferation do not differ significantly from normal homeostasis[37] Interestingly, most signaling pathways driving cell growth are involved in cell metabolism regulation[37]. Glucose uptake inhibition leads to cell death in a manner similar to what happens when growth factor signaling is inhibited[37]. Moreover, the excess nutrient uptake, consequence of increased cell growth receptor signaling, if not converted into aerobic glycolysis would greatly increase reactive oxygen species production, a byproduct of oxidative phosphorylation[37].

This metabolic shift is not exclusive of malignancy phenotypes; thus, it may result from reversion into a more embryonic state or an independent ability to undergo metabolic reprogramming[37]. Some metabolic activities are prompted by oncogenic drivers and may provide tumor dependencies to be exploited in the clinic[38]. For example, somatic mutations in genes encoding isocitrate dehydrogenase (NADP(+)) 1/2 (*IDH1*, *IDH2*) are abundant in a large variety of tumors and have been proposed to lead epigenetic changes that promote tumorigenesis through inhibition of normal cell

differentiation[39]. However, inhibition of 2-hydroxyglutarate, an oncometabolite of IDH-mutant tumors, did not decrease tumor growth, highlighting the importance of alternate and cooperating metabolic pathways[40]. In fact, the standard strategy of conducting *in vitro* screens followed by *in vivo* validation, which provided important therapeutic targets like the ones mentioned in the former sections, has particularly low efficacy for metabolic targets[38]. For example, in NSCLC, cultured cells used glutamine as the main carbon source for the tricarboxylic acid (TCA) cycle, while tumors *in vivo* showed greater dependency on glucose carbon contribution and no differential contribution of glutamine to the TCA cycle between tumor and normal tissue was found[41]. These results highlight the importance of proper preclinical model selection, as culture conditions are often non physiological and selective for higher proliferating cell clones[41]. Additionally, metabolically heterogeneity was observed within NSCLC patients, emphasizing the need to take the environmental context into account when selecting metabolic targets[42]. Effective strategies to target cancer metabolism will need to be supported by a better understanding of the reciprocal interactions between cancer-dependent and stromal cell signals[38], as well as with the host and diet microbiomes[43]. To improve patient stratification and therapeutic selection, we need cell culture strategies that retain tumor metabolic requirements, as well as better tools to assess quantitatively metabolic fluxes in co-culture contexts[38].

3. EXTRINSIC CHARACTERISTICS – HETEROTYPIC INTERACTIONS WITHIN THE TUMOR MICROENVIRONMENT

3.1 Epithelial to Mesenchymal Transition (EMT)

The considerable plasticity demonstrated by cancer cells allows them to transition between multiple and dynamic states separating epithelial and mesenchymal phenotypes[44]. Cells with partial EMT phenotype, which exhibit hybrid epithelial/mesenchymal characteristics, are involved in embryonic development and organ formation[45], wound healing and fibrosis in adult tissues[46], and cancer progression[44]. These transitioning states constitute final functional cell phenotypes;

therefore, it is important to contextualize EMT within the cellular process it is contributing to, namely invasion, survival, decreased proliferation, production of extracellular matrix (ECM) and resistance to therapy[44].

While oncogenic drivers, such as *RAS* and *EGFR* mutations, may elicit a shift towards the mesenchymal state (EMT), this induction is intimately connected with the signaling molecule network present in the tumor microenvironment (TME), which depends on the tissue of origin and on the network of cells that surround the tumor[44,47]. Key soluble factors secreted the cells comprising the TME that mediate EMT are transforming growth factor beta 1 (TGFB1) and interleukin (IL) 6. TGFB1 has a pleiotropic role as it may function both as a tumor suppressor, promoting growth arrest at early stages of tumorigenesis[48], or as tumor promoter, inducing EMT and cell migration and invasion[49]. The cues driving each behavior are not fully understood. Upon binding, TGFB1 signaling activates SMAD, PI3K/AKT or MAPK downstream pathways, depending on the cell type, and promotes EMT by upregulation of EMT-associated transcription factors (EMT-TF)[49] and downregulation of cadherin 1 (*CDH1*) and tight junction protein 1 (*TJP1*)[50,51]. TGFB1 has also been linked to other cellular processes triggered by EMT, such as the acquisition of stem-like characteristics by cancer cells[52]. IL6, on the other hand, is linked to chronic inflammation and has been shown to induce EMT by eliciting STAT3 phosphorylation in NSCLC and breast cancer (BC)[53,54], and by promoting cancer stem cell self-renewal[55]. Nevertheless, other TME growth factors and cytokines, as well as oxidative stress, hypoxia, morphogenic signaling (e.g., NOTCH and WNT) can induce expression of EMT-TF[44]. There is considerable crosstalk between the different pathways and cellular players, and no individual stimulation appears to be sufficient to induce the molecular and phenotypic changes associated with EMT[47].

EMT transitioning states result of a balance between several transcriptional drivers and suppressors, whose expression is regulated at different levels including epigenetic modifications, transcriptional control, alternative splicing, protein stability and subcellular localization[44]. The major EMT-TF are: the snail family transcriptional repressor 1/2 (*SNAI1/2*) and the zinc finger E-box binding homeobox 1 (*ZEB1/2*), strong

epithelial suppressors; and twist family bHLH transcription factor 1 (*TWIST1*), a mesenchymal inducer[44]. All these induce EMT through transcriptional suppression of various epithelial markers including *CDH1*, claudins and occludins, and upregulation of mesenchymal markers, such as vimentin and fibronectin 1[44]. These result is a change in cell polarity, matrix metalloprotease (MMP) expression and cytoskeleton arrangement, giving cells the ability to detach and invade surrounding tissue and, ultimately, enter the bloodstream and migrate in response to environmental stimuli[44].

Other functional implications of EMT include inhibition of cellular senescence and reduced susceptibility to apoptosis by inducing MAPK and PI3K/AKT survival pathways and BCL2 members[56]. Acquired chemoresistance is common in cells that underwent EMT, a feature that is independent on their metastatic potential[57,58]. Finally, the expression of EMT-TF can activate the expression of pro-inflammatory and immunosuppressive cytokines, thus modulating the immune infiltrate towards tumor promotion[59].

Cancer therapies should be designed in combinations that account for this shift in phenotype and network rewiring, thus acting preemptively[44]. However, the applicability of EMT for cancer treatment has been limited by the intrinsic heterogeneity of the phenomena in tumor cells *in vivo*, as well as of the TME[44]. The proportion and distribution of the different phenotypes also depends on the intrinsic molecular heterogeneity and cell of origin of tumors; for example, basal-like breast cancer (BLBC) subtype tends to have a higher proportion of cancer stem cell (CSC)-like cells with a more mesenchymal phenotype than BC from HER2 positive and luminal subtypes[44]. Additionally, cancers arising from mesoderm (sarcomas and melanoma) tend to display higher EMT score than solid tumors of epithelial origin[44]. Therefore, EMT's clinical significance should be evaluated in parallel with intrinsic molecular subtypes[44]. Thus, while reversing EMT may be a suitable strategy for fibrosis, the inherent complexity of the process in cancer progression suggests that it might be more effective to target and destroy cells that have undergone EMT[44]. Still, the lack of adequate preclinical models and advanced characterization techniques to visualize EMT *in vivo* is hampering

therapeutic development[44]. A pressing issue is the deciphering the full range of transitioning EMT states, its function in tumor progression, and their intracellular regulation[44].

3.2 Invasion and metastasis

Metastasis is a multistep process that involves invasion of adjacent tissue, intravasation into the blood stream, extravasation at a distant organ and colonization of the metastatic site, where it may lay dormant for years or progress into clinical metastatic disease (Fig. 1.4)[60]. Metastasis is still the main cause of cancer-related deaths[61], and each step is directly linked with reciprocal interactions maintained with elements of the TME (Fig. 1.4)[60].

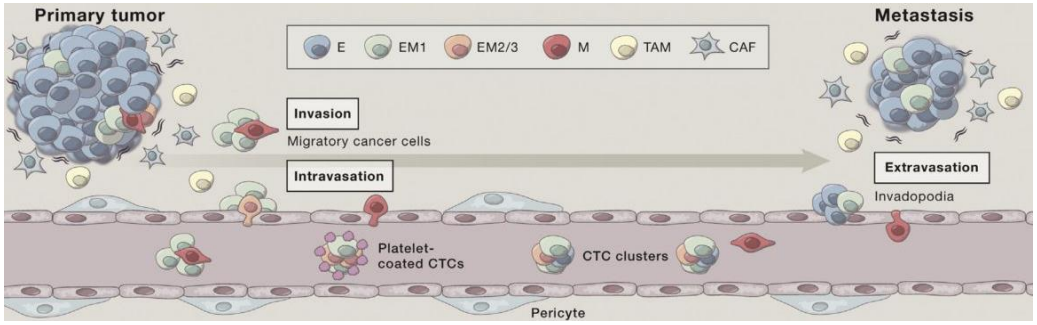

Figure 1.4: The metastatic process. Depiction of the different EMT stages cancer cells undergo during the metastatic cascade. The contribution of cells from the TME is also illustrated, namely tumor-associated macrophages (TAM) and cancer associated fibroblasts (CAF). These can be recruited prior and during the establishment of both primary and metastatic niches and contribute to the plasticity tumor cells exhibit in order to invade the surrounding tissues, survive within the bloodstream and colonize distant sites of metastasis. E: epithelial tumor cell; EM1 and EM2/3: intermediate EMT stages; M: mesenchymal tumor cell; CTC: circulating tumor cells or clusters. Adapted from Nieto *et al.*, Cell (2016)[44].

The ability of cancer cells to undergo metastasis is often preceded by the acquisition of a motile phenotype. While shifting towards a mesenchymal phenotype confers cancer cells higher motility and invasive capacities, its functional role in metastasis is still under intense investigation[60]. In a spontaneous breast-to-lung metastasis mouse model,

downregulation of *ZEB1* and *ZEB2* rendered tumor cells in a permanent epithelial state but did not impair lung metastasis[58]. In contrast, conditional *SNAI1* deletion ablated metastatic capability of breast cancer *in vivo*, while transient *SNAI1* overexpression increased both disseminated tumor cells and lung metastasis[62]. In line with these results, expression of *SNAI1*, *SNAI2* and *TWIST1* genes was strongly correlated with metastatic breast cancer progression, in contrast with *ZEB1*[63]. On the other hand, in a pancreatic cancer mouse model, downregulation of *TWIST1* and *SNAI1* had no impact on cell invasion and metastasis[57], while downregulation of *ZEB1* strongly impacted tumor initiation, invasion capability and metastasis formation during pancreatic cancer progression[64]. Therefore, there is considerable functional heterogeneity between EMT-TF, as well as tissue and cancer subtype specificity in their biological role. Thus, the functional contribution of EMT to metastasis and tumor progression needs to be investigated in a cancer type dependent manner[59]. Also, although EMT is activated in many tumor types, later stage markers such as vimentin are often not expressed, and hybrid phenotypes can increase cell motility both for individual cell migration and for collective migration[59]. Most low-grade tumors invade as cohesive multicellular aggregates of tumor cells, while high grade and mesenchymal tumors are more variable and present both collective migration and single-cell invasion of high EMT score phenotypes (Fig. 1.4)[65].

The fate of circulating tumor cells (CTC) is dependent on the interactions maintained during transit through the circulatory system and at the pre-metastatic niche[66]. CTC must overcome physical challenges, namely loss of attachment to a substrate and sheer stress, as well as avoid immune clearance[66]. This can be achieved by association with platelets in the bloodstream (Fig. 1.4). These avoid tumor cell recognition and cytotoxic activity of Natural killer (NK) cells, an effect mediated by local production of TGFB1, which inhibits NK activity[67]. Additionally, the local TGFB1 secretion sustains the expression of EMT-promoting intracellular signaling, thus compensating for the lack of the stromal factors that contributed to invasion in the primary tumor lesion[68]. This is in line with the strong TGFB1 response expressing signature found in circulating BC cells[69]. Most invasive solid tumors, however, undergo primarily collective cell

migration, where groups of cells invade the surrounding stroma while still maintaining cell-cell contacts[65]. Clusters of tumor cells observed in circulation arise from multicellular cluster detachment from the primary tumor, rather than being aggregated within blood vessels, as observed in a mouse model for BC metastasis[70]. CTC clusters in this model presented 23 to 50-fold increased metastatic potential[70].

Metastasis is, nevertheless, a very inefficient process; experimental data suggests that only 0.01% of CTC achieve productive colonization of a distant organ[66]. Moreover, in the case of breast cancer, dormant micrometastasis relapse decades after the original tumor has been removed, highlighting the fact that invasion and successful outgrowth are separate phenomena[2]. The process of distant colonization appears to be dependent on the presence of cells with CSC properties, the ability of these cells to undergo mesenchymal to epithelial transition (MET), and on the development of a supportive microenvironment[66]. MET is influenced by the microenvironment at the pre-metastatic niche, namely by the presence of cancer-associated fibroblasts (CAF) and metastasis-associated macrophages, as well as environmental factors such as hypoxia and angiogenesis (Fig. 1.4)[71–74].

3.3 Therapeutic resistance

Despite the advent of targeted molecular therapies, which often result from the dissection of the oncogenic pathways mediating malignancy, these remain in most cases poorly efficient and with mostly transient results[75]. Therapeutic resistance is, presently, the main obstacle in cancer treatment[76]. Identification of the underlying mechanisms is crucial to overcome current shortcomings improve clinical outcomes[76].

Cancer cell intrinsic mechanisms supporting acquired resistance include upregulation of drug efflux pumps and increased drug metabolism, as well as compensatory loss of specific oncogenes and emergence of enabling apoptotic defects[76]. Moreover, intrinsic intratumor heterogeneity across cancer types and tissue of origin also favors tumor evolution and therapeutic resistance[77]. Still, a great proportion of a tumors' heterogeneity is a result of the cells present in its surrounding microenvironment, both

in terms of composition and activation states[78]. Extrinsic determinants such as cytokines and growth factors supplied by the cells in the TME play a significant contribution in tumor evolution and disease recurrence[77]. Deciphering the intricate networks established between the different players in the provides knowledge into the biological mechanisms behind acquired anticancer therapy resistance, as well as a rational for combinatorial therapies[76]. These have also been instrumental in uncovering important new targets for therapeutic intervention, namely immunotherapies[76].

3.4 Tumor microenvironment (TME)

Tumors are shaped by environmental factors that enhance or dampen the effects of genetic and epigenetic alterations in the epithelial compartment[79]. The TME is a complex network of different cell types and soluble factors, intertwined within an ECM which provides physical support and directs cell signaling (Fig. 1.5)[76]. The acknowledgment of the dynamic and reciprocal heterotypic interactions between these different players has increased exponentially the complexity of cancer research.

The TME has a profound impact on tumor progression, invasion, metastasis and, ultimately, patient prognosis and therapeutic response[78]. Under normal physiological conditions, the microenvironment maintains tissue architecture and restricts cell growth, thus inhibiting tumor initiation and progression[80]. The concept of “seed and soil”, first proposed by Stephen Paget in 1889, states that tumor cells may only lead to tumor outgrowth when a supportive microenvironment emerges[78]. Thus, while tumor initiation appears mostly inevitable, its progression into a malignant state could potentially be managed with full knowledge of the intervening partners[81]. Understanding the phenotypic and functional diversity of stromal and immune cells within the TME, as well as the different axis mediating this crosstalk, is essential for cancer prevention, detection and treatment[81]. The cellular players include endothelial and perivascular cells, adipocytes and fibroblasts, and engaged immune cells including Mφ, dendritic cells, NK cells, myeloid derived suppressor cells (MSDC) and T and B cells. These acquire phenotypic and functional characteristics that are

distinct from their normal tissue resident counterparts and are reminiscent of a tissue recovering from wound healing[82]. On the other hand, deciphering this network provides cues to explain patients' differential response to treatment and to develop therapies that prolong disease free survival and patient's quality of life[83].

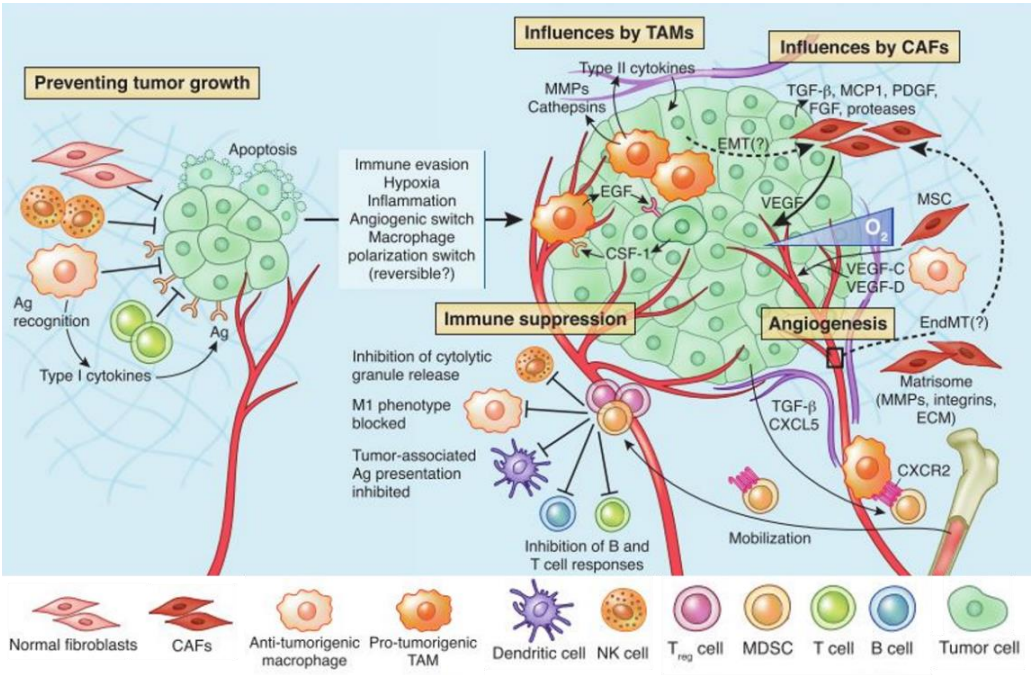

Figure 1.5: Different components of the tumor microenvironment. The balance between paracrine signaling and cell-cell interactions maintained at the tumor site dictate tumor progression and therapeutic response. Adapted from Quail *et al.*, Nat. Med. (2013)[78].

Fibroblasts and Mφ are key components within the TME and have been explored in the present work; therefore, are here reviewed further.

3.4.1 The stromal compartment - fibroblasts

Fibroblasts are a predominant cell type in the TME. Primary human fibroblasts have been described to inhibit tumor growth through direct cell-cell interaction as well as secretion of soluble factors[84,85]. However, upon contact with transformed cells, fibroblasts present an activated phenotype, with altered contractile and secretory characteristics when compared with fibroblasts from normal tissue[86], and a gene

expression profile similar to fibroblasts involved in wound healing[87,88]. Cancer-mediated fibroblast "education" into CAF is achieved through the secretion of growth factors, such as TGFB1, PDGF and fibroblast growth factor 2 (FGF2), whose production is also induced on fibroblasts at later stages[82]. CAF accumulation at the TME correlates with increased risk of relapse and reduced anti-tumor immunity in several cancer types[79,89,90]. Besides prognosis, these can also instruct therapeutic response. A gene expression signature characteristic of reactive stroma could predict resistance to neoadjuvant chemotherapy[91], indicating that combination therapies with drugs targeting CAF could contribute to overcome therapeutic resistance.

CAF influence most aspects of tumor biology. These have been functionally implicated in tumor formation[92], e.g., by contributing to genomic instability[81]. C-X-C motif chemokine ligand (CXCL) 12 and MMP secretion by CAF induces oxidative stress, leading to oncogenic transformation of epithelial cells[90,93,94]. CAF have also been linked with tumor subtype specification. A recent study reported that paracrine PDGFC signaling from BC cells induced hepatocyte growth factor (*HGF)*, insulin like growth factor binding protein 3 (*IGFBP3*) and stanniocalcin 1 (*STC1*) expression on CAF, which resulted in specification of a BLBC (ER negative) subtype on the tumor epithelial compartment[95]. CAF also enhance most tumor hallmarks, including cell proliferation, ECM remodeling and inflammation[79]. The highly secretory phenotype of CAF provides cytokines and growth factors that aid tumor development. In particular, CAF are an important source of RTK ligands, which ultimately contribute to tumor resistance to therapy[96,97]. Stromal HGF production activates MET receptor and consequent downstream MAPK and PI3K/AKT signaling pathways, leading to tumor rescue from RAF inhibitors[98]. Also, PDGFC production was shown to induce resistance to antiangiogenic therapy in lymphomas[99]. Stromal secretion of vascular endothelial growth factor (VEGF) A, PDGF and FGF2 promotes recruitment and proliferation of endothelial cells, enhancing angiogenesis[82]. CXCL12 is one of the main mediators of CAF tumorigenic potential; its expression has been observed in several tumors and it can induce tumor cell growth directly or through angiogenesis induction[93]. Moreover, its binding to C-X-C motif chemokine receptor (CXCR) 4 induces resistance to the estrogen receptor 1 (ER)

inhibitor, fulvestrant, in ER+ BC cells and reduced sensitivity to chemotherapeutic drugs in NSCLC[76]. CAF are also the main source of ECM at the tumor site, namely collagen, fibronectin and laminin, and induce desmoplasia in advanced carcinomas[100]. CAF were also shown to induce suppression of antitumor immunity[101]. The dense matrix formed at the TME was proposed to limit lymphocyte access to tumor sites[102]. In another study, depletion of CAF correlated with increased differentiation of T helper (Th) 1 cells, reduced recruitment of M2-like Mφ and was also correlated with increased CD8+T effector cell infiltration and activity[103]. Stromal expression of C-C motif chemokine ligand (CCL) 2, CCL3, CCL4, CCL5 has been shown to influence macrophage distribution and composition within the TME by recruitment of blood monocytes and immature myeloid cells[104]. CAF also contribute to the maintenance of an immunosuppressive TME through the production of CXCL8, IL4 and IL6, which polarize Mφ towards an M2-like phenotype[105]. Adaptive immunity is also dampened by the stromal compartment. Tumor infiltrating CD8+ T cells are often located in the adjacent tumoral areas and in direct contact with the fibroblast population. These CAF can directly decrease tumor antigen-specific CD8+ T cells through cross-presentation of antigens in concomitance with immune checkpoint expression (programmed cell death 1 ligand 2 - *PDCD1LG2* - and Fas ligand - *FASLG*)[106]. TGFB1 secretion also inhibits CD8+T and effector memory cells by inhibiting T cell receptor (TCR)-CD28 signaling[107,108], and thymic stromal lymphopoietin (TSLP) directs T cell into a Th2 phenotype[109].

It is important to note that CAF constitute a very heterogeneous population with multiple origins, and the effects of different CAF phenotypes are poorly understood[110]. Their intrinsic heterogeneity has been mainly studied in the context of single markers with a thoroughly elucidated functional role. CAF subpopulations expressing different levels of actin, alpha 2, smooth muscle, aorta (ACTA2), a broad activated fibroblast marker, can be found in wounds and sites of chronic inflammation. The tumor promoting activities of these CAFs have been dissected through co-transplantation into mice with cancer cells, or by disrupting their phenotype with drugs and evaluating tumor progression[2]. These termed myofibroblasts are a prominent

stromal population in several tumor types that correlate with poor prognosis and lead to therapeutic resistance[79,111]. Caveolin 1 (CAV1) and/or PDGFR-expressing CAF also constitute prognostic markers associated with low survival[81,112]. However, studies conducted using single or double marker identification of CAF may underestimate the complexity of the stromal compartment. The concurrent analysis of fibroblast activation protein alpha (FAP) and ACTA2 found phenotypically distinct CAF subpopulations in pancreatic cancer, that presented different spatial distribution[113]. Another recent study, comparing tumor and adjacent tissue fibroblasts in different subtypes of BC, found four distinct CAF subtypes by quantification of six different fibroblast markers (FAP, integrin β1, ACTA2, protein S100-A4, PDGFRB and CAV1)[79]. The different stromal subtypes differed not only in biomarker expression, but also functional effect, and their prevalence and distribution was dependent on tumor subtype, histological grade and immune microenvironment[79]. A specific CAF immunosuppression signature, which correlated with higher macrophage and lower CD8+T cell infiltration, was found to be preferentially present in triple negative BC (TNBC) and may be a promising target for combination therapy[79].

Not all CAF subpopulations aid tumor progression and since these are plastic cells, capable of acquiring multiple activating states, tumor promoting CAF phenotypes could be reversed[82]. However, we must better dissect stromal heterogeneity in the tumor milieu, which allied to the lack of functional biomarkers frustrates therapeutic strategies[103].

3.4.1 The immune compartment – macrophages

Myeloid cell recruitment to the tumor site has several pro-tumorigenic purposes, including tumor progression, increased angiogenesis and immunosuppression. These cells are recruited from blood monocytes and differentiate into multiple cell subsets, including MSDC, dendritic cells and Mφ, in response to TME stimuli produced by tumor and stromal cells[114]. Differentiated myeloid populations are a major source of endothelial, epithelial and stromal growth factors and matrix remodeling enzymes[2]. Clinical data shows that Mφ are a prominent myeloid infiltrate in the majority of

malignant human cancers and exert a strong influence on the immunologic state at the tumor site[115]. With few exceptions, these generally imply a poor prognosis[116–122] and display pro-tumorigenic properties, with reduced antigenic presenting capacity and low cytotoxic function[114].

Mφ encompass a diverse population of cells that is able to respond to inflammatory signals and tissue injury[115]. In steady-state, Mφ mainly exert phagocytic functions, neutralizing threats to the host and scavenging cell debris, while serving as a bridge between the innate and the adaptive arms of the immune system[123]. While usually classified into M1 or M2 phenotypes depending on their functional role in human immunity, Mφ are very plastic cells that change polarization state in response to environmental stimuli. Polarization involves remodeling in the cytokine secretion profile and in the expression of other signaling molecules, as well as surface receptors[114].

Several soluble factors produced by tumor and stromal cells were shown to induce monocyte recruitment, such as CCL2, colony stimulating factor 1 (CSF1), IL6, VEGF and PDGF[114,124]. The conditions observed at the tumor site that result of the aberrant metabolism of tumor cells, i.e. hypoxia, acidic pH and high lactate concentration, and of the release of danger signals by dying cells, triggers an inflammatory reaction resembling tissue damage[104,125,126]. In response, Mφ polarize into a wound-healing and tissue-repair phenotype, with functions of debris removal, production of trophic signals and immunosuppression[127]. Additionally, TME cytokines, such as IL4, IL10 and IL13, produced by tumor and stromal cells, further contribute to polarize Mφ into an M2-like pro-tumorigenic phenotype[128]. These tumor associated macrophages (TAM) secrete cytokines, growth factors, inflammatory substrates and proteolytic enzymes that contribute to cancer progression[128]. A lot of effort has been conducted towards dissection of the different identities and functions of Mφ present in tissue during the steady-state and during sterile inflammatory conditions, such as cancer[115]. Although there are Mφ populations present in all tumors, their amount, activation states and phenotypic markers differ from tissue to tissue and from patient to patient within the same tumor subtype[115]. TAM are traditionally associated with the M2 phenotype

since they suppress antitumor immunity through production of anti-inflammatory cytokines and contribute to the resolution of inflammation[114]. Nowadays, however, in light of the extensive network of transcriptional regulators at play during Mφ polarization, characterization of Mφ populations is based on a spectrum of phenotypes, that need further characterization[129]. Also, there have been additional Mφ molecular phenotypes identified that do not reflect the current M1/M2 paradigm[114]. The first single-cell analysis of the innate immune compartment in human cancer patients evidenced distinct myeloid cell subsets, and their differential contribution to anti-tumor T cell immunity[130]. Understanding the changes occurring within these subsets in the initial tumor lesion can provide immunomodulatory strategies targeting the innate immune compartment, that may enhance response to checkpoint blockade therapies[130].

TAM's pro-tumorigenic phenotype favors tumor growth by promoting tumor cell proliferation, invasion and metastasis, stimulating angionesis and ECM remodeling, and contributing to evasion from adaptive immunity (Fig. 1.6)[131]. At the invasive tumor front, several immune cells aid cell motility and invasion (Fig. 1.6 – E)[132,133]. Real-time multiphoton imaging showed that Mφ can associate with breast cancer cells at the tumor invasive edge and promote invasion[133]. Local production of TGFB1 and direct intercellular adhesion molecule 1 (ICAM1) / integrin subunit beta 2 (ITGB2)-mediated cell-cell contact by M2 Mφ induces cell dissociation and migration of single cells at the tumor front[134]. Increased invasion and metastatic ability may also result from a local induction of EMT, which is potentiated by soluble factors produced by stromal and inflammatory cells at the tumor periphery[44]. In a paracrine and self-sustaining loop, TME IL4 induces epidermal growth factor (EGF) production by TAM, which induces CSF1 secretion by tumor cells, further stimulating TAM survival and activation[132]. EGF, in turn, was shown to induce EGFR-mediated invasion by breast cancer cells, facilitating intravasation and promoting early metastasis (Fig. 1.6 – B, E)[132,135]. TAM, as well as other immune cells at the TME, secrete MMP, serine proteases and cathepsins that also facilitate invasion and metastasis by degrading ECM[114]. ECM remodeling can also cause the release of ECM-bound mitogenic factors that support angiogenesis (Fig. 1.6 –

E, F)[103]. Direct secretion of prostaglandin-endoperoxide synthase 2 (PTGS2), FGF2, PDGFB1 and VEGF by TAM can also increase angiogenesis and promote endothelial cell survival[103]. Myeloid cells were shown to contribute to the development of a favorable pre-metastatic niche, enhancing tumor cell colonization of distant organs[136]. A distinct subset of metastasis-associated macrophages was identified at perivascular sites of lung metastasis of PymT BC mouse model, which was required for efficient metastatic seeding and growth[137]. Macrophage education at the pre-metastatic niche appears to be a result of systemic release of exosomes by tumor cells, at least in liver colonization[138]. Finally, TAM contribute to the development of an immunosuppressive TME by directly inhibiting CD8+ T effector cell function or by the secretion of cytokines that recruit other immunosuppressive immune cells (Fig. 1.6 – D)[114]. Overexpression of PDL1/2 and CD80/86, ligands of the inhibitory receptors PD-1 and CTLA4, directly suppress cytotoxic CD8+T cell activity[114]. Production of cytokines and proteases, such as IL10, TGFB1, arginase 1 (ARG1), and prostaglandins, can also indirectly suppress T cell activation and proliferation (Fig. 1.6 – D)[114].

Thus, TAM infiltration can be a prognostic marker and a target for therapeutic intervention. The functional significance of TAM infiltrates was demonstrated by gene knockout of macrophage growth factor *CSF1*, or its direct effectors, in the polyoma middle T (PyMT) mouse model of BC. The KO decreased the macrophage infiltrate, which resulted in slowed tumor progression and decreased metastatic behavior[139,140]. Also, inhibition of CSF1R signaling, and consequent decreased TAM density, promoted the recruitment of CD8+ T cells to the tumor site, leading to reduction of cervical and mammary tumor growth[141]. In parallel, overexpression of *CSF1* in tumors stimulates macrophage infiltration, leads to tumor progression and metastasis, and is associated with poor prognosis in BC patients[140]. Finally, neutralizing antibodies against CSF1 or its receptor have the same effect in neuroblastoma mouse xenografts[142].

Promising results in both animal models and clinical trials targeting TAM suggests an important role in combination therapies[76]. Checkpoint blockade therapies focus on restoration of pre-existing antitumor cellular immunity, through rescue of exhausted

CD8+T cells or by depletion of regulatory T cells (Treg)[130]. However, the limited and heterogeneous response in different patients has sparked the need to develop accompanying strategies to further strengthen T cell responses. Mφ cross-present foreign antigens and produce T cell differentiation cytokines, playing an important role in managing T cell function at the tumor site[130]. Therefore, controlling the macrophage compartment or changing macrophage phenotype at the tumor site may serve as a synergistic role in potentiating T cell targeting therapies[130]. Indeed, decreased macrophage infiltration leads to higher efficacy of immunotherapies[143]. Interestingly, PD1/PDL1 blockade has also been shown to restore TAM phagocytic capacity and reduce tumor growth of colorectal cancer in mice models[144].

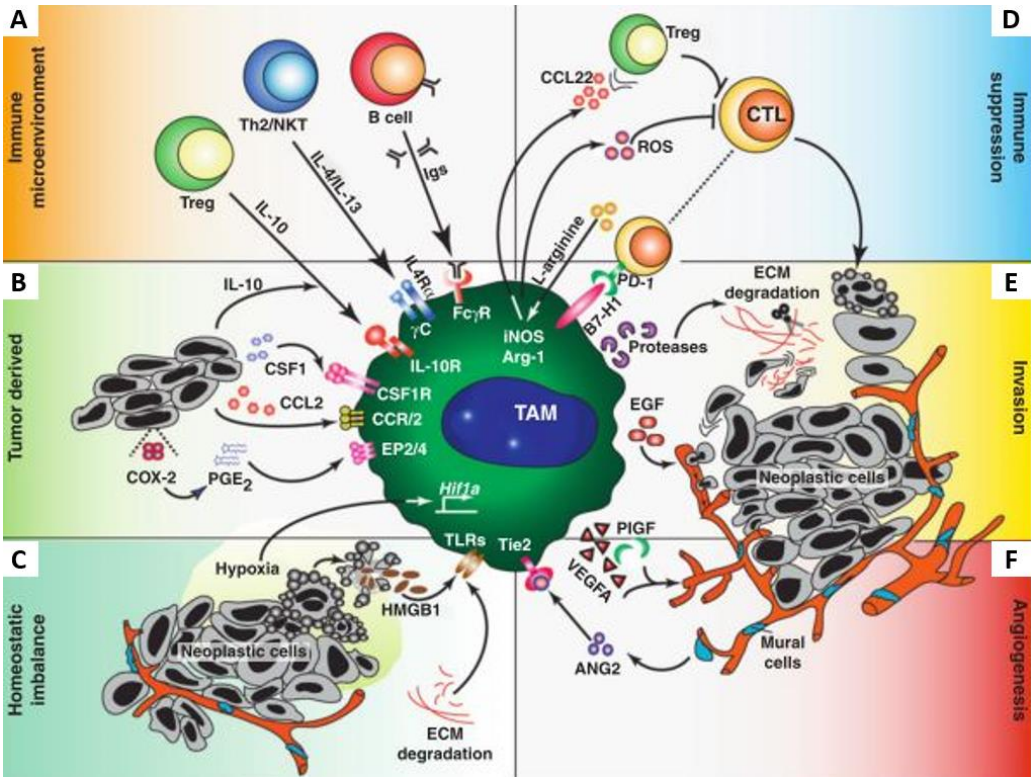

Figure 1.6: Tumor-associated macrophages (TAM) role within the tumor microenvironment (TME). A - C) TME factors promoting the polarization of macrophages towards a tumor promoting phenotype; **D – F)** tumor promoting roles of TAM. Adapted from Ruffell *et al.*, Trends Immunol (2012)[128].

4. EXPERIMENTAL TUMOR MODELING

Experimental tumor modeling has long supported the discovery of fundamental mechanisms of tumorigenesis and tumor progression, as well as provided platforms for the development of novel therapies. Still, the attrition rates observed today in clinical translation could be, in part, mitigated by more accurate recapitulation of environmental cues in research and preclinical models[145]. Since no model is a perfect representation of a real system, these must be chosen while considering the balance between their limitations and the necessary complexity to support the objectives of the study[146].

Two-dimensional (2D) cell culture systems provide the necessary throughput for fast screening of multiple compounds and key players in productive cell-cell interactions[98,147,148]. Nevertheless, these poorly predict drug response and lead to an overwhelming number of possible targets that, despite showing considerable efficacy in 2D culture assays or even animal models, are proven ineffective in clinical trials, prolonging patients' survival by a few months or a couple of years in metastatic disease[81,145]. It is now evident that, in these systems, cell-plastic connections prevail over cell-cell and cell-ECM interactions[149]. Thus, the need for more predictive drug discovery assays has prompted advances in cell culture techniques that permitted a fast evolution of complex *in vitro* cell models attempting to recapitulate tumor architecture[150]. Pioneering work by Mina Bissel evidenced that complex systems can be exploited to uncover molecular mechanisms of tumorigenesis and invasion. Blockade of ITGB1 reverted the malignant phenotype of BC cells in a three-dimensional (3D), forming reverted acini and re-establishing CDH1/catenin beta 1 (CTNNB1) complexes[151]. This phenomena had not been observed in 2D cultures and showed that epithelial tumor cells can change polarity in a microenvironment-dependent manner[152].

Most used 3D tumor models rely on spheroids for culturing the epithelial compartment[153]. Spheroids have been used for drug screening and to study tumor cell function, angiogenesis and tumor-immune interactions[154]. These constitute high-

throughput tools to select drug candidates and decrease animal use, as they present higher resistance to treatment, thus better resembling the drug response observed in solid tumors[155]. These are formed by spontaneous aggregation of cells in culture and present characteristics resembling the *in vivo* tumors, namely physical change in cell structure and polarity[152], tensile forces[156] and ECM production[157,158]. Also, these models maintain cell-cell interactions, gradients of nutrients, metabolites, oxygen and also ECM accumulation[159,160]. Finally, extensive studies have shown that tumor cell lines cultured under 3D conditions exhibit gene expression profiles closer to patient samples[154,161].

The thorough establishment of the influence of the TME on tumor progression and therapeutic response has spirited the development of *in vitro* models where some of these interactions can start to be dissected and exploited. Most heterotypic cell cultures incorporate CAF, which promote an inflammatory microenvironment and lead to drug resistance, though other cell types have been used, namely mesenchymal stem cells[162]. The fast development of immunotherapies, however, is driving the need for preclinical models that incorporate the immunological state of the TME, while maintaining compatibility with drug screening platforms and allowing straightforward functionality assessment[86].

Innovative strategies for research and preclinical studies of tumor-stroma-immune cell dynamic interactions pose a difficult challenge for the tumor modeling field[86]. Traditional co-culture techniques have brought significant insights into the crosstalk between cells from the TME. Conditioned media experiments have been extensively employed to study interactions between different cells; however, these preclude direct cell-cell interactions and dynamic crosstalk between the different cell types. Indirect co-cultures, on the other hand, allow for reciprocal and dynamic crosstalk between the different components but still, only through soluble factors[163]. Finally, direct co-culture assays add an extra layer of complexity on the readouts since either gene expression or protein analysis on individual cell subsets requires previous separation of the cell types; thus most analysis is ultimately based on imaging and secreted factors (Fig. 1.7 – A)[163]. Nevertheless, the contribution of cell-cell and cell-ECM components

is crucial for the tumorigenic phenotype and thus such interaction should be included in preclinical models. Several *in vivo* models have also been used to study tumor-TME interactions. Most relevant *in vivo* tumor-bearing models include patient- or cell line-derived xenografts (PDX/CDX), and genetically engineered mouse models (GEMM)[164]. Heterotypic implantation of human tumor cells in immunodeficient mouse models constitute effective alternatives to study tumorigenesis of specific tumor subtypes via genetic, phenotypic and functional analysis[164]. However, the lack of immune subset and the presence of murine stromal compartment render any considerations on the tumor-immune interactions and its impact on tumor progression unfeasible[86]. Xenografts that have incorporated the human immune compartment do exist, but are expensive and pose ethical dilemmas, while still not accurately translating results into the human setting[147]. GEMM, on the other hand, are very useful to study tumorigenesis of specific cancer subtypes. Here, the tumor-TME interactions are studied within a murine system, which may not represent the human situation[165–167]. Anti-CSF1 therapeutic approaches, for example, lead to complete tumor regression in mouse models of solid tumors but show lack of efficacy in human clinical trials[168].

3D heterotypic cellular models may provide the necessary complementary solution in terms of functionality, complexity and throughput, between in vivo experimental models or standard in vitro approaches and clinical oncology (Fig. 1.7)[86]. Spheroids appear uniquely qualified to decipher tumor-immune interactions. Transcriptional analysis of mesothelioma spheroids vs monolayers showed that the majority of upregulated genes are related with immune response, wound healing, lymphocyte stimulation and response to cytokine stimulation, while downregulated genes mainly include promotion of apoptosis[147,169]. Early reports show that cancer spheroids show increased migratory capacity when co-cultured with M2-like Mφ, resembling to some extent the effects described for TAM in human tumors[170]. Moreover, the reciprocal crosstalk between breast cancer spheroids from different subtypes and monocytes was shown to be dependent on the aggressiveness of each subtype[171].

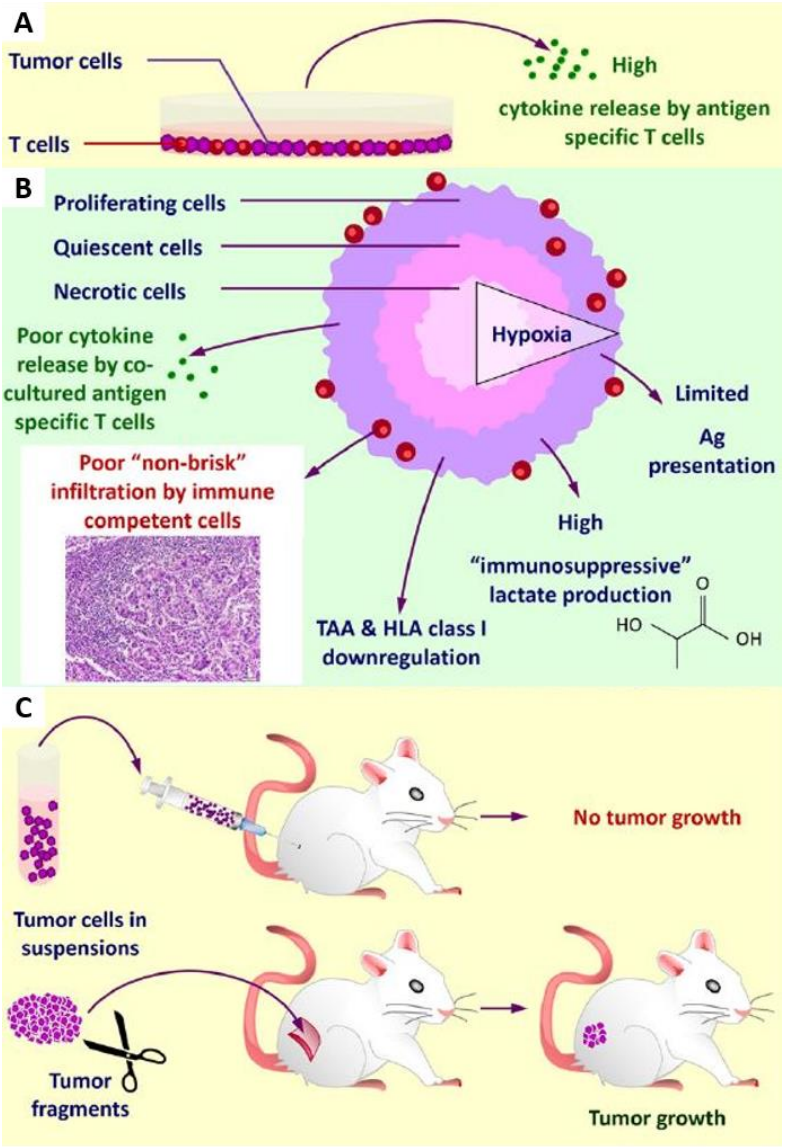

Figure 1.7: Different strategies to study tumor-immune interactions. **A)** Tumor-immune cell 2D direct co-culture; **B)** Tumor-immune 3D co-cultures based on spheroids, evidencing the lower ability to stimulate cytokine release by effector cells, as compared to 2D co-cultures. Different immunosuppressive characteristics of tumor spheroids are also depicted; **C)** *In vivo* mouse models evidencing the lower immunogenicity of tumor spheroids transplanted into immunocompetent mice, as compared to tumor single cell suspension. Adapted from Hirt *et al.*, Adv. Drug Deliv. Rev (2014)[86].

The co-culture with breast cancer spheroids from more aggressive phenotypes, namely BLBC, induced a pro-tumorigenic phenotype in the Mφ population, with consequent increased invasive potential for the tumor cells[171], features already described for these tumors *in vivo*[172]. Tumor spheroids also present diminished antigen presenting capacity and decreased proliferation (Fig. 1.7 – B)[86]. This leads to lower immunogenicity when compared to monolayers, decreasing tumor cells sensitivity to lymphocyte effector functions, which is also a prominent feature in different solid tumors *in vivo* (Fig- 1.7 – C)[86,103,147]. Additionally, the high lactate production is a key mechanism of action leading to an immunosuppressive TME in models encompassing tumor spheroids (Fig. 1.7 – B)[86].

Finally, the use of tumor biopsies or resected tumor sections embedded in a matrix can maintain heterogeneity of tumor cell populations and be a potential screening tool for patient-specific therapies[154]. Although these have been exploited, their application for drug discovery faces technical problems and limitations in sample material[150].

5. CANCER GENE THERAPY

Cancer diagnostics and therapeutics have evolved tremendously in the past decades, and now include strategies to target cancer cell intrinsic genetic aberrations and cell extrinsic mediators of malignancy[173]. Nonetheless, uncovering promising targets is not sufficient, efficient delivery platforms are still a bottleneck in the implementation of innovative therapies[174]. After many years of intense research delayed by significant setbacks related with negative outcomes in clinical trials, gene therapy is emerging as an important therapeutic approach[175]. Recent progress has been leveraged by the better understanding of the viral vector biology and a deeper knowledge of the target cells[175]. Currently, gene therapy-based treatments are approaching clinical approval by FDA and EMA for a myriad of diseases, from inherited immune disorders, hemophilia, eye and neurodegenerative disorders and lymphoid cancers[175]. Also, there is gene therapy product based on adeno-associated viral (AAV) vectors (Glybera) with granted marketing authorization in the European Union for the treatment of lipoprotein lipase deficiency[176].

For cancer gene therapy approaches to be successful, the development of gene delivery vectors that can safely and efficiently be used to bring genetic material into target cells is needed[177]. Non-viral vectors are easy to produce and readily amenable to engineering; however, these are difficult to deliver to target cells[177]. Viral vectors, on the other hand, can be exploited for their natural ability to efficiently reach and infect target cells. The prevalence of gene therapy clinical trials directed at cancer have long been focused on oncolytic viruses, which include adenovirus, herpes simplex virus, and reovirus[177,178]. Nevertheless, many viral vectors have been tested as gene delivery platforms, including adenovirus, retrovirus, vaccinia virus, herpesvirus, and AAV. Gene therapy approaches to target cancer cover a wide variety of strategies. These include delivery of suicide genes, such as the herpes simplex virus-thymidine kinase system and polyomavirus middle T antigen; vascular reprogramming by delivery of anti-angiogenic factors, such as PEDF, endostatin 34, Kringle 5 and Kallistatin; and strategies to activate the immune system, such as the delivery of cytokines or immunogenic cell surface molecules and tumor antigens[177].

5.1 Adeno-associated Viral Vectors (AAV)

The *in vivo* gene therapy field is currently dominated by recombinant adeno-associated viral vectors (rAAV). These have been increasingly used in clinical trials due to their safety profile and persistent transgene expression *in vivo*, when administered both locally and systemically[179].

The rAAV are engineered from adeno-associated viruses, which are nonpathogenic, naturally replication-deficient and mostly non-integrative. These characteristics greatly reduces the risks associated with their clinical application but also decreases the long-term expression potential in proliferative cells[180]. In central nervous system (CNS) disorders, namely congenital blindness, Parkinson´s disease and Leber's congenital amaurosis, AAV-based gene replacement therapies have successfully translated the results achieved in preclinical tests to humans[179,181,182]. This most likely reflects the good tropism found in some AAV variants towards CNS, together with the fact that retinal space is an immunoprivileged site[179]. Since humans are natural hosts for

adeno-associated virus, most people already have pre-existing humoral and cellular immunity against the AAV capsid, which reduces clinical efficacy[180]. Successful clinical translation of AAV-based therapies was preceded by a better understanding of anti-AAV immune responses, as well as by the development of strategies to circumvent such responses[175]. Over the years, several avenues to engineer AAV´s capsid have allowed the development of less immunogenic variants, as well as vectors presenting tropism better suited to the specific needs of the therapeutic target. Increased understanding of the AAV capsid structure, coupled with the presence of a known receptor at the target cell of interest enable rational design approaches[183]. The display of high affinity ligands for HER2 at the VP2 capsid protein of AAV2 increased their specificity for this BC subtype, which may be used in targeted therapies[184]. On the other hand, when there is no knowledge on the receptor to target, directed evolution approaches have been employed. Here, selective pressure is applied to identify relevant AAV variants[183]. For example, using different pools of human anti-AAV antibodies, several rounds of selective pressure enabled the identification of an AAV2 variant that could tolerate higher levels of neutralizing antibodies[185].

The delivery of high titer and high quality rAAV batches to meet clinical demands is supported by continuous improvement of upstream manufacturing and downstream purification processes[186]. The development of scalable platforms that allow generation of large quantity of high quality AAV batches are necessary to accommodate later stage clinical trials[187]. Manufacturing processes for rAAV are mostly based on two systems: stable producer cell lines and transient production systems[188]. Transient production involves either co-transfection of several plasmids or co-infection with different viruses that provide the helper functions and the vector construct, necessary to replicate and package the rAAV genome[179]. Laboratory scale platforms are mainly based on transfection of mammalian cells on 2D culture systems[179]. These are faster to implement and, by avoiding the use of helper virus, render the process much less time-consuming[186]. These systems enable rapid screen of multiple candidate vector construct for early assessment of lead candidates and can ensure production at preclinical and phase I/II clinical trial scale[186]. Several options for

scalability are already available including the use of multi-tray cell factories, roller bottles and suspension cultures[188]. Large scale production systems are based on suspension cultures of mammalian or insect cells[188]. Bioreactors routinely used for large scale suspension cultures include stirred-tank and WAVE bioreactors[188]. Insect cells in association with the baculovirus expression vector system (IC-BEVS) are currently one of the most used platforms for large scale rAAV production[189]. Insect cell-based platforms are scalable and GMP-compatible, since they achieve high cell density in suspension in serum-free conditions[188]. IC-BEVS can currently yield production batches suitable for later stage clinical trials and commercial use, with multiple products, mostly vaccines and gene therapy vectors, already approved for human and veterinary use, including Glybera[190].

6. AIMS AND SCOPE

The overarching aim of this thesis was to develop strategies that could improve the clinical translation of tumor biology insights. The work was divided into two main sections: A) development of therapeutic strategies to target cancer genetic vulnerabilities and B) development of 3D cellular models that incorporated the crosstalk between tumor cells and cells from the tumor microenvironment.

In ***Chapter I***, the state of the relevant to the present work was reviewed.

In the first part of the work (A), we took advantage of previously described genetic vulnerabilities of BLBC to pursue the development of a targeted therapeutic approach for this BC subtype. The lack of targeted therapies for BLBC does not reflect an absence of potential molecular targets. These do, however, need to be assessed for their preclinical efficacy to accurately evaluate their clinical potential. Therefore, in ***Chapter II***, we developed an rAAV-based gene therapy for the delivery of shRNA molecules targeting BLBC survival genes. To assess its effect, two different BLBC cell lines were transduced with the developed rAAV vectors and their effect on tumor cell viability and apoptosis induction was evaluated. Also, using an *in vivo* preclinical model – BLBC mouse xenografts - we planned to assess the effect of the developed therapeutic approach in BLBC cancer progression, by measuring the tumor volume over the course

of the treatment. Also, given the broad tropism of AAV2 serotype, and in order to avoid unspecific infection of non-relevant tissues *in vivo*, it was important to design a strategy to restrict AAV2 tropism towards BLBC. For this, in ***Chapter III***, sequential rounds of infection were conducted using different BLBC cell lines in an attempt to recover the variants with higher specificity. Thus, this would allow the development of a therapeutic strategy with specific toxicity for BLBC and that could be applied systemically.

The increasing realization that TME cues play a decisive role in the outcome of cancer drug response, urges its integration in preclinical tumor models. Several anticancer therapies require the presence of an engaged immune system to enhance their efficacy. These include untargeted approaches, namely chemo- and radiotherapy, as well as targeted molecular approaches aiming at inducing tumor cell death. Therefore, in ***Chapter IV***, we aimed at developing a 3D co-culture model that incorporated tumor, stromal and myeloid cell compartments. We hypothesized that by co-culturing relevant cell types present in the TME, and allowing cell-cell communication through both direct cell-cell contact and soluble factors, we would be able to mimic certain aspects of the TME. The inclusion of macrophages, in particular, could lead to the development of an immunosuppressive TME, present at NSCLC. Hence, a more accurate preclinical tumor model for both disease modeling and drug screening applications could be developed. This model was based on alginate microencapsulation of the different cells, which were cultured under stirred conditions. The model was characterized phenotypically and functionally, by treatment with both chemo and immunomodulatory challenges.

Finally, in ***Chapter V***, a general discussion of the work is presented, together with perspective on how this can impact future approaches in cancer research.

7. AUTHOR CONTRIBUTION & ACKNOWLEDGEMENTS

The author wrote this chapter based on the referred bibliography.

8. REFERENCES

1. Huch, M. & Rawlins, E. L. Cancer: Tumours build their niche. *Nature* **545,** 292–293 (2017).
2. Hanahan, D. & Weinberg, R. A. Hallmarks of Cancer: The Next Generation. *Cell* **144,** 646–

674 (2011).
3. Arteaga, C. L. & Engelman, J. A. ERBB receptors: From oncogene discovery to basic science to mechanism-based cancer therapeutics. *Cancer Cell* **25,** 282–303 (2014).
4. Lemmon, M. A. & Schlessinger, J. Cell Signaling by Receptor Tyrosine Kinases. *Cell* **141,** 1117–1134 (2010).
5. Slamon, D. J. *et al.* Human breast cancer: correlation of relapse and survival with amplification of the HER-2/neu oncogene. *Science* **235,** 177–82 (1987).
6. Burstein, H. J. The Distinctive Nature of HER2-Positive Breast Cancers. *N. Engl. J. Med.* **353,** 1652–1654 (2005).
7. Loibl, S. & Gianni, L. HER2-positive breast cancer. *Lancet* **389,** 2415–2429 (2017).
8. Moscatello, D. K. *et al.* Frequent expression of a mutant epidermal growth factor receptor in multiple human tumors. *Cancer Res.* **55,** 5536–9 (1995).
9. Ji, H. *et al.* The impact of human EGFR kinase domain mutations on lung tumorigenesis and in vivo sensitivity to EGFR-targeted therapies. *Cancer Cell* **9,** 485–495 (2006).
10. Morin-Ben Abdallah, S. & Hirsh, V. Epidermal Growth Factor Receptor Tyrosine Kinase Inhibitors in Treatment of Metastatic Non-Small Cell Lung Cancer, with a Focus on Afatinib. *Front. Oncol.* **7,** (2017).
11. Xu, A. M. & Huang, P. H. Receptor Tyrosine Kinase Coactivation Networks in Cancer. *Cancer Res.* **70,** 3857–3860 (2010).
12. Stommel, J. M. *et al.* Coactivation of Receptor Tyrosine Kinases Affects the Response of Tumor Cells to Targeted Therapies. *Science (80-.).* **318,** 287–290 (2007).
13. Alexander, P. B. *et al.* Distinct receptor tyrosine kinase subsets mediate anti-HER2 drug resistance in breast cancer. *J. Biol. Chem.* **292,** 748–759 (2017).
14. Remon, J. *et al.* Acquired resistance to epidermal growth factor receptor tyrosine kinase inhibitors in EGFR-mutant non-small cell lung cancer: A new era begins. *Cancer Treat. Rev.* **40,** 93–101 (2014).
15. Guix, M. *et al.* Acquired resistance to EGFR tyrosine kinase inhibitors in cancer cells is mediated by loss of IGF-binding proteins. *J. Clin. Invest.* **118,** 2609 (2008).
16. Mohammad, R. M. *et al.* Broad targeting of resistance to apoptosis in cancer. *Semin. Cancer Biol.* **35,** S78–S103 (2015).
17. Hoadley, K. A. *et al.* Multiplatform analysis of 12 cancer types reveals molecular classification within and across tissues of origin. *Cell* **158,** 929–944 (2014).
18. Kandoth, C. *et al.* Mutational landscape and significance across 12 major cancer types. *Nature* **502,** 333–339 (2013).
19. Kruiswijk, F., Labuschagne, C. F. & Vousden, K. H. p53 in survival, death and metabolic health: a lifeguard with a licence to kill. *Nat. Rev. Mol. Cell Biol.* **16,** 393–405 (2015).
20. Lalaoui, N., Lindqvist, L. M., Sandow, J. J. & Ekert, P. G. The molecular relationships between apoptosis, autophagy and necroptosis. *Semin. Cell Dev. Biol.* **39,** 63–69 (2015).
21. Croce, C. M. & Reed, J. C. Finally, An Apoptosis-Targeting Therapeutic for Cancer. *Cancer Res.* **76,** 5914–5920 (2016).
22. Tahir, S. K. *et al.* Potential mechanisms of resistance to venetoclax and strategies to circumvent it. *BMC Cancer* **17,** 399 (2017).
23. Akgul, C. Mcl-1 is a potential therapeutic target in multiple types of cancer. *Cell. Mol. Life Sci.* **66,** 1326–1336 (2009).
24. Marriott, H. M. *et al.* Dynamic changes in Mcl-1 expression regulate macrophage viability or commitment to apoptosis during bacterial clearance. *J. Clin. Invest.* **115,** 359–368 (2005).
25. Zhong, Q., Gao, W., Du, F. & Wang, X. Mule/ARF-BP1, a BH3-Only E3 Ubiquitin Ligase, Catalyzes the Polyubiquitination of Mcl-1 and Regulates Apoptosis. *Cell* **121,** 1085–1095 (2005).

26. Derenne, S. *et al.* Antisense strategy shows that Mcl-1 rather than Bcl-2 or Bcl-x L is an essential survival protein of human myeloma cells. *Blood* **100,** 194–199 (2002).
27. Wei, S.-H. *et al.* Inducing apoptosis and enhancing chemosensitivity to Gemcitabine via RNA interference targeting Mcl-1 gene in pancreatic carcinoma cell. *Cancer Chemother. Pharmacol.* **62,** 1055–1064 (2008).
28. Hussain, S.-R. A. *et al.* Mcl-1 Is a Relevant Therapeutic Target in Acute and Chronic Lymphoid Malignancies: Down-Regulation Enhances Rituximab-Mediated Apoptosis and Complement-Dependent Cytotoxicity. *Clin. Cancer Res.* **13,** 2144–2150 (2007).
29. Quinn, B. A. *et al.* Targeting Mcl-1 for the therapy of cancer. *Expert Opin. Investig. Drugs* **20,** 1397–1411 (2011).
30. Jesenberger, V. & Jentsch, S. Deadly encounter: ubiquitin meets apoptosis. *Nat. Rev. Mol. Cell Biol.* **3,** 112–121 (2002).
31. Manasanch, E. E. & Orlowski, R. Z. Proteasome inhibitors in cancer therapy. *Nat. Rev. Clin. Oncol.* **5,** 101–110 (2017).
32. Love, I. M., Shi, D. & Grossman, S. R. p53 Ubiquitination and Proteasomal Degradation. in *Methods in Molecular Biology* **962,** 63–73 (2013).
33. Pant, V. & Lozano, G. Limiting the power of p53 through the ubiquitin proteasome pathway. *Genes Dev.* **28,** 1739–1751 (2014).
34. Fennell, D. A., Chacko, A. & Mutti, L. BCL-2 family regulation by the 20S proteasome inhibitor bortezomib. *Oncogene* **27,** 1189–1197 (2008).
35. Lu, Z. & Hunter, T. Ubiquitylation and proteasomal degradation of the p21 Cip1 , p27 Kip1 and p57 Kip2 CDK inhibitors. *Cell Cycle* **9,** 2342–2352 (2010).
36. Chen, Z. J. Ubiquitin signalling in the NF-κB pathway. *Nat. Cell Biol.* **7,** 758–765 (2005).
37. Vander Heiden, M. G., Cantley, L. C. & Thompson, C. B. Understanding the Warburg Effect: The Metabolic Requirements of Cell Proliferation. *Science (80-.).* **324,** 1029–1033 (2009).
38. Vander Heiden, M. G. & DeBerardinis, R. J. Understanding the Intersections between Metabolism and Cancer Biology. *Cell* **168,** 657–669 (2017).
39. Losman, J.-A. & Kaelin, W. G. What a difference a hydroxyl makes: mutant IDH, (R)-2-hydroxyglutarate, and cancer. *Genes Dev.* **27,** 836–852 (2013).
40. Tateishi, K. *et al.* Extreme Vulnerability of IDH1 Mutant Cancers to NAD+ Depletion. *Cancer Cell* **28,** 773–784 (2015).
41. Davidson, S. M. *et al.* Environment Impacts the Metabolic Dependencies of Ras-Driven Non-Small Cell Lung Cancer. *Cell Metab.* **23,** 517–528 (2016).
42. Hensley, C. T. *et al.* Metabolic Heterogeneity in Human Lung Tumors. *Cell* **164,** 681–694 (2016).
43. Maddocks, O. D. K. *et al.* Serine starvation induces stress and p53-dependent metabolic remodelling in cancer cells. *Nature* **493,** 542–546 (2012).
44. Nieto, M. A., Huang, R. Y.-J., Jackson, R. A. & Thiery, J. P. EMT: 2016. *Cell* **166,** 21–45 (2016).
45. Li, Q. *et al.* A sequential EMT-MET mechanism drives the differentiation of human embryonic stem cells towards hepatocytes. *Nat. Commun.* **8,** 15166 (2017).
46. Savagner, P. *et al.* Developmental transcription factor slug is required for effective re-epithelialization by adult keratinocytes. *J. Cell. Physiol.* **202,** 858–866 (2005).
47. Said, N. A. B. M. & Williams, E. D. Growth Factors in Induction of Epithelial-Mesenchymal Transition and Metastasis. *Cells Tissues Organs* **193,** 85–97 (2011).
48. Siegel, P. M. & Massagué, J. Cytostatic and apoptotic actions of TGF-β in homeostasis and cancer. *Nat. Rev. Cancer* **3,** 807–820 (2003).
49. Pickup, M., Novitskiy, S. & Moses, H. L. The roles of TGFβ in the tumour microenvironment. *Nat. Rev. Cancer* **13,** 788–799 (2013).
50. Vogelmann, R. TGF -induced downregulation of E-cadherin-based cell-cell adhesion depends on PI3-kinase and PTEN. *J. Cell Sci.* **118,** 4901–4912 (2005).

51. Wu, J. *et al.* RBM38 is involved in TGF-β-induced epithelial-to-mesenchymal transition by stabilising zonula occludens-1 mRNA in breast cancer. *Br. J. Cancer* **117,** 675–684 (2017).
52. Katsuno, Y., Lamouille, S. & Derynck, R. TGF-β signaling and epithelial–mesenchymal transition in cancer progression. *Curr. Opin. Oncol.* **25,** 76–84 (2013).
53. Chen, W., Gao, Q., Han, S., Pan, F. & Fan, W. The CCL2/CCR2 axis enhances IL-6-induced epithelial-mesenchymal transition by cooperatively activating STAT3-Twist signaling. *Tumor Biol.* **36,** 973–981 (2015).
54. Sullivan, N. J. *et al.* Interleukin-6 induces an epithelial–mesenchymal transition phenotype in human breast cancer cells. *Oncogene* **28,** 2940–2947 (2009).
55. Lee, S. O. *et al.* IL-6 promotes growth and epithelial-mesenchymal transition of CD133+ cells of non-small cell lung cancer. *Oncotarget* **7,** 6626–6638 (2016).
56. Pradella, D., Naro, C., Sette, C. & Ghigna, C. EMT and stemness: flexible processes tuned by alternative splicing in development and cancer progression. *Mol. Cancer* **16,** 8 (2017).
57. Zheng, X. *et al.* Epithelial-to-mesenchymal transition is dispensable for metastasis but induces chemoresistance in pancreatic cancer. *Nature* **527,** 525–530 (2015).
58. Fischer, K. R. *et al.* Epithelial-to-mesenchymal transition is not required for lung metastasis but contributes to chemoresistance. *Nature* **527,** 472–476 (2015).
59. Brabletz, T., Kalluri, R., Nieto, M. A. & Weinberg, R. A. EMT in cancer. *Nat. Rev. Cancer* **18,** 128–134 (2018).
60. Mittal, V. Epithelial Mesenchymal Transition in Tumor Metastasis. *Annu. Rev. Pathol. Mech. Dis.* **13,** 395–412 (2018).
61. Mehlen, P. & Puisieux, A. Metastasis: a question of life or death. *Nat. Rev. Cancer* **6,** 449–458 (2006).
62. Tran, H. D. *et al.* Transient SNAIL1 Expression Is Necessary for Metastatic Competence in Breast Cancer. *Cancer Res.* **74,** 6330–6340 (2014).
63. Imani, S., Hosseinifard, H., Cheng, J., Wei, C. & Fu, J. Prognostic Value of EMT-inducing Transcription Factors (EMT-TFs) in Metastatic Breast Cancer: A Systematic Review and Meta-analysis. *Sci. Rep.* **6,** 28587 (2016).
64. Krebs, A. M. *et al.* The EMT-activator Zeb1 is a key factor for cell plasticity and promotes metastasis in pancreatic cancer. *Nat. Cell Biol.* **19,** 518–529 (2017).
65. Friedl, P., Locker, J., Sahai, E. & Segall, J. E. Classifying collective cancer cell invasion. *Nat. Cell Biol.* **14,** 777–783 (2012).
66. Lambert, A. W., Pattabiraman, D. R. & Weinberg, R. A. Emerging Biological Principles of Metastasis. *Cell* **168,** 670–691 (2017).
67. Kopp, H.-G., Placke, T. & Salih, H. R. Platelet-Derived Transforming Growth Factor- Down-Regulates NKG2D Thereby Inhibiting Natural Killer Cell Antitumor Reactivity. *Cancer Res.* **69,** 7775–7783 (2009).
68. Labelle, M., Begum, S. & Hynes, R. O. Direct Signaling between Platelets and Cancer Cells Induces an Epithelial-Mesenchymal-Like Transition and Promotes Metastasis. *Cancer Cell* **20,** 576–590 (2011).
69. Yu, M. *et al.* Circulating Breast Tumor Cells Exhibit Dynamic Changes in Epithelial and Mesenchymal Composition. *Science (80-.).* **339,** 580–584 (2013).
70. Aceto, N. *et al.* Circulating Tumor Cell Clusters Are Oligoclonal Precursors of Breast Cancer Metastasis. *Cell* **158,** 1110–1122 (2014).
71. del Pozo Martin, Y. *et al.* Mesenchymal Cancer Cell-Stroma Crosstalk Promotes Niche Activation, Epithelial Reversion, and Metastatic Colonization. *Cell Rep.* **13,** 2456–2469 (2015).
72. Qian, B.-Z. *et al.* FLT1 signaling in metastasis-associated macrophages activates an inflammatory signature that promotes breast cancer metastasis. *J. Exp. Med.* **212,** 1433–1448 (2015).

73. Nielsen, S. R. *et al.* Macrophage-secreted granulin supports pancreatic cancer metastasis by inducing liver fibrosis. *Nat. Cell Biol.* **18,** 549–560 (2016).
74. Plaks, V., Kong, N. & Werb, Z. The Cancer Stem Cell Niche: How Essential Is the Niche in Regulating Stemness of Tumor Cells? *Cell Stem Cell* **16,** 225–238 (2015).
75. Hanahan, D. & Coussens, L. M. Accessories to the Crime: Functions of Cells Recruited to the Tumor Microenvironment. *Cancer Cell* **21,** 309–322 (2012).
76. Sun, Y. Translational Horizons in the Tumor Microenvironment: Harnessing Breakthroughs and Targeting Cures. *Med. Res. Rev.* **35,** n/a-n/a (2015).
77. McGranahan, N. & Swanton, C. Clonal Heterogeneity and Tumor Evolution: Past, Present, and the Future. *Cell* **168,** 613–628 (2017).
78. Quail, D. F. & Joyce, J. A. Microenvironmental regulation of tumor progression and metastasis. *Nat. Med.* **19,** 1423–37 (2013).
79. Costa, A. *et al.* Fibroblast Heterogeneity and Immunosuppressive Environment in Human Breast Cancer. *Cancer Cell* **33,** 463–479.e10 (2018).
80. Bussard, K. M., Boulanger, C. A., Booth, B. W., Bruno, R. D. & Smith, G. H. Reprogramming Human Cancer Cells in the Mouse Mammary Gland. *Cancer Res.* **70,** 6336–6343 (2010).
81. Bissell, M. J. & Hines, W. C. Why don't we get more cancer? A proposed role of the microenvironment in restraining cancer progression. *Nat. Med.* **17,** 320–329 (2011).
82. Ronca, R., Van Ginderachter, J. A. & Turtoi, A. Paracrine interactions of cancer-associated fibroblasts, macrophages and endothelial cells. *Curr. Opin. Oncol.* **30,** 45–53 (2018).
83. Tang, H., Qiao, J. & Fu, Y.-X. Immunotherapy and tumor microenvironment. *Cancer Lett.* **370,** 85–90 (2016).
84. Alexander, D. B. *et al.* Normal cells control the growth of neighboring transformed cells independent of gap junctional communication and SRC activity. *Cancer Res.* **64,** 1347–58 (2004).
85. Alkasalias, T. *et al.* Inhibition of tumor cell proliferation and motility by fibroblasts is both contact and soluble factor dependent. *Proc. Natl. Acad. Sci.* **111,** 17188–17193 (2014).
86. Hirt, C. *et al.* "In vitro" 3D models of tumor-immune system interaction. *Adv. Drug Deliv. Rev.* **79–80,** 145–154 (2014).
87. Chang, H. Y. *et al.* From The Cover: Robustness, scalability, and integration of a wound-response gene expression signature in predicting breast cancer survival. *Proc. Natl. Acad. Sci.* **102,** 3738–3743 (2005).
88. Chang, H. Y. *et al.* Gene Expression Signature of Fibroblast Serum Response Predicts Human Cancer Progression: Similarities between Tumors and Wounds. *PLoS Biol.* **2,** e7 (2004).
89. Finak, G. *et al.* Stromal gene expression predicts clinical outcome in breast cancer. *Nat. Med.* **14,** 518–527 (2008).
90. Toullec, A. *et al.* Oxidative stress promotes myofibroblast differentiation and tumour spreading. *EMBO Mol. Med.* **2,** 211–230 (2010).
91. Farmer, P. *et al.* A stroma-related gene signature predicts resistance to neoadjuvant chemotherapy in breast cancer. *Nat. Med.* **15,** 68–74 (2009).
92. Bhowmick, N. a, Neilson, E. G. & Moses, H. L. Stromal fibroblasts in cancer initiation and progression. *Nature* **432,** 332–337 (2004).
93. Orimo, A. *et al.* Stromal Fibroblasts Present in Invasive Human Breast Carcinomas Promote Tumor Growth and Angiogenesis through Elevated SDF-1/CXCL12 Secretion. *Cell* **121,** 335–348 (2005).
94. Radisky, D. C. *et al.* Rac1b and reactive oxygen species mediate MMP-3-induced EMT and genomic instability. *Nature* **436,** 123–127 (2005).
95. Roswall, P. *et al.* Microenvironmental control of breast cancer subtype elicited through paracrine platelet-derived growth factor-CC signaling. *Nat. Med.* (2018).

doi:10.1038/nm.4494

96. Hale, M. D., Hayden, J. D. & Grabsch, H. I. Tumour-microenvironment interactions: role of tumour stroma and proteins produced by cancer-associated fibroblasts in chemotherapy response. *Cell. Oncol.* **36,** 95–112 (2013).
97. Dittmer, J. & Leyh, B. The impact of tumor stroma on drug response in breast cancer. *Semin. Cancer Biol.* **31,** 3–15 (2015).
98. Straussman, R. *et al.* Tumour micro-environment elicits innate resistance to RAF inhibitors through HGF secretion. *Nature* **487,** 500–504 (2012).
99. Crawford, Y. *et al.* PDGF-C Mediates the Angiogenic and Tumorigenic Properties of Fibroblasts Associated with Tumors Refractory to Anti-VEGF Treatment. *Cancer Cell* **15,** 21–34 (2009).
100. Dumont, N. *et al.* Breast Fibroblasts Modulate Early Dissemination, Tumorigenesis, and Metastasis through Alteration of Extracellular Matrix Characteristics. *Neoplasia* **15,** 249-IN7 (2013).
101. Kraman, M. *et al.* Suppression of Antitumor Immunity by Stromal Cells Expressing Fibroblast Activation Protein-. *Science (80-.).* **330,** 827–830 (2010).
102. Salmon, H. *et al.* Matrix architecture defines the preferential localization and migration of T cells into the stroma of human lung tumors. *J. Clin. Invest.* **122,** 899–910 (2012).
103. Turley, S. J., Cremasco, V. & Astarita, J. L. Immunological hallmarks of stromal cells in the tumour microenvironment. *Nat. Rev. Immunol.* **15,** 669–682 (2015).
104. Murdoch, C. Mechanisms regulating the recruitment of macrophages into hypoxic areas of tumors and other ischemic tissues. *Blood* **104,** 2224–2234 (2004).
105. Kim, J. H. *et al.* The role of myofibroblasts in upregulation of S100A8 and S100A9 and the differentiation of myeloid cells in the colorectal cancer microenvironment. *Biochem. Biophys. Res. Commun.* **423,** 60–66 (2012).
106. Lakins, M. A., Ghorani, E., Munir, H., Martins, C. P. & Shields, J. D. Cancer-associated fibroblasts induce antigen-specific deletion of CD8+ T Cells to protect tumour cells. *Nat. Commun.* **9,** 948 (2018).
107. Broderick, L. & Bankert, R. B. Membrane-Associated TGF- 1 Inhibits Human Memory T Cell Signaling in Malignant and Nonmalignant Inflammatory Microenvironments. *J. Immunol.* **177,** 3082–3088 (2006).
108. Ahmadzadeh, M. & Rosenberg, S. A. TGF- 1 Attenuates the Acquisition and Expression of Effector Function by Tumor Antigen-Specific Human Memory CD8 T Cells. *J. Immunol.* **174,** 5215–5223 (2005).
109. De Monte, L. *et al.* Intratumor T helper type 2 cell infiltrate correlates with cancer-associated fibroblast thymic stromal lymphopoietin production and reduced survival in pancreatic cancer. *J. Exp. Med.* **208,** 469–478 (2011).
110. Kalluri, R. & Zeisberg, M. Fibroblasts in cancer. *Nat. Rev. Cancer* **6,** 392–401 (2006).
111. Mink, S. R. *et al.* Cancer-Associated Fibroblasts Derived from EGFR-TKI-Resistant Tumors Reverse EGFR Pathway Inhibition by EGFR-TKIs. *Mol. Cancer Res.* **8,** 809–820 (2010).
112. Paulsson, J. *et al.* High expression of stromal PDGFRβ is associated with reduced benefit of tamoxifen in breast cancer. *J. Pathol. Clin. Res.* **3,** 38–43 (2017).
113. Öhlund, D. *et al.* Distinct populations of inflammatory fibroblasts and myofibroblasts in pancreatic cancer. *J. Exp. Med.* jem.20162024 (2017). doi:10.1084/jem.20162024
114. Aras, S. & Raza Zaidi, M. TAMeless traitors: Macrophages in cancer progression and metastasis. *Br. J. Cancer* **117,** 1583–1591 (2017).
115. Franklin, R. a. & Li, M. O. Ontogeny of Tumor-Associated Macrophages and Its Implication in Cancer Regulation. *Trends in Cancer* **2,** 20–34 (2016).
116. Komohara, Y. *et al.* Macrophage infiltration and its prognostic relevance in clear cell renal cell carcinoma. *Cancer Sci.* **102,** 1424–1431 (2011).

117. Campbell, M. J. *et al.* Proliferating macrophages associated with high grade, hormone receptor negative breast cancer and poor clinical outcome. *Breast Cancer Res. Treat.* **128,** 703–711 (2011).
118. Medrek, C., Pontén, F., Jirström, K. & Leandersson, K. The presence of tumor associated macrophages in tumor stroma as a prognostic marker for breast cancer patients. *BMC Cancer* **12,** 306 (2012).
119. Mahmoud, S. M. A. *et al.* Tumour-infiltrating macrophages and clinical outcome in breast cancer. *J. Clin. Pathol.* **65,** 159–163 (2012).
120. Ohri, C. M., Shikotra, A., Green, R. H., Waller, D. A. & Bradding, P. Macrophages within NSCLC tumour islets are predominantly of a cytotoxic M1 phenotype associated with extended survival. *Eur. Respir. J.* **33,** 118–126 (2009).
121. Dave, S. S. *et al.* Prediction of Survival in Follicular Lymphoma Based on Molecular Features of Tumor-Infiltrating Immune Cells. *N. Engl. J. Med.* **351,** 2159–2169 (2004).
122. Guo, Q. *et al.* New Mechanisms of Tumor-Associated Macrophages on Promoting Tumor Progression: Recent Research Advances and Potential Targets for Tumor Immunotherapy. *J. Immunol. Res.* **2016,** 1–12 (2016).
123. Williams, C. B., Yeh, E. S. & Soloff, A. C. Tumor-associated macrophages: unwitting accomplices in breast cancer malignancy. *npj Breast Cancer* **2,** 15025 (2016).
124. Qian, B.-Z. *et al.* CCL2 recruits inflammatory monocytes to facilitate breast-tumour metastasis. *Nature* **475,** 222–225 (2011).
125. Escribese, M. M., Casas, M. & Corbí, ángel L. Influence of low oxygen tensions on macrophage polarization. *Immunobiology* **217,** 1233–1240 (2012).
126. Colegio, O. R. *et al.* Functional polarization of tumour-associated macrophages by tumour-derived lactic acid. *Nature* **513,** 559–563 (2014).
127. Ostuni, R., Kratochvill, F., Murray, P. J. & Natoli, G. Macrophages and cancer: From mechanisms to therapeutic implications. *Trends Immunol.* **36,** 229–239 (2015).
128. Ruffell, B., Affara, N. I. & Coussens, L. M. Differential macrophage programming in the tumor microenvironment. *Trends Immunol.* **33,** 119–126 (2012).
129. Xue, J. *et al.* Transcriptome-Based Network Analysis Reveals a Spectrum Model of Human Macrophage Activation. *Immunity* **40,** 274–288 (2014).
130. Lavin, Y. *et al.* Innate Immune Landscape in Early Lung Adenocarcinoma by Paired Single-Cell Analyses. *Cell* **169,** 750–765.e17 (2017).
131. Solinas, G., Germano, G., Mantovani, A. & Allavena, P. Tumor-associated macrophages (TAM) as major players of the cancer-related inflammation. *J. Leukoc. Biol.* **86,** 1065–1073 (2009).
132. Wyckoff, J. *et al.* A Paracrine Loop between Tumor Cells and Macrophages Is Required for Tumor Cell Migration in Mammary Tumors. *Cancer Res.* **64,** 7022–7029 (2004).
133. Wyckoff, J. B. *et al.* Direct visualization of macrophage-assisted tumor cell intravasation in mammary tumors. *Cancer Res.* **67,** 2649–2656 (2007).
134. Bai, J. *et al.* Contact-dependent carcinoma aggregate dispersion by M2a macrophages via ICAM-1 and B2 integrin interactions. *Oncotarget* **6,** 25295–25307 (2015).
135. Yin, M. *et al.* Tumor-associated macrophages drive spheroid formation during early transcoelomic metastasis of ovarian cancer. *J. Clin. Invest.* **126,** 4157–4173 (2016).
136. Kitamura, T., Qian, B.-Z. & Pollard, J. W. Immune cell promotion of metastasis. *Nat. Rev. Immunol.* **15,** 73–86 (2015).
137. Qian, B. *et al.* A Distinct Macrophage Population Mediates Metastatic Breast Cancer Cell Extravasation, Establishment and Growth. *PLoS One* **4,** e6562 (2009).
138. Costa-Silva, B. *et al.* Pancreatic cancer exosomes initiate pre-metastatic niche formation in the liver. *Nat. Cell Biol.* **17,** 816–826 (2015).
139. Lin, E. Y., Nguyen, A. V., Russell, R. G. & Pollard, J. W. Colony-Stimulating Factor 1 Promotes

Progression of Mammary Tumors to Malignancy. *J. Exp. Med.* **193,** 727–740 (2001).
140. Qian, B. Z. & Pollard, J. W. Macrophage Diversity Enhances Tumor Progression and Metastasis. *Cell* **141,** 39–51 (2010).
141. Strachan, D. C. *et al.* CSF1R inhibition delays cervical and mammary tumor growth in murine models by attenuating the turnover of tumor-associated macrophages and enhancing infiltration by $CD8^+$ T cells. *Oncoimmunology* **2,** e26968 (2013).
142. Abraham, D. *et al.* Stromal cell-derived CSF-1 blockade prolongs xenograft survival of CSF-1-negative neuroblastoma. *Int. J. Cancer* **126,** 1339–1352 (2010).
143. Mok, S. *et al.* Inhibition of CSF-1 Receptor Improves the Antitumor Efficacy of Adoptive Cell Transfer Immunotherapy. *Cancer Res.* **74,** 153–161 (2014).
144. Gordon, S. R. *et al.* PD-1 expression by tumour-associated macrophages inhibits phagocytosis and tumour immunity. *Nature* **545,** 495–499 (2017).
145. Gu, L. & Mooney, D. J. Biomaterials and emerging anticancer therapeutics: engineering the microenvironment. *Nat. Rev. Cancer* **16,** 56–66 (2015).
146. Thomas, R. M., Van Dyke, T., Merlino, G. & Day, C.-P. Concepts in Cancer Modeling: A Brief History. *Cancer Res.* **76,** 5921–5925 (2016).
147. Nyga, A. *et al.* The next level of 3D tumour models: immunocompetence. *Drug Discov. Today* **21,** 1421–1428 (2016).
148. McMillin, D. W. *et al.* Tumor cell-specific bioluminescence platform to identify stroma-induced changes to anticancer drug activity. *Nat. Med.* **16,** 483–489 (2010).
149. Pampaloni, F., Reynaud, E. G. & Stelzer, E. H. K. The third dimension bridges the gap between cell culture and live tissue. *Nat. Rev. Mol. Cell Biol.* **8,** 839–845 (2007).
150. Lovitt, C. J., Shelper, T. B. & Avery, V. M. Cancer drug discovery: recent innovative approaches to tumor modeling. *Expert Opin. Drug Discov.* **11,** 885–894 (2016).
151. Weaver, V. M. *et al.* Reversion of the Malignant Phenotype of Human Breast Cells in Three-Dimensional Culture and In Vivo by Integrin Blocking Antibodies. *J. Cell Biol.* **137,** 231–245 (1997).
152. Inman, J. L. & Bissell, M. J. Apical polarity in three-dimensional culture systems: where to now? *J. Biol.* **9,** 2 (2010).
153. Benien, P. & Swami, A. 3D tumor models: history, advances and future perspectives. *Futur. Oncol.* **10,** 1311–1327 (2014).
154. Katt, M. E., Placone, A. L., Wong, A. D., Xu, Z. S. & Searson, P. C. In Vitro Tumor Models: Advantages, Disadvantages, Variables, and Selecting the Right Platform. *Front. Bioeng. Biotechnol.* **4,** 12 (2016).
155. Friedrich, J., Seidel, C., Ebner, R. & Kunz-Schughart, L. a. Spheroid-based drug screen: considerations and practical approach. *Nat. Protoc.* **4,** 309–24 (2009).
156. Levental, K. R. *et al.* Matrix Crosslinking Forces Tumor Progression by Enhancing Integrin Signaling. *Cell* **139,** 891–906 (2009).
157. Bissell, M. J., Kenny, P. A. & Radisky, D. C. Microenvironmental regulators of tissue structure and function also regulate tumor induction and progression: the role of extracellular matrix and its degrading enzymes. *Cold Spring Harb. Symp. Quant. Biol.* **70,** 343–56 (2005).
158. Xu, R. *et al.* Sustained activation of STAT5 is essential for chromatin remodeling and maintenance of mammary-specifi c function. *J. Cell Biol.* **184,** 57–66 (2009).
159. Hickman, J. a. *et al.* Three-dimensional models of cancer for pharmacology and cancer cell biology: Capturing tumor complexity in vitro/ex vivo. *Biotechnol. J.* **9,** 1115–1128 (2014).
160. Weiswald, L.-B., Bellet, D. & Dangles-Marie, V. Spherical Cancer Models in Tumor Biology. *Neoplasia* **17,** 1–15 (2015).
161. Hirschhaeuser, F. *et al.* Multicellular tumor spheroids: an underestimated tool is catching up again. *J. Biotechnol.* **148,** 3–15 (2010).

162. Chen, A. *et al.* Endothelial Cell Migration and Vascular Endothelial Growth Factor Expression Are the Result of Loss of Breast Tissue Polarity. *Cancer Res.* **69,** 6721–6729 (2009).
163. Regier, M. C., Alarid, E. T. & Beebe, D. J. Progress towards understanding heterotypic interactions in multi-culture models of breast cancer. *Integr. Biol.* **8,** 684–692 (2016).
164. Eferl, R. & Walker, J. M. *Mouse Models of Cancer*. **1267,** (Springer New York, 2015).
165. Masopust, D., Sivula, C. P. & Jameson, S. C. Of Mice, Dirty Mice, and Men: Using Mice To Understand Human Immunology. *J. Immunol.* **199,** 383–388 (2017).
166. Payne, K. J. & Crooks, G. M. Immune-Cell Lineage Commitment: Translation from Mice to Humans. *Immunity* **26,** 674–677 (2007).
167. Shay, T. *et al.* Conservation and divergence in the transcriptional programs of the human and mouse immune systems. *Proc. Natl. Acad. Sci.* **110,** 2946–2951 (2013).
168. Peyraud, F., Cousin, S. & Italiano, A. CSF-1R Inhibitor Development: Current Clinical Status. *Curr. Oncol. Rep.* **19,** 70 (2017).
169. Kim, H., Phung, Y. & Ho, M. Changes in Global Gene Expression Associated with 3D Structure of Tumors: An Ex Vivo Matrix-Free Mesothelioma Spheroid Model. *PLoS One* **7,** e39556 (2012).
170. Hauptmann, S., Zwadlo-Klarwasser, G., Jansen, M., Klosterhalfen, B. & Kirkpatrick, C. J. Macrophages and multicellular tumor spheroids in co-culture: a three-dimensional model to study tumor-host interactions. Evidence for macrophage-mediated tumor cell proliferation and migration. *Am. J. Pathol.* **143,** 1406–15 (1993).
171. Chimal-Ramírez, G. K. *et al.* MMP1, MMP9, and COX2 Expressions in Promonocytes Are Induced by Breast Cancer Cells and Correlate with Collagen Degradation, Transformation-Like Morphological Changes in MCF-10A Acini, and Tumor Aggressiveness. *Biomed Res. Int.* **2013,** 1–15 (2013).
172. Jiang, X. & Shapiro, D. J. The immune system and inflammation in breast cancer. *Mol. Cell. Endocrinol.* **382,** 673–682 (2014).
173. Coussens, L. M., Zitvogel, L. & Palucka, A. K. Neutralizing Tumor-Promoting Chronic Inflammation: A Magic Bullet? *Science (80-.).* **339,** 286–291 (2013).
174. Bianchini, G., Balko, J. M., Mayer, I. A., Sanders, M. E. & Gianni, L. Triple-negative breast cancer: challenges and opportunities of a heterogeneous disease. *Nat. Rev. Clin. Oncol.* **13,** 674–690 (2016).
175. Dunbar, C. E. Gene Therapy Comes of Age. *Science (80-.).* **359,** eaan7672 (2018).
176. Melchiorri, D. *et al.* Regulatory evaluation of Glybera in Europe — two committees, one mission. *Nat. Rev. Drug Discov.* **12,** 719–719 (2013).
177. Santiago-Ortiz, J. L. & Schaffer, D. V. Adeno-associated virus (AAV) vectors in cancer gene therapy. *J. Control. Release* **240,** 287–301 (2016).
178. Ledford, H. Cancer-fighting viruses win approval. *Nature* **526,** 622–623 (2015).
179. *Adeno-Associated Virus*. **807,** (Humana Press, 2011).
180. Luo, J. *et al.* Adeno-associated virus-mediated cancer gene therapy: Current status. *Cancer Lett.* **356,** 347–356 (2015).
181. Bainbridge, J. W. B. *et al.* Long-Term Effect of Gene Therapy on Leber's Congenital Amaurosis. *N. Engl. J. Med.* **372,** 1887–1897 (2015).
182. Kaplitt, M. G. *et al.* Safety and tolerability of gene therapy with an adeno-associated virus (AAV) borne GAD gene for Parkinson's disease: an open label, phase I trial. *Lancet* **369,** 2097–2105 (2007).
183. Kotterman, M. a & Schaffer, D. V. Engineering adeno-associated viruses for clinical gene therapy. *Nat. Rev. Genet.* **15,** 445–451 (2014).
184. Münch, R. C. *et al.* Displaying High-affinity Ligands on Adeno-associated Viral Vectors Enables Tumor Cell-specific and Safe Gene Transfer. *Mol. Ther.* **21,** 109–118 (2013).

185. Maheshri, N., Koerber, J. T., Kaspar, B. K. & Schaffer, D. V. Directed evolution of adeno-associated virus yields enhanced gene delivery vectors. *Nat. Biotechnol.* **24,** 198–204 (2006).
186. Snyder, R. O. An Overview of rAAV Vector Product Development for Gene Therapy. in (ed. Childers, M. K.) 21–37 (Springer New York, 2016). doi:10.1007/978-1-4939-3228-3_2
187. Berns, K. I. & Muzyczka, N. AAV: An Overview of Unanswered Questions. *Hum. Gene Ther.* **28,** 308–313 (2017).
188. Merten, O., Schweizer, M., Chahal, P. & Kamen, A. A. Manufacturing of viral vectors for gene therapy: part I. Upstream processing. *Pharm. Bioprocess.* **2,** 183–203 (2014).
189. Merten, O.-W. AAV vector production: state of the art developments and remaining challenges. *Cell Gene Ther. Insights* **2,** 521–551 (2016).
190. Ylä-Herttuala, S. Endgame: Glybera Finally Recommended for Approval as the First Gene Therapy Drug in the European Union. *Mol. Ther.* **20,** 1831–1832 (2012).

CHAPTER II

EVALUATION OF AAV-MEDIATED DELIVERY OF SHRNA TO TARGET BASAL-LIKE BREAST CANCER GENETIC VULNERABILITIES

This chapter was adapted from:

Pinto C, Silva G, Garrido M, Bandeira VS, Nascimentos A, Ribeiro AS, Oliveira M, Paredes J, Coroadinha AS, Peixoto C, Barbas A, Brito C, Alves PM. *Evaluation of AAV-mediated delivery of shRNA to target basal-like breast cancer genetic vulnerabilities* (submitted)

ABSTRACT

Adeno-associated viral vectors (AAV) for gene therapy applications are gaining momentum after the clinical approval of Glybera, with more therapies moving into later stages of clinical development and towards market approval, namely for cancer therapy. The development of cytotoxic vectors is often hampered by side effects arising when non-target cells are infected, and their production can be hindered by toxic effects of the transgene on the producing cell lines. In this study, we evaluated the potential of rAAV-mediated delivery of short hairpin RNAs (shRNA) to target basal-like breast cancer (BLBC) genetic vulnerabilities. Our results show that by optimizing the stoichiometry of the plasmids upon transfection and time of harvest, it is possible to increase the viral titers and quality. All obtained rAAV-shRNA vectors efficiently transduced the BLBC cell lines MDA-MB-468 and HCC1954. In MDA-MB-468, transduction with rAAV-shRNA vector targeting the *PSMA2* was associated with significant decrease in cell viability and apoptosis induction. Importantly, rAAV2-PSMA2 also induced reduced tumor growth in a BLBC mouse xenograft model, thus representing a promising therapeutic vector against this type of cancer.

TABLE OF CONTENTS

1. INTRODUCTION

Gene therapy has the opportunity to expand beyond conventional drug based therapeutics and deliver a targeted treatment through regulation of endogenous genes[1]. As our knowledge on cancer´s onset and progression evolves, tumor-specific phenotypic characteristics are uncovered that can be explored in this context, to achieve higher specificity and potency of the developed therapies[2]. Basal-like breast cancer (BLBC) patients can greatly benefit from the development of such therapies. Although this subtype represents up to 20% of worldwide breast cancer (BC) incidence, it is responsible for a disproportionate number of deaths as it often leads to relapse with distant metastasis[3]. The lack of molecular markers and deficient characterization, impaired by an heterogeneous molecular presentation, leads to lack of targeted therapies and leaves clinicians with cytotoxic chemotherapeutic drugs as the only treatment option[3,4]. Standard treatment for these patients, namely surgery, radiation and chemotherapy, often fails to completely eradicate the disease, is incapable of maintaining sustained protection, and is accompanied by serious side effects, such as cytotoxicity to non-cancerous cells[5,6]. Therefore, there is a strong unmet medical need for targeted therapies for BLBC with improved clinical efficacy, targeted effect with lower side effects, and longer patient survival times[6,7]. A lot of effort has been conducted towards the discovery of actionable molecular targets for this disease[8]. Recently, Petrocca et al conducted a genome-wide small interfering RNA (siRNA) screen to identify selective genetic vulnerabilities causing lethality in this BC subtype[9]. Although promising, these leads still face considerable challenges reaching the clinic due to ineffective delivery platforms[10].

Recombinant adeno-associated viral (rAAV) vectors have been increasingly successful as gene therapy delivery platforms and have proven to be a promising approach to treat a variety of human diseases[11–13]. The increasing number of preclinical studies and human clinical trials has demonstrated their favorable safety profile, efficacious gene delivery, and robust and persistent transgene expression *in vivo*, with manageable immune response and minor adverse effects upon injection[6,14,15]. In fact, an rAAV1-based vector for the treatment of a lipoprotein lipase deficiency became the first

commercially-approved gene therapy product for clinical applications by the European Commission[16].

rAAV vectors' potential for cancer applications has also been demonstrated in several *in vitro* cancer studies, i*n vivo* pre-clinical cancer models, and clinical trials, with a wide variety of approaches, such as the delivery of anti-angiogenesis factors (PEDF, endostatin 34, Kringle 5, Kallistatin), suicide genes (HSV-TK system and polyomavirus middle T antigen), immunostimulatory molecules (TRAIL, Interferons, Interleukins), DNA-encoded small RNA molecules for post-transcriptional regulation of oncogenes, immunogenic cell surface molecules and tumor antigens[5,6,17].

Herein we describe an rAAV-based therapeutic approach to target BLBC. Signature genetic dependencies previously identified for this BC subtype (i.e. *MCL1*, *PSMA2* and *PSMB4*)[9] were targeted using rAAV-mediated delivery of shRNA. Consequent downregulation of the target genes led to a decrease in cell viability and induced apoptosis in BLBC cell lines. Furthermore, intratumoral injections of rAAV vectors targeting *PSMA2* resulted in slowed tumor growth in a BLBC xenograft model. Moreover, our results indicate that optimization of plasmid stoichiometry upon transfection and time of harvest should be done in a transgene dependent manner, with the goal of circumventing potential cytotoxic effects of the transgene in the producer cell line and yield rAAV batches of higher quality.

2. MATERIALS AND METHODS

2.1 Cell culture

HEK293T (ATCC CRL-3216™) and HT1080 cells (ATCC® CCL121) cells were cultured in high glucose (4.5 g/L) DMEM supplemented with 10% (v/v) fetal bovine serum (FBS). The basal breast cancer cell lines HCC1954 and MDA-MB-468, kindly provided by professor Judy Lieberman (Harvard Medical Scholl, USA) were cultured in RPMI 1640 medium supplemented with 10% (v/v) FBS, 6 mM HEPES and 5 µM 2-Mercaptoethanol. Media and cell culture reagents were from Gibco Life Technologies. Cells were incubated at 37 °C in a humidified atmosphere with 5% CO_2 in air.

2.2 Construction of pAAV-shRNA plasmids

An AAV2 vector plasmid carrying a CMV-promoter driven GFP gene flanked by ITRs, and a puromycin resistance gene under the control of a hEF1 promoter outside the AAV2 expression cassette with no shRNA (pAAV-Puro) was generated based on the AAV2 vector construct pAAV-MSC-CMV-eGFP-CytbAS (kind gift from Prof. U. Michel, University Medicine Göttingen, Germany), after removal of the extra CMV promoter. To construct the pAAV2-shRNA vectors, DNA fragments containing the H1 promoter, gene specific or control scramble shRNA sequences, and the BstBI and HindIII restriction sites, at the 5´and 3´extremities, respectively, were chemically synthesized (GenScript) and cloned into the BstBI/HindIII site of pAAV-Puro inside the AAV2 expression cassette. The generated pAAV-shRNA plasmids were amplified in E. coli Stbl3 cells (Invitrogen), and their sequence integrity and orientation were confirmed by restriction analysis and sequencing. Gene specific shRNA sequences were obtained from the RNAi consortium database (http://www.broadinstitute.org/rnai/public/). The scramble control shRNA sequences, not targeting any known human or mouse genes, were from Sigma. The shRNA catalog numbers are: PLK1shRNA: TRCN0000006247; MCL1shRNA: TRCN0000196390; PSMA2shRNA: TRCN0000003879; PSMB4shRNA: TRCN0000003914; Ctrl1shRNA: SHC202; and Ctrl2shRNA: SHC016.

2.3 Production, purification and titer determination of rAAV-shRNA vectors

rAAV-shRNA vectors were produced in HEK293T cells by 2- or 3-plasmid transfection system using 5 μg DNA/1x10^6 cells, with linear polyethylenimine (PEI; Polysciences) or $CaPO_4$ as transfection reagents. In the 2-plasmid system HEK293T cells (seeded at 4-5x10^4 cell/cm^2 20-24h before) were co-transfected at 70-80% confluency with individual pAAV-shRNA plasmids, generated above, plus the pDG plasmid[18], encoding the *rep* and *cap* genes and the adenovirus encoding products essential for AAV vector production, using different plasmid ratios as indicated below. 3-plasmid transfection

was performed with plasmids: pAAV-shRNA, pAAV-Helper - encoding adenovirus gene products required for the production of infective AAV particles, and pAAV-RC - encoding the rep and cap genes (necessary trans-acting elements for replication and packaging of the viral genome) (all from Stratagene/Agilent), at a plasmid molar ratio of 1:1:1. All plasmids, except pAAV-shRNA, were amplified in E. coli DH5α cells (Invitrogen). Plasmid DNA was purified with the EndoFree plasmid kit from Qiagen, as per supplier´s instructions. Transfections with the $CaPO_4$ method were performed using the Calcium Phosphate Transfection Kit from Sigma (CAPHOS) as per kit´s instructions. Transfections of HEK293T cells with PEI were performed as per standard protocols using optimized DNA:PEI ratio of 1:1.8 (μg), as previously described[19]. 48-72h post transfection, cells were lysed with 0.1% Triton-X100 (Sigma), releasing the intracellular vectors into the supernatant. Media with lysed cells was collected and incubated with 30 unit/ml Benzonase® nuclease (Merck Millipore) and sterile 2 mM $MgCl_2$ (Sigma) for 1h at 37C, for removal of host cell and unpacked DNA. The solution was clarified by centrifugation (4000*xg*/30min/4^0C) and the vector-containing supernatant (primary viral stock) was filtered through 0.45-μm pore size filters (Merck Millipore). Purification of the different rAAV-shRNA vectors was performed by affinity chromatography using the AVB Sepharose High Performance resin (GE Healthcare), according to manufacturer's instructions. Purity was monitored by SDS-PAGE followed by InstantBlue™ and endotoxin content assessed with the chromogenic LAL test kit (Endosafe-PTS). All vectors used in this study passed the endotoxin test.

Viral productivities were assessed in primary viral stocks and purified vectors. Viral particle (vp) titration was performed using the AAV titration kit ELISA (PROGEN Biotechnik GmbH), according to manufacturer's instructions. For rAAV-shRNA vector genome (vg) quantification, viral DNA was extracted and purified with the high pure viral nucleic acid kit (Roche). Vg titer was quantified by real-time PCR quantification (qPCR) of encapsidated CMV promoter DNA fragment driving the expression of the GFP transgene, in at least 3 different serial dilutions of extracted viral DNA stocks, against a linearized pAAV-Ctrl1shRNA plasmid DNA standard curve. Eight serial dilutions of the plasmid standard (containing 10^8, 10^7, 10^6, 10^5, 10^4, 10^3, 10^2, and 10^1 copies of plasmid

DNA) were used to generate a standard curve for absolute quantification of vector samples. All reactions were performed in triplicate using CMV specific primers (Forward: 5´-GCGCCTCTTATACCCACGTAG-3' and reverse: 5´-TAACACCGCCCCGGTTT-3´) and the SYBR Green I Master mix (Roche). Analysis of qPCR results was carried out with LC480 software. Infectious particle (ip) titration was performed in HT1080 fibrosarcoma cells as previously described[19]. Briefly, cells were transduced at 50% confluency with serial dilutions of the viral stocks for 2h. After 48h incubation in complete media cells were harvested and the percentage of GFP^+/infected cells was quantified by flow cytometry (Cyflow Space, Partec).

2.4 pAAV-shRNA plasmid transfection

HEK293T cells at 60-70% confluency were transiently transfected with individual pAAV-shRNA constructs at 5 µg DNA per $1x10^6$ cells using PEI as transfection reagent, at a DNA:PEI ratio of 1:2 (µg). After 8h incubation, medium was replaced, and cells further cultured. After 24-48h, cells were imaged by fluorescence microscopy for the expression of GFP transgene and harvested for RNA extraction for gene expression studies and GFP^+ cell quantification by flow cytometry (Cyflow Space, Partec).

2.5 rAAV-shRNA vector transduction and Fluorescence activated cell sorting

HCC1954 and MDA-MB-468 cells at 60-70% confluency were transduced with individual rAAV2-shRNA vectors at a multiplicity of infection (MOI) of $4x10^4$ vg/cell in 2% serum containing media. After 8h incubation, medium was replaced by complete media and transduced cells were FACS sorted for GFP expression 24h and 48h thereafter. Following FACS isolation, cells were immediately used for RNA extraction for gene expression studies or further cultured for viability and apoptosis assays. Sorting was conducted at the Instituto Gulbenkian de Ciência Flow Cytometric facility in Moflo (Beckman Coulter) and FACSAria (Becton Dickinson) cytometers.

2.6 Gene expression analysis

Total RNA from cells was extracted with Qiagen RNeasy Mini Kit as per manufacturer´s instructions with DNAse digestion. cDNA was synthesized, from equal amounts of RNA, by reverse transcription using the Advantage RT-for-PCR kit (Clontech Laboratories, Mountain View, CA), or the High Fidelity cDNA Synthesis Kit (Roche), as per the manufacturer's Instructions. Gene expression was quantified on Roche LightCycler 480 (LC480) using gene specific primers and the SYBR Green I Master mix (Roche). All experiments were performed in triplicate and the melting-curve data were collected to check product specificity. mRNA transcripts were normalized to both hypoxanthine phosphoribosyltransferase 1 (*HPRT1*) and ribosomal protein L22 (RPL22) mRNA levels in the same sample, and the results were calculated as fold change relative to control cells using the advanced relative quantification method from the LC480 software. The primers used were (forward and reverse, respectively): HPRT1: 5´-CCTGGCGTCGTGATTAGTGAT-3´ and 5´- AGACGTTCAGTCCTGTCCATAA-3'; MCL1: 5´-TGCTTCGGAAACTGGACATCA-3´ and 5´- TAGCCACAAAGGCACCAAAAG-3´; PLK1: 5´-AAAGAGATCCCGGAGGTCCTA-3´ and 5´- GGCTGCGGTGAATGGATATTTC-3´; PSMA2: 5´-GAGCGCGGGTACAGCTTTT-3´ and 5´- ACCACACCATTTGCAGCTTTA-3; PSMB4: 5´-GAAGCGTTTTTGGGGTCGC-3´ and 5´-GAGTGGACGGAATGCGGTA-3; RPL22: 5´-CACGAAGGAGGAGTGACTGG-3´ and 5´-TGTGGCACACCACTGACATT-3´.

2.7 Cell viability and apoptosis

To investigate the effects of rAAV-shRNA vectors on cell viability, sorted-transduced cells were plated in 96-well plates at different cell densities and incubated for 48-120h. After each 24h incubation period, cell viability was assessed using the PrestoBlue™ cell viability reagent (Life Technologies), according to the manufacturer's instructions. For apoptosis assays transduced cells were plated in 24-well plates, at different cell densities, and the number of apoptotic cells was determined by flow cytometry using the FLICA apoptosis kit (Immunochemistry Technologies) as per the manufacturer's instructions.

2.8 Mouse xenografts and vector delivery

All animal experiments were carried out in accordance with the Guidelines for the Care and Use of Laboratory Animals, directive 86/609/EEC. Human BLBC model was established in N:NIH(s)II:nu/nu nude mice with MDA-MB-468 cells. Briefly, $2x10^6$ MDA-MB-468 cells were injected into the mammary fat pad of Female N:NIH(s)II:nu/nu nude mice. Three to four mice were kept per cage, with food and water *ad libitum,* and examined daily. Mice weight and tumor volume were measured twice a week until tumors reached an average volume of 100-150 mm^3. Mice were then distributed into different experimental groups, with equal average tumor volume, for treatment initiation. rAAV2-shRNA intratumoral injections were performed twice a week, for 3-4 weeks. Tumors were measured in two perpendicular dimensions and the volume was estimated by the formula [volume = (length) x $(width)^2/2$] for approximating the volume of an ellipsoid.

3. RESULTS

3.1 Development of an rAAV vector expressing eGFP and an shRNA targeting BLBC genetic vulnerabilities

3.1.1 Design and validation of AAV-shRNA plasmids

Building on the overrepresentation of proteasome machinery leads identified as BLBC intrinsic vulnerabilities in a previous study[9], two proteasome subunits were chosen as potential targets – proteasome subunit alpha 2 (PSMA2) and proteasome subunit beta 4 (PSMB4). Another persistent susceptibility identified was MCL1, BCL2 family apoptosis regulator (MCL1), an anti-apoptotic protein that was the third target chosen for the present study. shRNA sequences targeting these genes (MCL1sh, PSMA2sh and PSMB4sh) were obtained from a publicly available database (https://www.broadinstitute.org/rnai/trc). An shRNA targeting polo like kinase 1 (PLK1), a Ser/Thr protein kinase highly expressed during mitosis[20], was also obtained. Inhibition of this protein has been previously shown to decrease proliferation and induce apoptosis in cancer cells[21,22], thus PLK1sh was used as positive control. Additionally, two scramble shRNA (Ctrl1sh and Ctrl2sh), with no known targets in

human or mouse cells, served as negative controls. All shRNA sequences were cloned into a pAAV expression vector, co-expressing an eGFP reporter gene to facilitate the monitoring of target cell transduction. Validation of shRNA knockdown efficiency of the different plasmid constructs was assessed by transient transfection of HEK293T cells. Target gene knockdown efficiencies ranging from 40 to 90% were obtained, depending on the shRNA (Fig. 2.1), showing that the designed sequences caused potent and specific target gene silencing.

3.1.2 Platform implementation for endotoxin-free rAAV-shRNA vector production

Production processes based on transient transfection of HEK293T cells constitute a versatile platform, that enables a rapid performance screen of multiple rAAV vectors for the most promising lead[14,23,24]. Therefore, for production of rAAV-shRNA vectors, 2 and 3-plasmid transfection using $CaPO_4$ or PEI as transfection agent, were tested.

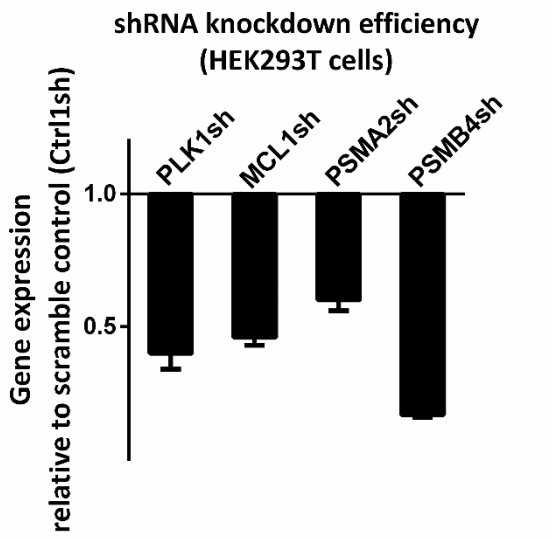

Figure 2.1: Validation of AAV-shRNA plasmids for downregulation of BLBC genetic vulnerabilities. qRT-PCR analysis of *PLK1*, *MCL1*, *PSMA2*, *PSMB4* gene expression 24h post-transfection of HEK293T cells with the different plasmid constructs. mRNA levels were normalized against the housekeeping *RPL22* mRNA levels within the same sample and are shown as fold change relative to the respective levels in control cells transfected with scramble negative control Ctrl1sh plasmid.

Initial assessment of vector productivity was conducted using rAAV-Ctrl1sh to circumvent effects arising from target gene knockdown on the production cell line (HEK293T), which could mask the results. As observed in Fig. 2.2 – A, there were no significant differences in the productivity (vg/cell) obtained with the two transfection reagents tested. While low cost and high transfection rates can make $CaPO_4$ the obvious choice for small scale productions, the similar yields obtained in these preparations led us to pursue with PEI transfection, for easier scalability and more consistent results[24]. Regarding the transfection systems, as observed in Fig. 2.2 – B, 2-plasmid transfection system delivered significantly higher production yields. On average, the viral vector titer, as per vg/cell, was up to 5-fold higher with the 2-plasmid system relative to the 3-plasmid.

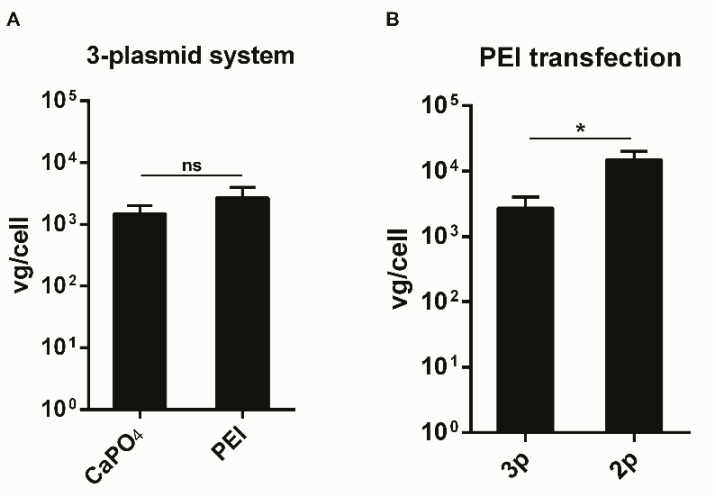

Figure 2.2: Platform implementation for rAAV-shRNA vector production. Evaluation of rAAV vector productivity following HEK293T cell transfection using **A)** different transfection agents (CaPO4 vs. PEI) and **B)** different transfection conditions (2- vs. 3-plasmid system). *, p <0.05, statistical significance was determined using two-tailed Student´s t-test.

Quality control of each AAV vector preparation in terms of total viral particles, packaged viral genomes and infectious particles is critical before potency assays are conducted, since different rAAV variants produced potentially have different ratios of the referred parameters. Standard upstream methods for rAAV vector production combine the

plasmid carrying the transgene (pAAV) and the helper/packaging plasmid (pDG) in a 1:1 equimolar ratio, and set time of harvest (TOH) at 72 hours post transfection (hpt). As observed in Table 2.1, this combination led to a high vp/vg ratio.

Table 2.1: Optimization of plasmid ratio and harvesting time of rAAV-shRNA vectors.

Harvesting time	pDG:pAAVshRNA	vg/cell	ip/cell	vp/vg
48h post TF	1:1	1.3E+04	7.3E+01	94
	1:3	2.9E+04	9.9E+01	29
	1:9	2.1E+04	6.0E+01	26
72h post TF	1:1	1.2E+04	5.2E+01	130
	1:3	1.4E+04	8.3E+01	105
	1:9	9.1E+03	6.0E+01	87

In order to decrease this ratio and, consequently, decrease empty capsids produced, different combinations of the referred parameters were tested. Table 1 shows that decreasing time of harvest to 48hpt consistently decreased vp/vg ratio. Also, increasing the proportion of pAAV in the transfection mix further decreased empty capsid production. The final optimized protocol was set at pDG:pAAV = 1:3 and toh = 48hpt for the higher ip yield.

Six rAAV-shRNA vectors, two encoding control scramble shRNA (rAAV-Ctrl1sh, rAAV-Ctrl2sh) and four gene target shRNA (rAAV-PK1sh, rAAV-MCL1sh, rAAV-PSMA2sh, rAAV-PSMB4sh) were produced and purified by affinity chromatography. SDS-PAGE followed by InstantBlue™ staining revealed high purity levels for all batches (Fig. 2.3).

The titers obtained after purification (10^{13} vp/ml; 0.4-1 x 10^{12} vg/ml; 10^{10} ip/ml – Table 2) are within reported ranges[15,25]. Batch quality, in terms of vp/vg/ip, was maintained within a small range, suggesting that the optimized protocol overcome possible side effects arising from RNAi machinery activation in HEK293T cells.

Nevertheless, rAAV-shRNA targeting genetic vulnerabilities showed a tendency to have higher vp/vg ratios.

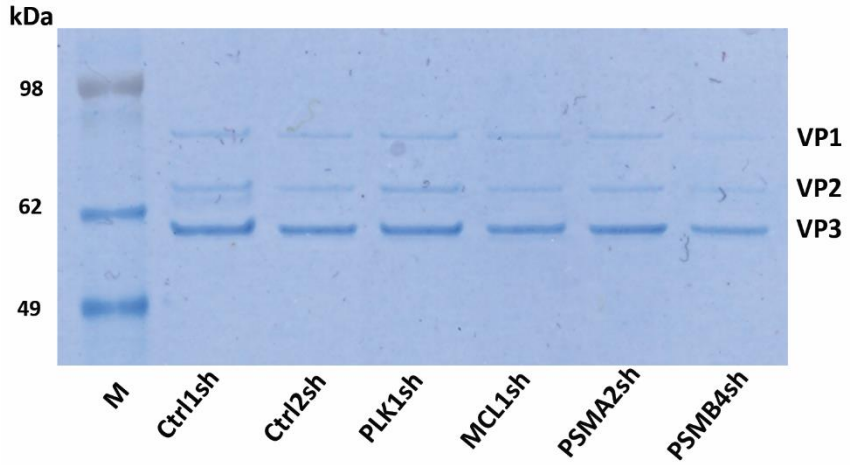

Figure 2.3: Purified rAAV-shRNA vector characterization. Purification of different rAAV-shRNA vectors was performed by affinity chromatography using the AVB Sepharose high performance resin. Six rAAV-shRNA vectors (two negative scramble controls, one positive control, and three rAAV-shRNA vectors targeting three different BLBC dependency genes) were obtained. Purity of rAAV-shRNA vectors was monitored by SDS-PAGE followed by Instant Blue staining. M: protein standard; VP1, VP2, VP3: AAV structural proteins.

Table 2.2: Purified rAAV-shRNA vector yields.

rAAV-shRNA		vp/mL	vg/mL	ip/mL
scramble control	Ctrl1sh	1.3E+13	1.1E+12	2.1E+10
	Ctrl2sh	4.0E+13	9.3E+11	3.4E+10
positive control	PLK1sh	2.7E+13	3.6E+11	2.0E+10
BLBC genetic vulnerabilities	MCL1sh	3.3E+13	4.3E+11	1.7E+10
	PSMA2sh	4.3E+13	1.8E+12	4.3E+10
	PSMB4sh	3.6E+13	4.7E+11	1.6E+10

3.2 *PSMA2* downregulation decreases cell viability and induces apoptosis in BLBC cell lines

3.2.1 rAAV-shRNA target gene knockdown efficiency

rAAV-shRNA vector transduction efficiency was assessed in two BLBC cell lines – HCC1954, a poorly differentiated epithelial cell line derived from a ductal carcinoma with no lymph node invasion; and MDA-MB-468, a cell line with epithelial morphology derived from a metastatic site. All vectors developed had comparable levels of transduction efficiency for each of the cell lines – around 60% for MDA-MB-468 and approximately 80% for HCC1954 (Fig. 2.4).

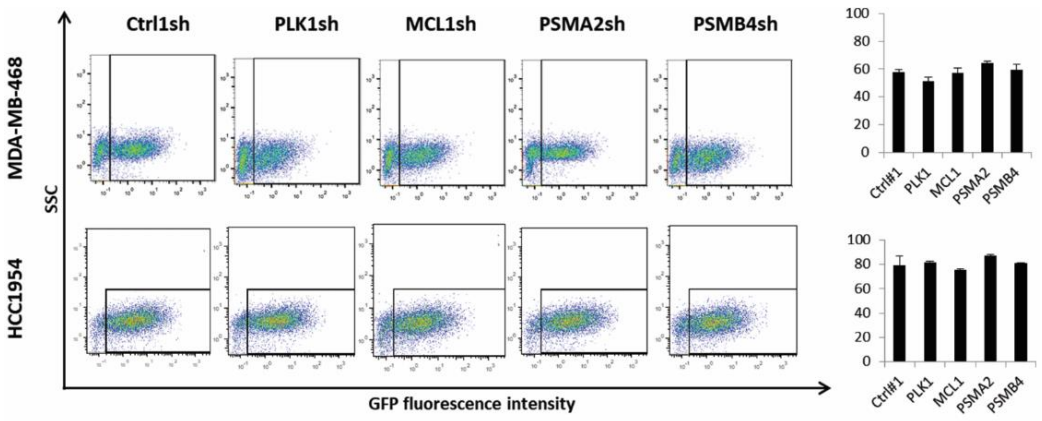

Figure 2.4: Transduction efficiency of rAAV-shRNA viral vectors in BLBC cell lines. Exponentially growing MDA-MB-468 and HCC1954 cells were transduced with the indicated viral vectors (4.6E+4 vg/cell each). rAAV vector transduction efficiency was monitored 48h post transduction by flow cytometry detection of eGFP. Plots show representative data obtained for each cell line. Graphics present percentage of transduced cells (mean ± SD).

Target gene knockdown after rAAV-mediated delivery of shRNA to HCC1954 and MDA-MB-468 cell lines was also assessed. rAAV-PSMA2sh showed a consistent downregulation of the target gene in both cell lines, of around 80% knockdown efficiency (Fig. 2.5). However, the other rAAV-shRNA vectors assessed showed either no detectable gene knockdown (rAAV-MCL1sh), or levels that did not surpass 50% knockdown efficiency (rAAV-PLK1sh, rAAV-PSMB4sh). These results significantly differ

from the levels obtained after HEK293T transient transfection, likely reflecting differences in the shRNA delivery system and target cell. Nevertheless, since the level of gene knockdown that translates into an observable phenotype is likely to depend on the gene of interest and on the expected outcome, it is difficult to predict if the knockdown efficiency observed will have a functional effect.

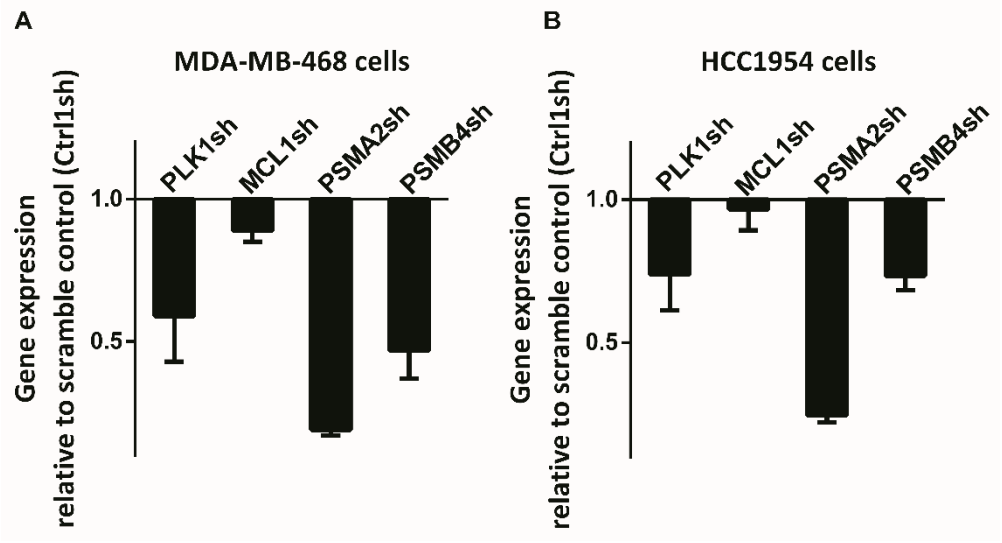

Figure 2.5: Target gene knockdown efficiency of rAAV-shRNA vectors in BLBC cell lines. Exponentially growing **A)** MDA-MB-468 and **B)** HCC1954 cells were transduced with the indicated viral vectors (4.6E+4 vg/cell each). Twenty-four or forty-eight hours post transduction cells were sorted and processed. Total RNA was extracted and the mRNA levels of PLK1, MCL1, PSMA2 and PSMB4 were determined by qRT-PCR. mRNA levels were normalized against housekeeping HPRT1 and RPL22 genes within the same sample and are shown as fold change relative to the respective levels in cells transduced with rAAV-Ctrl1sh vector (mean ± SD) of three independent experiments.

3.2.2 *In vitro* biological activity

To evaluate whether downregulation of the target genes has an impact in BLBC tumorigenic potential, the effects of their knockdown were evaluated in terms of impact on cell viability and apoptosis induction in HCC1954 and MDA-MB-468 cell lines. In MDA-MB-468, a generalized decrease in viability of around 30% was observed after

rAAV-mediated delivery of PLK1sh, PSMA2sh and PSMB4sh, when compared to cells transduced with scramble control (Fig. 2.6 – A).

These results indicate that even a moderate level of gene knockdown may deliver the desired effect. Therefore, further optimization of the shRNA sequences for the genetic

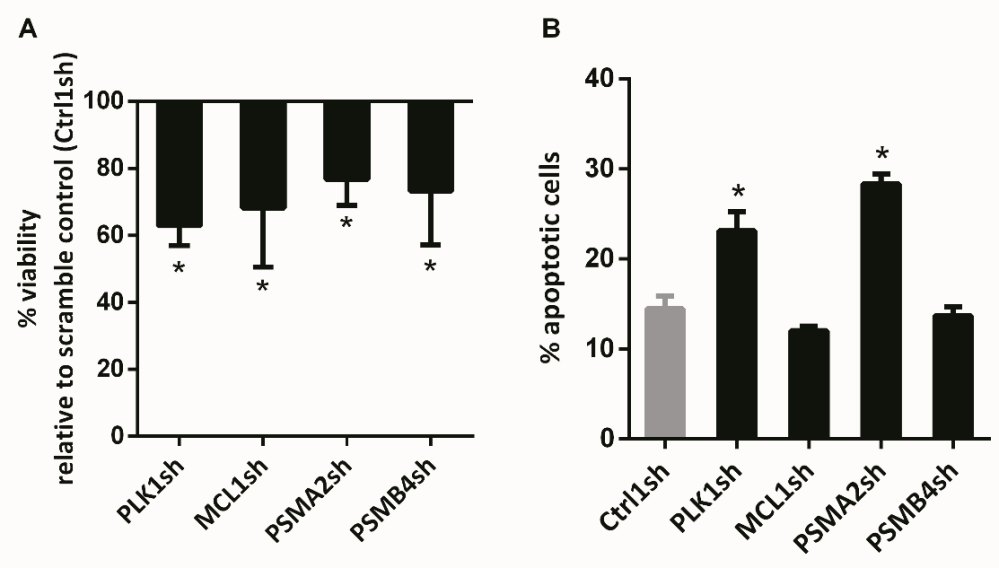

Figure 2.6: Functional effects of rAAV-shRNA vectors in BLBC cell lines. Exponentially growing MDA-MB-468 cells were transduced with the indicated viral vectors (4.6E+4 vg/cell each). Twenty-four and forty-eight hours thereafter, transduced cells were sorted and further cultured. **A)** Cell viability was measured using Presto Blue fluorometric assay at different culture time points. Cellular viability was calculated as a percentage relative to cells transduced with rAAV-Ctrl1sh vector. Shown is mean percent viability of transduced cells at 72h post-transduction ± SD from 3 independent experiments. **B)** Sorted cells were seeded, and apoptosis determined by FLICA apoptosis kit by flow cytometry. The graphics show average cell apoptosis (± SD) of 3 independent experiments, at day 5 post-transduction. *, $p < 0.05$ vs. values in cells transduced with scramble control (Ctrl1sh). Statistical significance was determined using the two-tailed Student´s t-test.

vulnerabilities here exploited could be warranted, in an attempt to increase gene knockdown to potentiate the functional effect. In terms of apoptosis induction in these cells, a statistically significant increase was achieved with rAAV-PSMA2sh, with up to 2-fold increase in the percentage of apoptotic cells compared with the scramble control

(Fig. 2.6 – B). This is in line with the displayed knockdown efficiency of the referred vector. In HCC1954 cells, significant decrease of cell viability was observed only for rAAV-PLK1sh viral vector, and there was no significant effect on apoptosis induction by any of the viral vectors tested in these cells (data not shown). The different biologic activities of the viral vectors between MDA-MB-468 and HCC1954 might be due to their different molecular signatures and oncogenic status[26].

3.3 Effect of rAAV-PSMA2sh intratumoral injections BLBC mouse xenografts

To evaluate whether the predicted genetic vulnerabilities can be harnessed for BC therapy using the developed technology, we assessed whether *PSMA2* knockdown could suppress tumor growth *in vivo* using BLBC mouse xenografts. When tumors were circa 100 mm^3, mice were treated with rAAV-PSMA2sh, rAAV-PLK1sh, rAAV-Ctrl1sh or PBS, using two vector dosages, by intratumoral injections. Tumor progression was monitored every 3 days by measuring the tumor volume in each condition.

As an aggressive tumor model, growth of tumor mass was rapid, especially for control groups treated with PBS or with the scramble controls, in both vector dosages tested (Fig. 2.7).

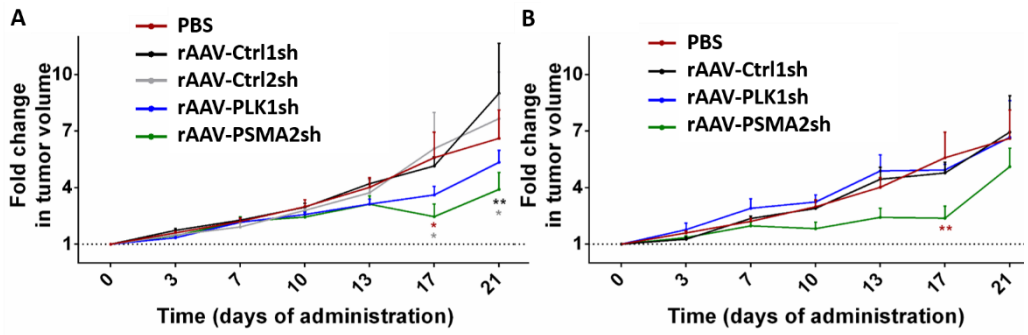

Figure 2.7: Effect of rAAV-shRNA vectors on tumor growth rate of BLBC xenografts. A) and **B)** Fold change in tumor volume progression in mice injected with $2x10^9$ or $2x10^8$ vg/tumor/injection, respectively. Data are mean ± SEM. The statistical difference between the groups was determined by Two-way ANOVA using the Graphpad 6 (Prism®) software (**p<0.01, *p<0.05).

However, mice treated with rAAV-PSMA2 showed a consistent reduction in tumor growth over time, apparent after day 13 of treatment (Fig. 2.7). Interestingly, for rAAV-PLK1sh, a reduction in tumor growth is only apparent for the highest dose, possibly reflecting the lower gene downregulation achieved with this construct and consequent lower impact on cell viability.

No significant differences were observed in the gain or loss of mice weight. Moreover, no major macroscopic alterations were observed in the liver of mice treated with either vector, suggesting that the rAAV2-shRNA viral injections did not prompt significant side-effects nor hepatotoxicity.

The impact of rAAV-shRNA intratumoral injections on tumor growth of BLBC mouse xenografts was analyzed independently for a separate group of mice. These mice suffered from a bacterial infection and had to be subjected to antibiotic treatment over the course of the experiment. Here, both rAAV-PSMA2 and scramble control led to a persistent decrease in tumor growth over time (Fig. 2.8).

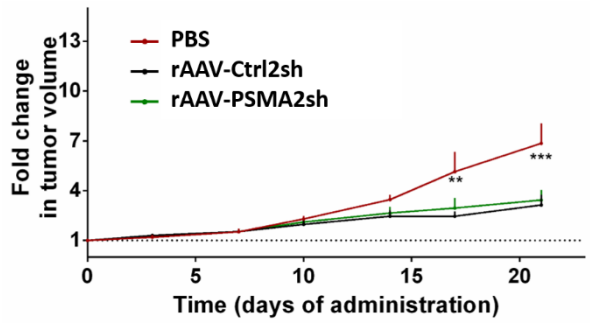

Figure 2.8: Effect of rAAV-shRNA vectors on tumor growth rate of BLBC xenografts. Fold change in tumor volume of mice injected with $2x10^9$ VG/tumor/injection. Data are mean ± SEM. The statistical difference between the groups was determined by Two-way ANOVA using the GraphPad™ 6 (Prism®) software (***p<0.001, **p<0.01).

Previous studies had already reported that some of the antibiotics commonly used in cell culture can significantly alter gene expression of human liver[27] and keratinocyte cell lines[28]. Others have even proposed the use of antibiotics for anticancer therapy, including breast cancer[29]. Therefore, the antibiotic treatment appears to be inducing

slower tumor growth over time and, consequently, affecting tumor's response to the treatment in the model used.

Previous reports showed that different BLBC cell lines underwent caspase-dependent apoptosis after infection with AAV2. This was correlated with differential expression of non-structural proteins in these cell lines, and was concomitant with increased expression of proliferation markers c-Myc and Ki-67[30]. Since we are not working with wtAAV2, the rAAV2 vectors used do not express non-structural proteins, therefore a different mechanism is responsible for this effect. Additionally, no differences were found in the expression of proliferation (Fig. 2.9 – A) or apoptosis (Fig. 2.9 – B) markers between the different rAAV2-shRNA viral vectors tested. The mechanisms at play here could possibly be a result of a synergistic effect of the antibiotics and unspecific toxicity related with the rAAV capsid, which was unaltered between all rAAV variants produced.

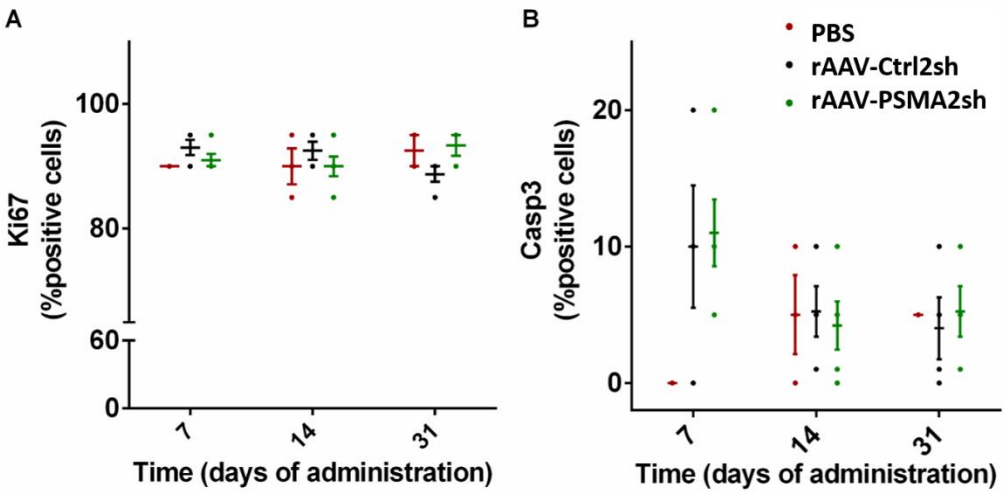

Figure 2.9: Evaluation of BLBC xenografts proliferation and apoptotic indexes over the course of the treatment. Immunohistochemical analysis of tumor samples derived from BLBC xenografts after treatment at the referred time points. Data are mean ± SEM.

4. DISCUSSION

This study evaluates the potential of rAAV-mediated shRNA delivery for the downregulation of genes necessary for the survival of BLBC cells. Our results indicate that standard upstream methods for rAAV production, based on transient transfection

of HEK293T cells, lead to high empty capsid titer in the final formulation of rAAV vectors encoding shRNA constructs. We showed that by increasing the transgene/packaging plasmid ratio in the transfection mix, which likely reduces the probability of empty capsid formation, the vp/vg ratio was improved and ip titers were slightly increased. Additionally, the combination of the optimal ratio with a decrease in the time of harvest to 48hpt, further lowered empty viral vector titers. A lower vp/vg ratio is instrumental for the successful employment of gene therapy approaches as empty capsids will decrease therapy potency and increase immune responses to capsid proteins.

The success of anticancer therapeutics using the referred approach, or even the correct interrogation as to possible clinical utility, is dependent on the development of suitable delivery systems for safe and efficient introduction of shRNA molecules into tumor cells. AAV was shown to be a viable option, as rAAV vectors are among the most promising gene therapy products developed to date. After numerous successful applications in the treatment of monogenic diseases by gene replacement[31–33], AAV arsenal has been broadened to comprise several anti-cancer therapies[5] and different clinical modalities that include RNAi and genome engineering strategies such as CRISPR/Cas9[34]. The low transgene loading capacity, often impairing rAAV-mediated gene therapy, is not an issue with these approaches, and makes such small DNA-encoded RNA molecules ideal transgenes for these vectors.

Also pivotal for successful therapy is maximizing vector production while maintaining batch consistency. However, reaching high titers during upstream processing entails high expression of the transgene in producer cells. While few concerns arise when dealing with inert gene products, that generally set the gold standard for vector titer production, the biological activity of cytotoxic transgenes for cancer therapy on producer cell lines may impact its protein synthesis capacity, metabolism and viability, or impact vector assembly itself[35]. Concerning shRNA applications, the activation of the RNAi machinery in HEK293T cells during rAAV production, combined with the extra burden of producing heterologous proteins, decreased cell viability over time (which was lower at 72hpt – data not shown), and impaired the quality of vector preparations. Our findings add to a growing body of literature on strategies to circumvent such side

effects. These include the addition of extra proteins and extensive genetic manipulation of the transgene[35], addition of aptamers[36], the inhibition of transgene expression on producer cells via siRNA or by activation of toxic genes only through the excision of spacer DNA by Cre-recombinase delivered via a second vector[37]. The simpler strategy applied here is flexible enough to allow transgene-dependent optimization if required, while reaching yields comparable to current rAAV production platforms[23,25].

To assess the potential of this strategy to be used as a BLBC therapeutic approach, we transduced BLBC cell lines with rAAV vectors expressing shRNA against previously identified genetic vulnerabilities of this BC subtype. rAAV-PSMA2 transduction caused a specific and potent decrease in *PSMA2* expression in both cell lines tested, as compared to cells transduced with rAAV carrying a scramble shRNA. The reduced expression of *PSMA2* resulted in a decrease of viability and increased apoptosis in MDA-MB-468 cells. Furthermore, rAAV2-PSMA2 intratumoral injections in BLBC mouse xenografts led to a consistent decrease in tumor growth over time, when compared to PBS or scramble controls. These results are consistent with Petrocca et al, which indicated that proteins from the proteasome machinery are fundamental for BLBC cell viability[9], and suggest that this could be a promising therapeutic vector against this type of cancer.

Although previously conducted clinical trials have led to regulatory approval of proteasome inhibitors for the treatment of various diseases, including multiple myeloma and mantle-cell lymphoma, acquired resistance mechanisms commonly arise and undermine effectiveness of the therapy[38]. Also, preclinical efficacy of these inhibitors for solid tumors could not be translated into the clinic, indicating the importance for development of suitable delivery platforms, as even the most potent therapeutic can fail in the clinic due to inefficient delivery[38].

Therapeutic posttranscriptional gene silencing via shRNA can target each gene's mRNA, as well as the considered undruggable genome[10]. In contrast to proteasome inhibitors, this approach offers the possibility to evolve in a sequence specific manner, which could overcome resistance mechanisms arising from genetic mutations. Also, it possesses superior advantages over other strategies with proven clinical efficacy,

including small-molecule inhibitors, such as imatinib for the treatment of chronic myeloid leukemia[39], and monoclonal antibodies, such as Trastuzumab for HER2-positive early breast cancer[40]. Small-molecule inhibitors have low degree of specificity when it comes to target modulation, which can lead to adverse side effects, and often do not restrict the entire function of a protein, leading to inefficient anti-oncogenic effects[41–44]. On the other hand, monoclonal antibodies are restricted to membrane or circulating proteins[42].

Taken together, this study showed evidence that further optimization of standard upstream rAAV production platforms, based on transient transfection of HEK293T cells, has the potential to overcome transgene cytotoxicity in vector-producing cells. Moreover, our results provide proof-of-concept that rAAV-mediated delivery of shRNA targeting BLBC dependency genes can be a promising approach for the treatment of this disease. The strategy here developed represents an improvement on traditional employment of suicide gene therapy for cancer. Classical suicide gene approaches will kill cells indiscriminately and rely solely on targeted delivery for specificity. Directing therapy to cancer specific dependency genes will confer a higher degree of specificity and safety to the treatment. Nevertheless, it still maintains the possibility to be combined with capsid engineering approaches for an additional layer of specificity[45,46]. This strategy might also be suitable for treatment of other malignancies. The shRNA can be customized to any tumor dependency and tailored to different subtypes or different tumors. Also, a combination of rAAV batches encoding different transgenes can be used to decrease the emergence of tumor resistance.

Finally, given the indication for therapeutic potential of these targets, evaluation of clinical efficacy in more relevant models of tumorigenesis should be warranted. Although a modest decrease in tumor progression was observed in BLBC mouse xenograft models, these mice are immunocompromised and thus do not portray the immunogenicity of the therapy developed. It is now established that several anticancer therapeutics that induce apoptosis in tumor cells can trigger an antigen-specific immune response[47]. This, in turn, reactivates the immune system against tumor cells, enhancing therapeutic response. Consequently, the assessment of anticancer drugs is

now shifting towards the use of immunocompetent mice for proper evaluation of the therapeutic outcome[47]. With the development of *in vitro* human models that incorporate immune cells, testing promising leads in a human setting may also be possible[48].

5. AUTHOR CONTRIBUTION & ACKNOWLEDGEMENTS

The author participated in the experimental setup and design, performed part of the experiments, analyzed the data and wrote the manuscript. The author acknowledges Dr Judy Lieberman for scientific support. The work was supported by FCT grant PTDC/BBB-BIO/1240/2012 and PhD fellowship PD/BD/52202/2013 to C. Pinto. Also, iNOVA4Health unit "iNOVA4Health Research Unit (LISBOA-01-0145-FEDER-007344), which is co-funded by Fundação para a Ciência e Tecnologia / Ministério da Ciência e do Ensino Superior, through national funds, and by FEDER under the PT2020 Partnership Agreement, is acknowledged.

6. REFERENCES

1. Naldini, L. Gene therapy returns to centre stage. *Nature* **526,** 351–360 (2015).
2. Miest, T. S. & Cattaneo, R. New viruses for cancer therapy: meeting clinical needs. *Nat. Rev. Microbiol.* **12,** 23–34 (2013).
3. Schneider, B. P. *et al.* Triple-negative breast cancer: Risk factors to potential targets. *Clin. Cancer Res.* **14,** 8010–8018 (2008).
4. Caldas-lopes, E. *et al.* Hsp90 inhibitor PU-H71, a multimodal inhibitor of malignancy, induces complete responses in triple-negative breast cancer models. *PNAS* **106,** 8368–8373 (2009).
5. Luo, J. *et al.* Adeno-associated virus-mediated cancer gene therapy: Current status. *Cancer Lett.* **356,** 347–356 (2015).
6. Santiago-Ortiz, J. L. & Schaffer, D. V. Adeno-associated virus (AAV) vectors in cancer gene therapy. *J. Control. Release* **240,** 287–301 (2016).
7. Carey, L., Winer, E., Viale, G., Cameron, D. & Gianni, L. Triple-negative breast cancer: disease entity or title of convenience? *Nat. Rev. Clin. Oncol.* **7,** 683–92 (2010).
8. Bianchini, G., Balko, J. M., Mayer, I. A., Sanders, M. E. & Gianni, L. Triple-negative breast cancer: challenges and opportunities of a heterogeneous disease. *Nat. Rev. Clin. Oncol.* **13,** 674–690 (2016).
9. Petrocca, F. *et al.* A genome-wide siRNA screen identifies proteasome addiction as a vulnerability of basal-like triple-negative breast cancer cells. *Cancer Cell* **24,** 182–96 (2013).
10. Kacsinta, A. D. & Dowdy, S. F. Current views on inducing synthetic lethal RNAi responses in the treatment of cancer. *Expert Opin. Biol. Ther.* **16,** 161–172 (2016).
11. Testa, F. *et al.* Three-Year Follow-up after Unilateral Subretinal Delivery of Adeno-Associated Virus in Patients with Leber Congenital Amaurosis Type 2. *Ophthalmology* **120,**

1283–1291 (2013).
12. Brimble, M. A., Reiss, U. M., Nathwani, A. C. & Davidoff, A. M. New and improved AAVenues: current status of hemophilia B gene therapy. *Expert Opin. Biol. Ther.* **16,** 79–92 (2016).
13. Kaplitt, M. G. *et al.* Safety and tolerability of gene therapy with an adeno-associated virus (AAV) borne GAD gene for Parkinson's disease: an open label, phase I trial. *Lancet* **369,** 2097–2105 (2007).
14. *Adeno-Associated Virus*. **807,** (Humana Press, 2011).
15. Samulski, R. J. & Muzyczka, N. AAV-Mediated Gene Therapy for Research and Therapeutic Purposes. *Annu. Rev. Virol.* **1,** 427–451 (2014).
16. Bryant, L. M. *et al.* Lessons Learned from the Clinical Development and Market Authorization of Glybera. *Hum. Gene Ther. Clin. Dev.* **24,** 55–64 (2013).
17. Ledford, H. Cancer-fighting viruses win approval. *Nature* **526,** 622–623 (2015).
18. Grimm, D., Kay, M. A. & Kleinschmidt, J. A. Helper virus-free, optically controllable, and two-plasmid-based production of adeno-associated virus vectors of serotypes 1 to 6. *Mol. Ther.* **7,** 839–850 (2003).
19. *Viral Vectors for Gene Therapy*. *Methods in Molecular Biology* **737,** (Humana Press, 2011).
20. Zitouni, S., Nabais, C., Jana, S. C., Guerrero, A. & Bettencourt-Dias, M. Polo-like kinases: structural variations lead to multiple functions. *Nat. Rev. Mol. Cell Biol.* **15,** 433–452 (2014).
21. Liu, Z., Sun, Q. & Wang, X. PLK1, A Potential Target for Cancer Therapy. *Transl. Oncol.* **10,** 22–32 (2017).
22. Bhola, N. E. *et al.* Kinome-wide Functional Screen Identifies Role of PLK1 in Hormone-Independent, ER-Positive Breast Cancer. *Cancer Res.* **75,** 405–414 (2015).
23. Snyder, R. O. An Overview of rAAV Vector Product Development for Gene Therapy. in (ed. Childers, M. K.) 21–37 (Springer New York, 2016). doi:10.1007/978-1-4939-3228-3_2
24. van der Loo, J. C. M. & Wright, J. F. Progress and challenges in viral vector manufacturing. *Hum. Mol. Genet.* **25,** R42–R52 (2016).
25. Kotin, R. M. Large-scale recombinant adeno-associated virus production. *Hum. Mol. Genet.* **20,** R2–R6 (2011).
26. Grigoriadis, A. *et al.* Molecular characterisation of cell line models for triple-negative breast cancers. *BMC Genomics* **13,** 619 (2012).
27. Ryu, A. H., Eckalbar, W. L., Kreimer, A., Yosef, N. & Ahituv, N. Use antibiotics in cell culture with caution: genome-wide identification of antibiotic-induced changes in gene expression and regulation. *Sci. Rep.* **7,** 7533 (2017).
28. Nygaard, U. H. *et al.* Antibiotics in cell culture: friend or foe? Suppression of keratinocyte growth and differentiation in monolayer cultures and 3D skin models. *Exp. Dermatol.* **24,** 964–965 (2015).
29. Lamb, R. *et al.* Antibiotics that target mitochondria effectively eradicate cancer stem cells, across multiple tumor types: Treating cancer like an infectious disease. *Oncotarget* **6,** 4569–4584 (2015).
30. Alam, S. *et al.* Adeno-associated virus type 2 infection activates caspase dependent and independent apoptosis in multiple breast cancer lines but not in normal mammary epithelial cells. *Mol. Cancer* **10,** 97 (2011).
31. Cideciyan, A. V. *et al.* Vision 1 Year after Gene Therapy for Leber's Congenital Amaurosis. *N. Engl. J. Med.* **361,** 725–727 (2009).
32. Valori, C. F. *et al.* Systemic Delivery of scAAV9 Expressing SMN Prolongs Survival in a Model of Spinal Muscular Atrophy. *Sci. Transl. Med.* **2,** 35ra42-35ra42 (2010).
33. Nathwani, A. C. *et al.* Long-Term Safety and Efficacy of Factor IX Gene Therapy in Hemophilia B. *N. Engl. J. Med.* **371,** 1994–2004 (2014).

34. Valdmanis, P. N. & Kay, M. A. Future of rAAV Gene Therapy: Platform for RNAi, Gene Editing, and Beyond. *Hum. Gene Ther.* **28,** 361–372 (2017).
35. Maunder, H. E. *et al.* Enhancing titres of therapeutic viral vectors using the transgene repression in vector production (TRiP) system. *Nat. Commun.* **8,** 14834 (2017).
36. Strobel, B. *et al.* Riboswitch-mediated Attenuation of Transgene Cytotoxicity Increases Adeno-associated Virus Vector Yields in HEK-293 Cells. *Mol. Ther.* **23,** 1582–1591 (2015).
37. Lee, E. J. & Jameson, J. L. Cell-Specific Cre-Mediated Activation of the Diphtheria Toxin Gene in Pituitary Tumor Cells: Potential for Cytotoxic Gene Therapy. *Hum. Gene Ther.* **13,** 533–542 (2002).
38. Manasanch, E. E. & Orlowski, R. Z. Proteasome inhibitors in cancer therapy. *Nat. Rev. Clin. Oncol.* **5,** 101–110 (2017).
39. Druker, B. J. *et al.* Five-Year Follow-up of Patients Receiving Imatinib for Chronic Myeloid Leukemia. *N. Engl. J. Med.* **355,** 2408–2417 (2006).
40. Smith, I. *et al.* 2-year follow-up of trastuzumab after adjuvant chemotherapy in HER2-positive breast cancer: a randomised controlled trial. *Lancet* **369,** 29–36 (2007).
41. Kikani, C. K., Dong, L. Q. & Liu, F. "New"-clear functions of PDK1: Beyond a master kinase? *J. Cell. Biochem.* **96,** 1157–1162 (2005).
42. Pecot, C. V, Calin, G. A., Coleman, R. L., Lopez-Berestein, G. & Sood, A. K. RNA interference in the clinic: challenges and future directions. *Nat. Rev. Cancer* **11,** 59–67 (2011).
43. Weihua, Z. *et al.* Survival of Cancer Cells Is Maintained by EGFR Independent of Its Kinase Activity. *Cancer Cell* **13,** 385–393 (2008).
44. Lim, S. T., Mikolon, D., Stupack, D. G. & Schlaepfer, D. D. FERM control of FAK function: Implications for cancer therapy. *Cell Cycle* **7,** 2306–2314 (2008).
45. Chen, M. *et al.* Efficient Gene Delivery and Expression in Pancreas and Pancreatic Tumors by Capsid-Optimized AAV8 Vectors. *Hum. Gene Ther. Methods* **28,** 49–59 (2017).
46. Sayroo, R. *et al.* Development of novel AAV serotype 6 based vectors with selective tropism for human cancer cells. *Gene Ther.* **23,** 18–25 (2016).
47. Galluzzi, L., Buqué, A., Kepp, O., Zitvogel, L. & Kroemer, G. Immunogenic cell death in cancer and infectious disease. *Nat. Rev. Immunol.* 2–5 (2016). doi:10.1038/nri.2016.107
48. Nyga, A. *et al.* The next level of 3D tumour models: immunocompetence. *Drug Discov. Today* **21,** 1421–1428 (2016).

CHAPTER III

ENGINEERING AAV2 VECTOR TROPISM THROUGH *IN VITRO* DIRECTED EVOLUTION

ABSTRACT

Basal-like breast cancer (BLBC) has currently no validated surface biomarkers that could direct targeted therapies. Thus, the only therapeutic option for these patients is still chemotherapy, which entails toxic side-effects. Here, we used a peptide library displayed on AAV vectors to select for AAV capsids with restricted tropism and that could mediate BLBC-specific transduction. By following a directed evolution approach through sequential infection rounds in BLBC cell lines, we were able to select a single peptide motif enrich within the library. Overall tropism for this AAV variant was maintained for all the cancer cell lines tested, spanning different subtypes of breast and lung cancer, as well as a fibrosarcoma cell line. Transduction efficiency of the selected variant was decreased for embryonic kidney and hepatic cell lines when compared to wild-type (wt) AAV2 capsids. On the other hand, transduction efficiency was increased for human dermal fibroblasts and normal mammary epithelial cells. Therefore, we were successful in selecting an AAV variant (AAV-X7) with altered tropism when compared to vectors carrying the wild-type AAV2 capsid. However, this variant presents limited potential for BLBC targeted therapy since it still is able to infect normal breast epithelial cells. Further studies are needed to understand which receptors mediate AAV-X7 cell binding.

TABLE OF CONTENTS

1. INTRODUCTION

Breast cancer (BC) is an heterogeneous disease in terms of molecular phenotypes and disease outcomes. Over the years, extensive research has been directed at dividing BC into subgroups that could instruct clinical decisions. Both transcriptomic and genomic studies have classified BC into "intrinsic" subtypes which are mostly defined by the expression of three biomarkers: endocrine receptors for oestrogen (ER) and progesterone (PR), and altered expression of *HER2*[1,2]. ER+ BC (Luminal A/B subtypes) are the most common and present a good prognosis when treated with endocrine therapies, although relapses still occur[3]. The HER2-enriched subgroup has also seen its prognosis drastically improved with the development of targeted therapies for this receptor[4]. Basal-like breast cancer (BLBC), on the other hand, currently has no validated biomarkers, other than absent or low expression of *ER*, *PR* and *HER2*. In fact, more than 90% of BLBC are negative for all three receptors; thus, these do not respond to available targeted therapies. Therefore, there is an urgent need for identification of biomarkers that could help target BLBC and improve prognosis[5].

AAV vectors´ extensive preclinical and clinical studies have highlighted their safe and efficacious profile for gene therapy[6]. Moreover, the increasing understanding of AAV capsid structure has facilitated the rational design of AAV variants with clinical potential[7,8]. On the other hand, progress in AAV capsid library development has supported directed evolution approaches[9,10]. Here, wild-type (wt) capsid encoding genes are mutated using different approaches, generating large peptide libraries displayed in AAV vectors[11]. These are then subjected to selective pressure to isolate novel AAV variants with enhanced properties for *in vivo* gene delivery, such as increased infection efficiency and lower immunogenicity profiles[11].

Since there are no known cellular receptors available for BLBC targeting, we used a directed evolution approach to select for an AAV variant with increased tropism and transduction efficiency towards this BC subtype. For this, we used a random peptide library displayed on AAV2 vectors (AAV library)[12]. The peptides were inserted at the site of attachment to the viral receptors, at the surface of the vector capsid, thereby

decreasing AAV2 vectors´ endogenous tropism[12]. After multiple rounds of infection of the AAV library on BLBC cell lines a single AAV variant was selected, which enabled efficient transduction of BLBC cell lines. Nevertheless, a broader analysis of its tropism revealed that it was still able to infect cells from other tissues, thus limiting its potential for BLBC directed therapy.

2. MATERIALS AND METHODS

2.1 Cell culture

HEK293T, AAV293 and HT1080, MCF7 and HepG2 cell lines were cultured in high glucose (4.5 g/L) DMEM supplemented with 10% (v/v) fetal bovine serum (FBS). Basal breast cancer (BLBC) cell lines HCC1187, HCC1954, HCC1806, HCC1937, MDA-MB-231, MDA-MB-468, were cultured in RPMI 1640 medium supplemented with 10% (v/v) FBS, 6 mM HEPES and 5 µM 2-Mercaptoethanol. H1650 cell line was cultured in RPMI 1640 medium supplemented with 10% (v/v) FBS. Human Dermal Fibroblasts (HDF), from Innoprot, were cultured in IMDM supplemented with 10% (v/v) FBS. Primary breast epithelial cells were cultured in WIT-P™ Culture Medium (Stemgent). Media and cell culture reagents were from Gibco Life Technologies, unless otherwise specified. Cells were incubated at 37 °C in a humidified atmosphere with 5% CO_2 in air.

2.2 AAV peptide library biopanning

PBEC and BCLC cell lines were infected with an AAV display peptide library kindly supplied by Prof. Martin Trepel's group, University Medical Center Hamburg-Eppendorf[12]. After 8hrs cells were washed with PBS followed by incubation with wild-type Ad5 at an MOI of 100pfu/cell in serum free media. After 1h incubation, cell´s culture media was added, and cell were further cultured for 72hrs. Replicated AAV particles were harvested from supernatant and from cell, concentrated using vivaspin columns, and used for the subsequent rounds of infection. wtAd5 harvested from each selection round was inactivated by incubating the lysate and supernatant for 45 min at 55ºC. This biopanning cycle was repeated 3 to 5 times.

2.3 PCR-amplification and sequencing of insert sequences

Replicated AAV particles recovered after selected round were recovered, incubated for 10 min at 90°C to inactivate wtAd5 and release the AAV genomes from the particles, and insert sequences were amplified using primers 5'-CCCGTGGCTACGGAGC-3' and 5'-TGACATCTGCGGTGGCC-3', as previously described[12]. PCR products were analyzed by gel electrophoresis and purified using PCR purification Kit (Quiagen cat#28106). A ligantion reaction using T4 DNA ligase was performed and the product was analyzed by gel electrophoresis. Bands ranging from 800 and 1500 bp were cut from the gel and purified with the Peqlab gel extraction kit, cloned into pJet2.1 vector (Fermentas cat# K1232), and transformed using electrocompetent DH5alfa cells. Randomly selected clones were sequenced.

2.4 Phage library biopanning

Selection of peptides was performed using Ph.D.-12™ Phage Display Peptide Library (NEB #E8111L). Briefly, primary breast epithelial cells were used to deplete the phage library of non-specific binders. The cells were washed twice with PBS and blocked with PBS containing 1% bovine serum albumin (BSA) at 37°C for 1 h. Approximately, $1x10^{11}$ pfu phages were added and mixed gently for 1 h at 37˚C. During this time, target cells were pre-washed and blocked. The supernatant containing unbound phages was transferred to blocked target cells and incubated for 2hrs on at 37˚C. After four intensive washes of cells with PBS containing 0.2% Tween-20, bound phages were eluted from cells by incubation with 0.2 M glycine–HCl, pH 2.2 for 15 min. The eluate was immediately neutralized by the addition of 200 µl of 1 M Tris–HCl buffer at pH 9.1. Selected phages were amplified in E. coli for next rounds. At the third round of biopanning clones were sequenced by colony PCR.

2.5 Production and purification of AAV vectors

Selected capsid modified AAV vectors were produced and purified as described in Chapter II – section 2.3.

2.6 *In vitro* vector characterization

All cells were transduced using the capsid modified AAV vectors as described in Chapter II – section 2.5. Percentage of transduced cells was analyzed by identification of GFP+ cells by flow cytometry.

3. RESULTS

3.1 Selection of peptides targeting human basal-like breast cancer cells

Using a random peptide library displayed on AAV vectors (AAV library) previously developed[12], a directed evolution approach was followed using different strategies, as depicted in Fig. 3.1.

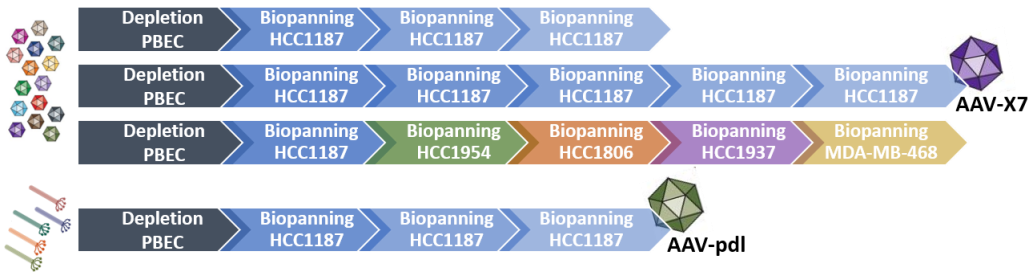

Figure 3.1: Schematic representation of the different strategies followed for *in vitro* directed evolution AAV library on BLBC cells. Images were adapted from Kotterman *et al.*, Nat Rev Gen (2014) and New England Biolab® protocol.

To decrease these vectors ability to infect normal mammary tissue and restrict AAV2 tropism, the AAV library was subjected to an initial depletion step, using primary breast epithelial cells (PBEC). All the AAV variants unable to bind and internalize were recovered in the supernatant. Following the depletion step, to select for AAV capsids with high transduction efficiency and selective tropism toward BLBC, cell lines from the referred BC subtype were infected with the depleted supernatant.

HCC1187 cell line was chosen for the initial screenings due to its high tumorigenic phenotype. After AAV library infection, these cells were superinfected with Ad5 for amplification of internalized clones. Amplified clones were recovered and used in

subsequent rounds of infection to select and enrich for AAV variants with ability to efficiently bind, enter and replicate in BLBC cell lines. One peptide motif was enriched upon screening the AAV library. Sequencing of the DNA region coding for the 7-peptide motif inserted in the AAV library of the selected clones was done after three and five selection rounds. DNA sequencing revealed a 15% enrichment of one peptide motif only after five rounds of biopanning using the first strategy. The enriched peptide motif was RDGERPG (X7).

To avoid selection of an AAV variant specific for the HCC1187 cell line and increase the chances of finding a variant that would allow broad infection of multiple BLBC, a second strategy was followed, consisting of using different BLBC cell lines for the biopanning selection steps (Fig. 3.1). Unfortunately, this approach did not result in enrichment of AAV variants. As an alternative, a screening using a phage-display peptide library was performed with the HCC1187 cell line, which resulted in enrichment in a single peptide motif - PNLHAWVP (pdl).

The two peptide motifs identified were cloned into AAV2 rep-cap plasmid and used for the production of AAV vectors displaying the selected peptides: AAV-X7 and AAV-pdl, respectively. As a positive control, an AAV variant containing the wild-type AAV2 capsid was also produced and used for comparison in further studies (wtAAV2).

3.2 Tropism evaluation

To validate the targeting potential of the selected peptide for AAV-mediated gene transfer, BLBC cell lines were transduced with the developed AAV variants, and its transduction efficiency was compared to that of AAV vectors carrying the wt capid (wtAAV2). The AAV vectors produced carried eGFP reporter gene to facilitate transduction monitoring via flow cytometry. Tropism was evaluated by analyzing the transduction efficiency of both control (wtAAV2) and capsid modified AAV vectors (AAV-X7 and AAV-pdl) in different cell lines. The AAV variant containing the pdl peptide motif (AAV-pdl) showed decreased transduction efficiency in all cell types tested (data not shown). This may indicate that the insertion of the peptide motif arising from the phage library caused a disruption in the AAV2 capsid, impairing its infectivity.

Regarding the AAV-X7 variant, transduction efficiency in all BLBC cell lines tested was maintained when compared to wtAAV2 (Fig. 3.2). To evaluate cell-type specificity, transduction efficiency was also evaluated for normal breast epithelial control cells, as well as for cells from irrelevant tissues. Similarly to BLBC cells, the AAV-X7 vector transduced the cancer cell lines MCF7 (luminal A breast cancer), HT1080 (fibrosarcoma) and H1650 (lung adenocarcinoma) at levels similar to those of wild-type vector (Fig. 3.2).

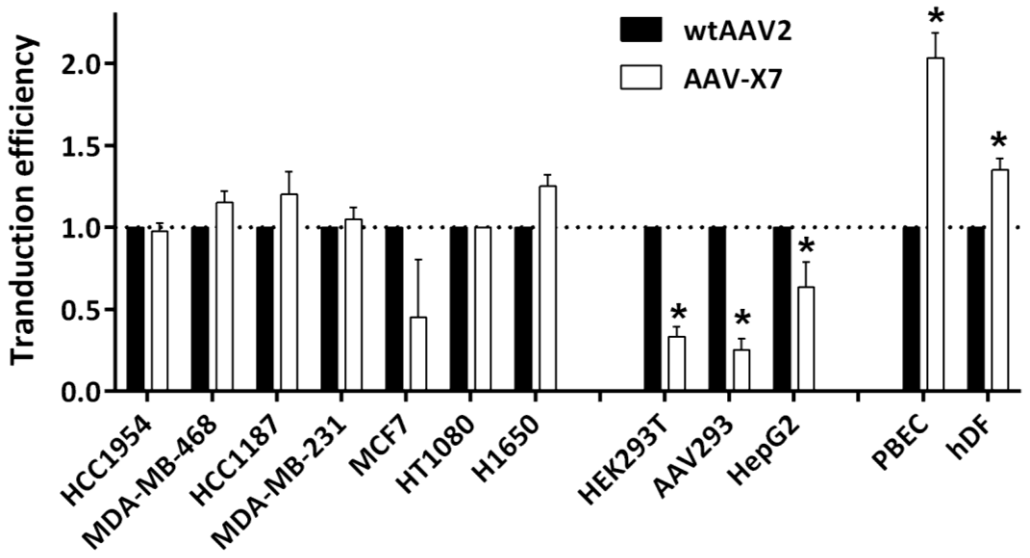

Figure 3.2: Transduction efficiency and tropism evaluation of AAV variant expressing the selected peptide motif. The indicated cells were transduced with control wild type AAV2 (wtAAV2) or capsid-modified AAV-X7 vectors at $4.57x10^3$ VG/cell. Transduction efficiency monitored 48h thereafter by detection of GFP+ cells by flow cytometry. Transduction efficiency of AAV-X7 was calculated relative to transduction efficiency of cells transduced with wtAAV2 vector. Plots show fold change in percentage transduced cells (mean $\pm$ SD) of several independent experiments, each done in duplicate. *, $p < 0.05$. Statistical significance was determined using the two-tailed Student´s t-test.

Proof of tropism alteration arose when hepatic (HepG2) and embryonic kidney (HEK293T and AAV293) cell lines were tested. In these cells, transduction efficiency of AAV-X7 was reduced by 40% to 80% depending on the cell line (Fig. 3.2). On the other hand, AAV-X7 vector showed increased transduction efficiency towards normal breast

epithelial cells (2-fold) and human dermal fibroblasts (1.4-fold) when compared to the wild-type control vector (Fig. 3.2); thus, impairing its potential for BLBC targeting.

4. DISCUSSION

Several studies have shown the feasibility of engineering AAV capsid for binding to alternative receptors. The development of systematic tools to generate vectors targeting any cell-type of interest, such as peptide libraries displayed on AAV vectors, can facilitate the process of finding variants of interest[12].

Since there are no known targets for basal-like breast cancer (BLBC), with the goal of finding AAV variants with improved efficiency for BLBC cell-directed gene transfer, the AAV library developed by Muller *et al.* was panned on BLBC cell lines. Several strategies were followed using sequential rounds of panning i) on the same cell line, or ii) using multiple BLBC cell lines. Although the second strategy would increase the chances of finding AAV variants that target BLBC, independently of their intrinsic heterogeneity, it did not support enrichment in any particular peptide motif. This may indicate that the cell lines used are too diverse, decreasing the probability of finding a common receptor target. Such heterogeneity has also been reported for BLBC patients[5].

Sequential rounds of infection using the same cell line resulted in 15% enrichment in a single peptide motif – RDGERPG. The targeting properties of the AAV variant incorporating the selected peptide (AAV-X7) were evaluated *in vitro*, by comparing its transduction efficiency with that of the wtAAV2 capsid in cell lines from different tissues. Transduction efficiency of AAV-X7 for BLBC was maintained when compared to the wtAAV2 capsid. However, AAV-X7 was still effective in transducing normal breast epithelium and human dermal fibroblasts. This suggests that there will be unspecific targeting of non-relevant tissues *in vivo*, thus impairing its use as a therapy for BLBC. When compared to the wtAAV2 capsid, AAV-X7 presented decreased transduction efficiency for human embryonic kidney and hepatocellular carcinoma cell lines. These represent cell lines from different tissue-of-origin and cellular morphology (epithelial vs mesenchymal); thus, it is unclear how restricted is the tropism of the developed variant.

Further tests are required for proper characterization of the selected AAV and discovery of the targeted receptor.

The incorporation of peptides selected from different platforms, namely phage display, within AAV capsids has been successful. It presents important advantages over bispecific conjugates for systemic treatment due to the possible instability of the vector-conjugate complex and immunogenicity of the adaptor[12]. The development of phage display peptide libraries increased power and throughput of screening methods. These are efficient tools for fast selection of ligands for different molecular targets and have been successfully screened for binding specificity to endothelial cells *in vitro*[13], on tumor tissue sections[14] and *in vivo*[15,16]. Here, we used a phage display peptide library as an alternative approach to identify relevant BLBC-binding peptides. After three rounds of biopanning on a BLBC cell line, we identified a single peptide motif enriched in the clones sequenced. The sequence – PNLHAWVP – presented high homology to a peptide ligand for breast ductal carcinoma, previously identified by Lu *et al.*, in a similar biopanning campaign[17]. This highlights the power and reproducibility of the screening technology; nevertheless, it may indicate that the tropism of the engineered AAV capsid will not be restricted to BLBC. AAV vectors displaying the selected peptide presented low transduction efficiency in all cell lines tested. Upon incorporation into the viral capsid, the peptide conformation may be altered, or it may interfere with the proper assembly of the viral capsids. Moreover, since these peptides are selected for binding and not necessarily entry into the target cell, if the target receptor does not support internalization of the ligand, the developed vectors will not be suitable for gene transfer[12]. Further analysis are required to understand what is impairing transduction for AAV-pdl.

Lastly, additional strategies are currently ongoing to select recombinant virus with specific tropism towards BLBC cells. These include the use of a more stringent depletion strategy (by increasing the number of infection cycles using primary breast epithelial cells), prior to biopanning in BLBC cell lines.

Breast cancer cell lines have been essential for elucidating BC biology and finding novel therapeutics[18,19]. Also, several studies have reported that the heterogeneity of gene expression and genomic aberration profiles is maintained to a certain extent within the BC cell lines currently available[20,21]. Nevertheless, the routine culturing of these cells under non-physiological culture conditions may impair biological studies. Therefore, biopanning for peptide motifs with restricted tropism towards BLBC using cellular models that more accurately reflect the biology of this subtype can be pursued. These include 3D cellular models where the tumor architecture, and thus relevant cell-cell interactions and surface receptors, are maintained. This is expected to increase the chances of finding a peptide motif suitable to develop an AAV-based therapy against breast cancer.

Moreover, biopanning using *in vivo* animal models is also an alternative. This allows for the simultaneous selection of relevant peptide motifs, while avoiding peptides that bind to the other tissues. It is important to note that selection would be done in a murine environment, thus differences compared with human tissues may arise.

5. AUTHOR CONTRIBUTION & ACKNOWLEDGEMENTS

The author participated on the experimental setup and design, performed the experiments, analyzed the data and wrote the chapter. The author acknowledges Dr Gabriela Silva for contributing to the experimental setup and design, experiments and data analysis. The author acknowledges Dr. Ana Barbas and Inês Barbosa for performing part of the experiments. The work was supported by FCT grant PTDC/BBB-BIO/1240/2012 and PhD fellowship PD/BD/52202/2013 to C. Pinto. Also, iNOVA4Health unit "iNOVA4Health Research Unit (LISBOA-01-0145-FEDER-007344), which is co-funded by Fundação para a Ciência e Tecnologia / Ministério da Ciência e do Ensino Superior, through national funds, and by FEDER under the PT2020 Partnership Agreement, is acknowledged.

6. REFERENCES

1. Koboldt, D. C. *et al.* Comprehensive molecular portraits of human breast tumours. *Nature*

490, 61–70 (2012).
2. Parker, J. S. *et al.* Supervised Risk Predictor of Breast Cancer Based on Intrinsic Subtypes. *J. Clin. Oncol.* **27,** 1160–1167 (2009).
3. Turner, N. C., Neven, P., Loibl, S. & Andre, F. Advances in the treatment of advanced oestrogen-receptor-positive breast cancer. *Lancet* **389,** 2403–2414 (2017).
4. Loibl, S. & Gianni, L. HER2-positive breast cancer. *Lancet* **389,** 2415–2429 (2017).
5. Bianchini, G., Balko, J. M., Mayer, I. A., Sanders, M. E. & Gianni, L. Triple-negative breast cancer: challenges and opportunities of a heterogeneous disease. *Nat. Rev. Clin. Oncol.* **13,** 674–690 (2016).
6. Samulski, R. J. & Muzyczka, N. AAV-Mediated Gene Therapy for Research and Therapeutic Purposes. *Annu. Rev. Virol.* **1,** 427–451 (2014).
7. Martino, A. T. *et al.* Engineered AAV vector minimizes in vivo targeting of transduced hepatocytes by capsid-specific CD8+ T cells. *Blood* **121,** 2224–2233 (2013).
8. Zhong, L. *et al.* Next generation of adeno-associated virus 2 vectors: Point mutations in tyrosines lead to high-efficiency transduction at lower doses. *Proc. Natl. Acad. Sci.* **105,** 7827–7832 (2008).
9. Sallach, J. *et al.* Tropism-modified AAV Vectors Overcome Barriers to Successful Cutaneous Therapy. *Mol. Ther.* **22,** 929–939 (2014).
10. Naumer, M., Popa-Wagner, R. & Kleinschmidt, J. a. Impact of capsid modifications by selected peptide ligands on recombinant adeno-associated virus serotype 2-mediated gene transduction. *J. Gen. Virol.* **93,** 2131–2141 (2012).
11. Kotterman, M. a & Schaffer, D. V. Engineering adeno-associated viruses for clinical gene therapy. *Nat. Rev. Genet.* **15,** 445–451 (2014).
12. Müller, O. J. *et al.* Random peptide libraries displayed on adeno-associated virus to select for targeted gene therapy vectors. *Nat. Biotechnol.* **21,** 1040–1046 (2003).
13. Mutuberria, R. *et al.* Isolation of human antibodies to tumor-associated endothelial cell markers by in vitro human endothelial cell selection with phage display libraries. *J. Immunol. Methods* **287,** 31–47 (2004).
14. Ruan, W., Sassoon, A., An, F., Simko, J. P. & Liu, B. Identification of Clinically Significant Tumor Antigens by Selecting Phage Antibody Library on Tumor Cells in Situ Using Laser Capture Microdissection. *Mol. Cell. Proteomics* **5,** 2364–2373 (2006).
15. Urich, E. *et al.* Cargo Delivery into the Brain by in vivo identified Transport Peptides. *Sci. Rep.* **5,** 14104 (2015).
16. Li, X.-B., Schluesener, H. J. & Xu, S.-Q. Molecular addresses of tumors: selection by in vivo phage display. *Arch. Immunol. Ther. Exp. (Warsz).* **54,** 177–181 (2006).
17. Lu, R.-M. *et al.* Targeted Drug Delivery Systems Mediated by a Novel Peptide in Breast Cancer Therapy and Imaging. *PLoS One* **8,** e66128 (2013).
18. Lacroix, M. & Leclercq, G. Relevance of Breast Cancer Cell Lines as Models for Breast Tumours: An Update. *Breast Cancer Res. Treat.* **83,** 249–289 (2004).
19. Barretina, J. *et al.* The Cancer Cell Line Encyclopedia enables predictive modelling of anticancer drug sensitivity. *Nature* **483,** 603–307 (2012).
20. Grigoriadis, A. *et al.* Molecular characterisation of cell line models for triple-negative breast cancers. *BMC Genomics* **13,** 619 (2012).
21. Keller, P. J. *et al.* Mapping the cellular and molecular heterogeneity of normal and malignant breast tissues and cultured cell lines. *Breast Cancer Res.* **12,** R87 (2010).

CHAPTER IV

3D-3-CULTURE: A TOOL TO UNVEIL MACROPHAGE PLASTICITY WITHIN THE TUMOR MICROENVIRONMENT

This chapter was adapted from:

Rebelo SP*, Pinto C*, Martins TR, Harrer N, Estrada MF, Loza-Alvarez P, Cabeçadas J, Alves PM, Gualda EJ, Sommergruber W, Brito C. (*equal contribution) *3D-3-culture: A tool to unveil macrophage plasticity in the tumour microenvironment.* Biomaterials 163, 185–197 (2018).

*equal contribution

ABSTRACT

The tumour microenvironment (TME) shapes disease progression and influences therapeutic response. Most aggressive solid tumours have high levels of myeloid cell infiltration, namely tumour associated macrophages (TAM). Recapitulation of the interaction between the different cellular players of the TME, along with the extracellular matrix (ECM), is critical for understanding the mechanisms underlying disease progression. This particularly holds true for prediction of therapeutic response(s) to standard therapies and interrogation of efficacy of TME-targeting agents. In this work, we explored a culture platform based on alginate microencapsulation and stirred culture systems to develop the 3D-3-culture, which entails the co-culture of tumour cell spheroids of non-small cell lung carcinoma (NSCLC), cancer associated fibroblasts (CAF) and monocytes. We demonstrate that the 3D-3-culture recreates an invasive and immunosuppressive TME, with accumulation of cytokines/chemokines (IL4, IL10, IL13, CCL22, CCL24, CXCL1), ECM elements (collagen type I, IV and fibronectin) and matrix metalloproteinases (MMP1/9), supporting cell migration and promoting cell-cell interactions within the alginate microcapsules. Importantly, we show that both the monocytic cell line THP-1 and monocytes from healthy donors infiltrate the tumour tissue and transpolarize into an M2-like macrophage phenotype expressing CD68, CD163 and CD206, resembling the TAM phenotype in NSCLC. The 3D-3-cultures were challenged with chemo- and immunotherapeutic agents and the response to therapy was assessed in each cellular component. Specifically, the macrophage phenotype was modulated upon treatment with the CSF1R inhibitor BLZ945, resulting in a decrease of the M2-like macrophages. In conclusion, the crosstalk between the ECM and tumour, stroma and immune cells in microencapsulated 3D-3-cultures promotes the activation of monocytes into TAM, mimicking aggressive tumour stages. The 3D-3-culture constitutes a novel tool to study tumour-immune interaction and macrophage plasticity in response external stimuli, such as chemotherapeutic and immunomodulatory drugs.

TABLE OF CONTENTS

1. INTRODUCTION

Cell-cell and cell-matrix interactions, involving tumour, stromal and immune cells, are critical in all steps of tumour development and have been extensively studied in recent years. Moreover, reports on their impact on patient prognosis and therapeutic response are also increasing[1,2]. Immune checkpoint blockade and adoptive T-cell therapy approaches have introduced immunotherapies as viable clinical modalities, alongside chemotherapeutics and targeted agents[3]. However, there are still considerable challenges in understanding why in some tumour types immunotherapy has no clinical effect and why certain patients fail to respond to the treatment[4–6]. Undeniably, there is a need to understand the mechanistic effects of a therapy within the immune regulatory context of a given tumour microenvironment (TME), leading to more effective approaches, and harnessing the full potential of the TME as a therapeutic target[7].

Non-small cell lung cancer (NSCLC), one of the most lethal malignant diseases, is typically associated with extensive myeloid cell infiltration[8,9]. Infiltrating myeloid cells are key mediators of immune suppression, neovascularization, invasiveness, metastasis and poor response to therapy. Consequently, those cells constitute an important target for the development of novel immunotherapies[10,11]. In most solid tumours, including NSCLC, macrophages constitute the main myeloid infiltrate, representing up to 50 % of the tumour mass[12,13]. Circulating monocytes are recruited to the tumour tissue and can be transpolarized towards the M1-like or M2-like phenotype. Tumour associated macrophages (TAM) have been linked with the M2-like phenotype, exerting tumour-promoting effects such as induction of proliferation, angiogenesis, ECM remodelling and evasion from adaptive immunity such as secretion of arginase 1[14]. In contrast, M1 macrophages have a tumour suppressive effect[13]. The presence of TAM infiltrate affects tumour response to standard-of-care drug treatments[15] and were shown to be an important therapeutic target. For instance, by inhibiting the colony stimulating factor 1 receptor (CSF-1R), which is the main route of activation and survival of monocytes, the tumour progression both in murine models as well as in patients was controlled, resulting in an extended survival rate[16–18]. Most of the knowledge on

TAM infiltrate has been derived from histological examination of patient samples in retrospective cohort studies where myeloid cells have been identified by a few immunohistochemistry markers, providing no information about the TAM function *per se*[10,19]. Therefore, technological developments are urgently needed including the development of *in vitro* models that can recapitulate tumour-immune interactions in a TME relevant context, while allowing rapid and thorough characterization of the immune compartment, to screen and functionally assess novel therapeutics in high throughput platforms[4].

Preclinical models consist mainly of human tumour-derived cell lines, propagated in 2D culture or used in the implementation of mouse xenografts, and on genetically engineered mouse models (GEMM) of human tumorigenesis[20]. Although 2D cultures provided important insights into potential anticancer agents at early stages of drug development, they cannot recapitulate the gradients of nutrients, oxygen and drug penetration occurring *in vivo* and do not account for key TME triggers[21,22]. Human cell line-derived xenografts differ considerably from primary human tumours in terms of proliferative capacity and TME[23,24]. In addition, the immune system is often compromised, thus these models cannot reliable support immunomodulatory drug development[24]. Immune-competent and genetically engineered mouse models (GEMM) overcome some of the drawbacks, as they allow for the presence of the complete immune system. However, those models are still based on murine stromal and immune components[24,25]. For most aggressive cancers, including several lung cancers, drug candidates arising from 2D cell-line screens and mouse xenograft models present poor clinical translation[22]. The discrepancy between these models and the human situation in key physiological features, such as human tumour-stroma, tumour-immune cell interactions and gradients of drug penetration in the tissue have a significant impact on the therapeutic response[22]. Therefore, the combination of *in vivo* cell models with advanced *in vitro* cell models offers a complementary approach to study the mechanisms underlying tumour development in the context of the TME. 3D cellular models have the potential to advance drug discovery and streamline progression of novel candidates through drug discovery pipelines. The need for more

predictive drug assays triggered advances in cell culture techniques that led to the appearance of complex *in vitro* models[21]. Tumour spheroids offer an alternative to high throughput monolayer-based assays and are complementary to mouse models[20]. Several methods for spheroid production are currently available, such as low adhesion plates, the hanging drop method, cell-seeded matrices and scaffolds, micropatterning and agitation based methods[26]. Tumour spheroids can mimic drug response of primary human tumours and have proven useful in the study of tumour physiology, such as metabolic and chemical gradients, hypoxic environment and cell-cell and cell-matrix interactions[20,21,27,28]. Heterotypic cellular models have been successfully employed in unravelling new aspects of cancer biology[23,26]. Most heterotypic models include stromal cells, such as cancer-associated fibroblasts (CAF), which have been shown to enhance the inflammatory environment, promote tumour progression and lead to drug resistance[29]. Reports of *in vitro* models of immune interaction with tumours from diverse pathologies are mostly focused on the tumour phenotype and its modulation by the macrophages via secreted factors[30–33]. In lung cancer, it has been reported that the presence of macrophages promotes a metastatic phenotype due to the presence of MMP-1 and VEGF[34]. However, the dynamic interaction between both cell types and the effect of TME heterogeneity on the response to chemotherapeutic or immune-targeted agents has scarcely been assessed in these types of models. Most studies focusing on macrophage and tumour interaction in response to therapy still rely on mouse models using *in vivo* imaging tools that, although capable deciphering tumour architecture and cell interaction networks, are technically demanding and not compatible with high throughput screening[19,35]

In the present work, we establish a 3D cell model (3D-3-culture), enclosing three cellular components: NSCLC cells as tumour spheroids, CAF and monocytes. The model is based on the alginate microencapsulation strategy previously described by our group, which allows direct interaction between different cell types and is compatible with continuous monitoring and functional assessment in long-term culture using stirred systems[26,29]. Here we demonstrate the recruitment of human monocytes into tumour tissue and their polarization into a M2-like phenotype without directed differentiation by the

addition of exogenous cytokines, thus recreating the TAM phenotype *in vitro*. Moreover, the TME response to therapy is assessed, depicting the differences in each cellular compartment upon treatment and demonstrating that the macrophage phenotype can be modulated in response to chemo- and immunotherapy.

2. MATERIAL AND METHODS

2.1 Cell lines

The NSCLC cell line NCI-H157 originally obtained from ATTC (ATCC: #CRL-5802) was stably transfected with the pRSF91.dtTomato-Blasti plasmid[36]. Briefly, $1x10^6$ NCI-H157 cells were centrifuged at 90x*g* (1200 rpm, 7min.) at room temperature (RT), resuspended in 100 µl Amaxa nucleofector solution, 2 µg of vector DNA were added and carefully mixed. The cell suspension was transferred into an Amaxa cuvette and the cells transfected according to the manufacturer's program (Amaxa Nucleofector™ nuclear transfection apparatus - Lonza; Amaxa Kit Program: V X-0011). After the electroporation procedure, 500 µl of a pre-warmed culture medium containing serum and supplements were added. Culture medium composition was: RPMI media with 11 mM glucose and 2 mM GlutaMAX™ (Cat. # 61870, Life Technologies) supplemented with 10% (v/ v) FBS (Life Technologies), 1% (v/ v) penicillin/ streptomycin (Life Technologies), 12 mM HEPES (Life technologies), 1 mM Sodium Pyruvate (Life Technologies) and 0.1 mM of non-essential amino acids (Life Technologies). The cell suspension was then transferred into a 6-well cell culture plate and an additional 1 ml of the pre-warmed complete medium was added per well. Cells were incubated in a humidified incubator at 37°C and 5% CO2. Selection was at 30 µg/ml Blasticidin.

Lung derived cancer-associated fibroblasts (CAF) were isolated as described previously[37]. The local ethics committee “Ethik-Kommission der Medizinischen Fakultät am Universitätsklinikum Tübingen” approved the study (project number 396/2005V and 159/2011BO2) and a written informed consent was obtained from the patient. CAF were immortalized using a virus co-expressing hTERT and GFP (Lenti-hTERT-eGFP; Cat No- LG508, BioGenova), as described[38–40]. CAF were cultivated in

RPMI media with 11 mM glucose and 2 mM GlutaMAX™ supplemented with 10% (v/ v) FBS and 1% (v/ v) penicillin/ streptomycin (all from Life Technologies).

THP-1 cell line was purchased from ATCC (ATCC: TIB-202) cultured in RPMI media with 11 mM glucose and 2 mM GlutaMAX™ supplemented with 10% (v/v) FBS and 1% (v/v) penicillin/streptomycin (all from Life Technologies). For monitoring during the co-culture experiments, the THP-1 cell line was labelled with the fluorescent dye Cell tracker™ deep red (Invitrogen), according to manufacturer´s instructions.

Tagged cell lines were used to monitor the different cell lines in co-culture. For fluorescent-based assays / analysis, cultures were performed with non-tagged cell lines. All the cultures were maintained at 37°C in a humidified atmosphere of 5% CO2 and were sub–cultured every 3-4 days.

2.2 Peripheral blood-derived monocytes (PBM)

Peripheral blood mononuclear cells (PBMC) were isolated from buffy coats obtained from Portuguese Blood Institute. The buffy coats were diluted in phosphate buffer saline (PBS) containing 2% (v/v) FBS and 2 mM EDTA, layered on top of Lymphoprep™ (Stemcell Technologies) and centrifuged at 950*xg* for 25 minutes. The PBMCs were recovered from the interface and were washed with PBS containing 2% (v/ v) FBS and 2 mM EDTA. Monocytes were isolated from PBMCs by negative selection through magnetic separation using EasySep™ human monocyte isolation kit (Cat. #19359, Stemcell technologies) and cultured in RPMI media with 11 mM glucose and 2 mM GlutaMAX™ supplemented with 10% (v/ v) FBS and 1% (v/ v) penicillin/streptomycin (Basal Media). Primary monocytes monolayer cultures were maintained in basal media.

2.3 Microencapsulated cultures

NCI-H157 cell line was inoculated as a single cell suspension into 125 mL stirred-tank spinner vessels with flat centered cap and angled side arms (Corning) at a concentration of $3x10^5$ cells/mL with an agitation range of 80-100 rpm to induce aggregation. After 3 days, the spheroids were collected, centrifuged at low speed and combined with single-cells of CAF and THP-1/PBM in a ratio of 1:1:1. The spheroid and single-cell mix was

encapsulated in 1.1 % (w/ v) of Ultra Pure Ca^{2+} MVG alginate (UP MVG NovaMatrix, Pronova Biomedical), prepared in NaCl 0.9 % (w/ v) solution. The control groups were the combination of the cellular components (double co-cultures) at a ratio of 1:1 or alone (mono-culture). The microencapsulation was performed in an electrostatically driven unit, VarV1 (Nisco, Zurich, Switzerland) to generate beads with a diameter ranging from 600-700 µm. Alginate polymerization was attained with a solution of 20 mM $BaCl_2$ in 115 mM NaCl/ 5mM L-Histidine pH 7.4. The microcapsules were collected, washed in NaCl 0.9 % (w/ v) and cultured in RPMI media with 11 mM glucose and 2 mM GlutaMAX™ supplemented with 10% (v/ v) FBS and 1% (v/ v) penicillin/ streptomycin at a concentration of 1-3 × 10^5 cell/mL. Cultures were maintained until day 21 when using the THP-1 cell line and until day 10 when using the PBM in stirred conditions and 50% media exchange was performed at each 3-4 days. Samples were collected periodically for determination of culture viability, cell concentration and culture characterization[26,29].

2.4 Spheroid and capsule size

Capsule size was determined by measuring Ferret's diameter and the average tumor spheroid diameter was determined by the average of three diameters per spheroid, using the open source ImageJ software version 1.47 m (http://rsbweb.nih.gov/ij/)[26,29].

2.5 Drug studies

For the 3D-3-culture set up with the THP-1 cell line, the cultures were incubated with drugs 8 days after microencapsulation (day 11 of culture) at a concentration of 25 capsule/mL. Dose-response curves were performed, and cultures were incubated with established concentrations of Paclitaxel ($1x10^{-8}$ M), Cisplatin ($1x10^{-6}$ M) and Blz945 ($1x10^{-7}$ and $1x10^{-6}$ M). Drug incubation lasted 6 days, with media replenishment. For the 3D-3-culture set up with PBM, the cultures were incubated with BLZ945 4 days after microencapsulation (day 7 of culture) and the drug treatment lasted 3 days. After the drug treatment, metabolic activity, cell proliferation and apoptosis were assessed as

described below. For BLZ945 treatment, the macrophage phenotype was characterized by analysis of gene expression and immunodetection of cell surface markers.

2.6 Cell viability

Cell viability was assessed through a fluorescent membrane integrity assay to discriminate live from dead cells. Microcapsules were incubated with 10 µg/mL of fluorescein diacetate (FDA; Sigma-Aldrich) and 1 µM of TO-PRO® 3 (Invitrogen) and were observed under a fluorescence microscope (DMRB6000, Leica). Cells that accumulated the metabolized product of FDA were considered live and cells stained with TO-PRO® 3 were considered dead.

2.7 Apoptosis levels

Apoptosis levels in cultures after exposure to a drug were measured by NucView Apoptosis Assay (Cat. #30062, Biotium). Treated and non-treated cultures were incubated with the caspase 3 substrate Nucview for 90 minutes at 37°C and fixed with 4% (w/ v) formaldehyde with 4% (w/ v) sucrose in PBS for 20 minutes. The samples were mounted in Prolong® Gold antifade reagent containing DAPI (Cat. #P36935, Life Technologies).

2.8 Cell proliferation

Alginate microcapsules were dissolved in chelating solution (10 mM HEPES pH 7.4 with 100 mM EDTA) and centrifuged either at 50x*g* for 1 minute to recover the tumor spheroids or at 400x*g* for 5 minutes to recover all the cell components. Pellets were solubilized in water subjected to ultra-sounds to lyse cells. Cell proliferation was measured by the amount of DNA present in the samples using Quant-iT™ PicoGreen® dsDNA Assay Kit (Invitrogen). DNA quantification was used to quantify the number of cells throughout the culture and in drug studies. Cell proliferation was also assessed by the incorporation of Click-iT® EdU (Life Technologies) during DNA replication, according to manufacturer's instructions. Alginate microcapsules were incubated overnight with 10 µM of EdU and fixed with 4% (w/ v) formaldehyde with 4% (w/ v) sucrose in PBS for

20 minutes. The samples were mounted in Prolong® Gold antifade reagent containing DAPI (Life Technologies) and the fluorescence was measured in an Andor spinning disk microscope (Revolution XD, Andor).

2.9 Metabolic Activity

The reduction capacity of the cultures was measured by Presto-Blue™ Viability Reagent reduction assay (Cat. #A13262, Life Technologies), according to the manufacturer´s instructions. The samples were incubated with 1x Presto blue for 30 minutes at 37^{o}C and the fluorescence was read at 560 nm excitation and 590 nm emission in the micro plate reader Infinite®200 PRO (NanoQuant, Tecan Trading AG). ATP levels were measured by CellTiter–Glo® 3D Cell Viability Assay (Promega) according to the manufacturer's instructions. Cell media was removed from each well and capsules were dissolved and centrifuged for 3 minutes at 500x*g*. Subsequently, equal volumes of CellTiter-Glo® reagent and the correspondent media were added to the wells. Plates were incubated at room temperature for 120 minutes on a shaker and luminescence was measured in the micro plate reader Infinite®200 PRO (NanoQuant, Tecan Trading AG).

2.10 Immunofluorescence microscopy

Samples were collected and fixed in 4% (w/v) formaldehyde with 4% (w/v) sucrose in PBS for 20 minutes. Then, they were dehydrated in 30% (w/ v) sucrose for approximately 5 hours and embedded in Tissue-Tek® O.C.T. (Sakura) and frozen at -80C for cryosectioning. The frozen samples were sliced with a thickness of 10µm in a cryostat (Cryostat CM 3050S, Leica). The cryosections were permeabilized for 10 minutes with 0.1% (v/v) Triton X- 100 (Sigma-Aldrich), blocked with 0.2% (w/ v) fish-skin gelatin (FSG; Sigma-Aldrich) in PBS for 30 minutes. Primary and secondary antibodies were prepared in 0.125% (w/v) of FSG in PBS and incubated for 2 or 1.5 hours. The samples were mounted in Prolong® Gold antifade reagent containing DAPI (Life Technologies). The primary antibodies used were anti-collagen type I, IV, fibronectin, vimentin (all from Abcam), N-cadherin (R&D systems), E-cadherin (Santa Cruz Biotechnology) and

phalloidin for detection of F-actin (Invitrogen). Samples were visualized using a fluorescence microscope (DMRB6000, Leica).

2.11 Light-sheet fluorescence microscopy

The custom-made light-sheet microscope used for these experiments is an evolution of the SPIM-Fluid system [41]. CW lasers with excitation wavelengths of 488 nm (Cobolt, MLD 50 mW), 515 nm (TOPTICA, iBeam Smart 515-S 100 mW) and 637 nm (Cobolt, MLD 150 mW) are used for excitation. The light sheet is created by a pair of galvanometric mirrors (Thorlabs, GVSM002), conjugated with the illumination objectives (Nikon, PlanFluor 4x, NA 0.13). We use a 50/ 50 beamsplitter cube (Thorlabs, CCM1-BS013) to create double side illumination, increasing the quality of the images. On each arm, laser beams are expanded using a telescope system, composed of two achromatic doublets (Thorlabs, AC254-050-A-ML (f= 50 mm) and AC254-200-A-ML (f= 200 mm)), creating a flat top Gaussian beam profile. A relay lens set, with two achromatic lenses (Thorlabs, AC254-075-A-ML (f=75 mm)) is used in the right arm, so the planes are properly conjugated. Detection is performed in an up-right configuration, using water dipping objectives (Nikon, PlanFluor 10x, NA 0.3). An achromatic doublet (AC254-200-A-ML) forms an image onto a Hamamatsu Orca Flash4.0 cMOS camera chip. Different emissions filters (Chroma and Semrock: 520/ 15 (GFP), 590/ 50 (tdTomato), 638LP (Cell tracker deep red)) are selected using a motorized filter wheel (Thorlabs, FW102C).

Samples were fixed as described above, and directly imaged without any further manipulation. In order to increase the throughput of the system, samples are loaded into FEP tubes (which refractive index is matched to water, 1.33) and transported towards the detection objective field of view using a syringe pump (Tecan, Cavro Centris). Scanning of the encapsulated aggregates is performed by vertical translation of the tubes, using a motorized stage (PI M-501.1DG), through a fixed horizontal light sheet plane. This allowed a straightforward the evaluation of hundreds of 3D-3-cultures with different co-culture combination and at different time points. All the components of the microscope are controlled using the custom-made software (LabView) and the image processing is carried on Fiji.

2.12 Immunohistochemistry

Samples were fixed as described above and embedded in 1% (w/ v) high melting temperature agarose (Lonza), dehydrated in graded alcohols and then embedded in paraffin wax. Paraffin blocks were sectioned (3 mm) for Hematoxylin & Eosin and immunohistochemical staining. Immunohistochemistry was carried out in a BenchMark ULTRA Automated IHC/ISH slide staining system from Ventana Medical Systems, Inc. according to instrument specifications. Briefly, antigen retrieval was performed in the instruments using the standard antigen retrieval solutions. Staining was performed using as primary antibodies the following clones: Anti-CD45 (clone 2B11 + PD7/26 from Agilent/DAKO), CD68 PG-M1 clone PGM1 from Agilent/DAKO and CD163 (clone 10D6 from Leica Biosystems). OptiView DAB IHC Detection Kit from Ventana Medical Systems, Inc. was used as the visualization system for all. Sections of human tonsil were included in all slides as positive and negative controls. The resulting staining was evaluated by bright field microscopy. Quantification was performed using the image analysis software Image J, by applying the colour deconvolution plug in and determining the DAB-positive and negative areas. The results are expressed as the percentage of positive staining within the alginate capsule.

2.13 Flow Cytometry

Alginate microcapsules were dissolved with a chelating solution as indicated above and centrifuged at 600x*g* for 5 minutes. To analyze the surface expression of immune cells, CD45 (Cat. #555483, BD Pharmingen™, San Diego, USA), CD163 (Cat. #FAB1607A, R&D Systems) and CD206 (Cat. #321114, Biolegend) were used. The cell suspensions were incubated with the primary antibodies conjugated with a fluorophore for 45 minutes in PBS. The samples were centrifuged, washed and analyzed in a CyFlow space (Partec).

2.14 Cytokine analysis

Supernatant media were collected at day 4 and day 17 and centrifuged at 1000g for 5 minutes. Samples were snap- frozen and stored at -80^{o}C until use. The Bio-Plex Pro™ Human Chemokine Panel, 40-Plex #171AK99MR2 was applied and samples were

analyzed in a Bio-Plex® 200 System according to the manufacturer´s protocol (http://www.bio-rad.com/webroot/web/pdf/lsr/literature/10031990.pdf).

2.15 Gene expression analysis

Alginate microcapsules were dissolved with a chelating solution as indicated above, centrifuged at 400x*g* for 5 minutes. Pellets were snap- frozen and kept at -80^{o}C until RNA isolation. Total RNA was extracted from samples with the High Pure Isolation kit (Roche) and then converted to cDNA with Transcriptor High Fidelity cDNA synthesis kit (Roche), both according to the manufacturer's instructions. Real Time-PCR was performed using SYBR-Green (SYBR Green I Master Kit, Roche) in LightCycler 480 (Roche). Gene expression calculations were based in relative quantification using the comparative CT method ($2^{-\Delta\Delta CT}$) and RPL22 and HPRT1 endogenous expression were used as controls.

3. RESULTS

3.1 Advanced stage NSCLC spheroids maintain mesenchymal phenotype in 3D-3-culture

With the goal of establishing *in vitro* tumor models of NSCLC that incorporate the myeloid compartment found at the tumor site, 3D-3-cultures were established. Our strategy employed alginate microencapsulation and stirred culture described previously by our group [26,29], and summarized in Fig. 4.1 – A. The 3D-3-cultures were set up within alginate microcapsules of an average diameter of 652 ± 26 µm, with three cellular compartments – NSCLC (NCI-H157) tumor spheroids, cancer associated fibroblasts (CAF) and a monocytic cell line (THP-1) (Fig. 4.1 – B). Microencapsulated cells were maintained in stirred suspension culture for up to three weeks and presented high viability throughout culture time (Fig. 4.1 – C). Cell proliferation was homogeneous within the tumor spheroids and also in the remaining cellular compartments, as evidenced by Edu staining (Fig. 4.2 – A). Cell proliferation resulted in a 10-fold increase in tumor cell concentration by week 3 (Fig. 4.2 – B), which was comparable to tumor cell growth in

monocultures and in double co-culture controls. Even though no statistical differences in the average spheroid diameter were observed between the 1st and 3rd week of

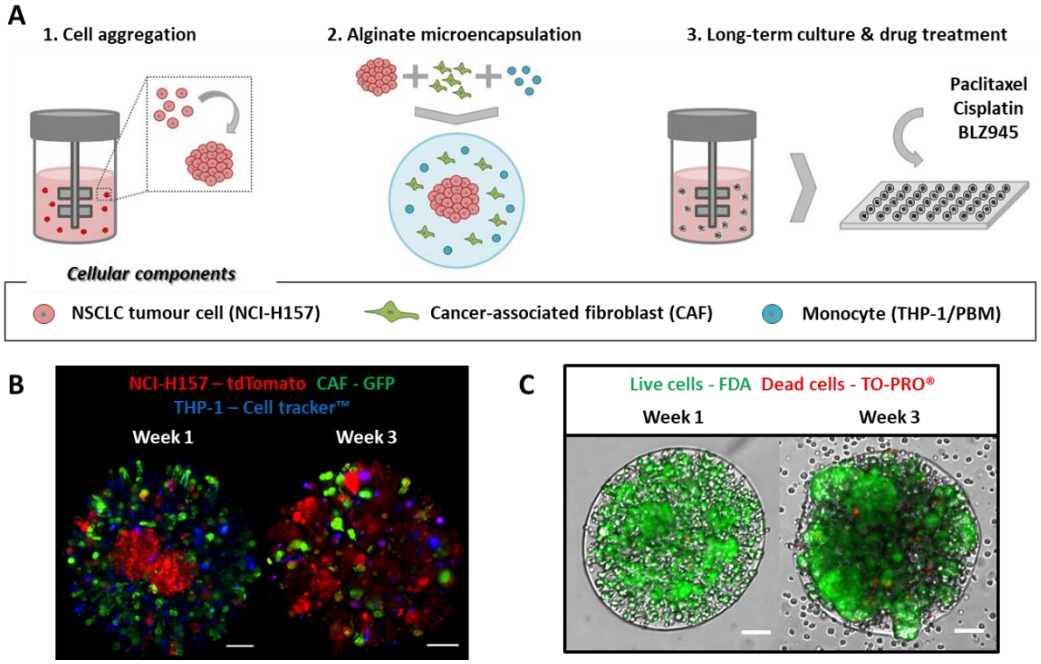

Figure 4.1 - Experimental approach and culture monitoring over time. A) Schematic representation of the experimental approach: 1 - Tumor cells were inoculated as single cells in stirred-tank vessels to promote cell aggregation. 2 - After 3 days, tumor spheroids and single-cells of CAF and THP-1 or PBM were mixed and encapsulated in alginate, resulting in microcapsules enclosing the three cellular components. 3 - The alginate microcapsules were maintained in long-term culture while culture characterization and drug treatments were performed. The representation is not to scale. **B)** Alginate microcapsules of the 3D-3-cultures in the 1st and 3rd week of culture visualized by light-sheet fluorescence microscopy. The cellular types are labelled by tdTomato (red) – NSCLC spheroids; GFP (green) – CAF; Cell tracker™ (blue) – THP-1. **C)** Live/dead assay of 3D-3-cultures in the 1st and 3rd week of culture: FDA (green) – live cells; TO-PRO-3 (red) – dead cells. Scale bars represent 100 µm.

culture, the number of spheroids per capsule increased over time and a high dispersion in the diameter of spheroids was observed in the 3rd week of culture (supplementary Fig. S4.1), which is in line with the increase in cell concentration. These results suggest that the presence of stromal and monocytic cell types had no major effect on tumor

proliferation and that there were no nutrient or spatial restrictions within the microcapsules.

Along the culture period, multiple spheroids and clusters of cells were found spread within the microcapsules in 3D-3-cultures, constituted by tumor, CAF and THP-1 cells (Fig. 4.1 – B). In contrast, 1-3 large spheroids were found in the microcapsules of tumor monocultures (Fig. 4.2 – A). Tumor spheroids within 3D-3-cultures were composed of cells positive for N-cadherin and vimentin, with low E-cadherin expression (data not shown) and presented loose cell architecture, as evidenced by F-actin staining (Fig. 4.2 – C), showing that NCI-H157 cells maintain their typical mesenchymal phenotype upon microencapsulated spheroid culture.

Moreover, collagen type I (Col I), collagen type IV (Col IV) and Fibronectin (FN) accumulated in the alginate microcapsules intercalated with cell spheroids, clusters and single cells, in a tissue-like phenotype (Fig 4.2 – D). The accumulation of ECM (*e.g.* Col I) was marked in the edges of the alginate microcapsules, in which the cells aligned in between the collagen fibers, displaying a migratory phenotype. These results suggest that the model set up was permissive to cell movement within the microcapsules, accommodating cell-cell interactions occurring between the different cell compartments, which may be promoted by the ECM accumulation[42,43].

3.2 Myeloid cells infiltrate into the tumor spheroids and display a TAM-like phenotype

To fully assess the model's capability of recapitulating the immune contexture, namely the trans-polarization of monocytic THP-1 cells into myeloid M2-like macrophages and their infiltration into human NSCLC tumors, the M2-like macrophage population was characterized in detail.

$CD45^+$ (protein tyrosine phosphatase, receptor type, C/PTPRC; pan leukocyte marker) cells were detected in small clusters around larger tumor spheroids and as single-cells dispersed in between the latter, both in 3D-3-cultures and in tumor-immune co-culture

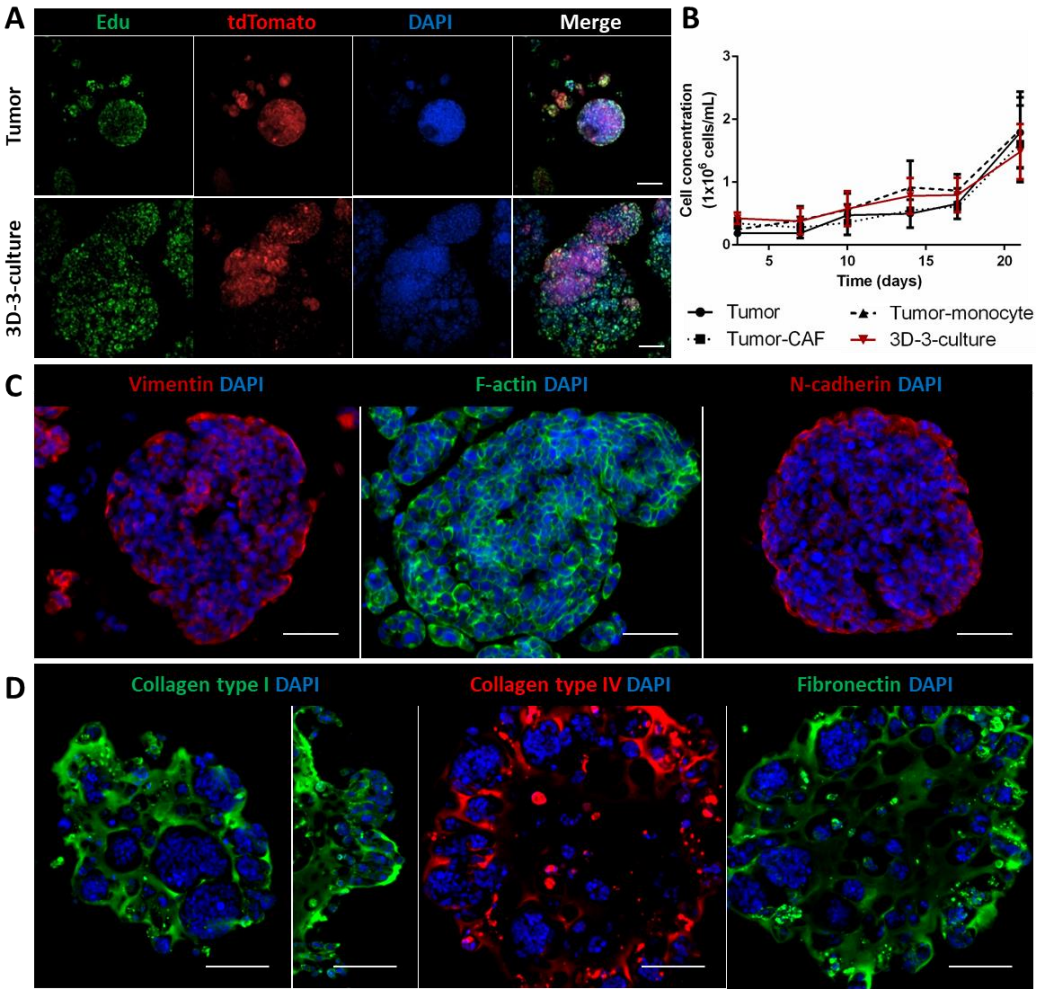

Figure 4.2 - Phenotypic characterization of tumor spheroids and ECM accumulation in alginate microcapsules. A) Cell proliferation and morphology of tumor spheroids in mono- (upper panel) and 3D-3-cultures (lower panel) at day 14 of culture. From the left: Edu (green) – proliferative cells; tdTomato (red) - NCI-H157; DAPI (blue) – Nuclei and merge of all channels. **B)** Tumor cell concentration profile of mono-, double co-cultures and 3D-3-culture along 3 weeks of culture; data are mean ± SEM from three independent experiments. **C-D)** Immunofluorescence microscopy of 3D-3-culture alginate microcapsules in 10 µm thick cryosections, at day 21, of **C)** Tumor cells: Vimentin (red), F-actin (Phalloidin; green); N-cadherin (red) and Nuclei (DAPI; blue). Scale bars represent 50 µm and **D)** ECM: Collagen type I (green), Collagen type IV (red), Fibronectin (green) and Nuclei (DAPI; blue). Scale bars represent 100 µm.

controls (Fig.4.3 – A). Furthermore, the presence of $CD45^+$ cells distributed within tumor

spheroids suggests that alginate microcapsules allow cell migration and that the generated TME within the microcapsules drives the infiltration of myeloid cells into the tumor spheroids. The immunohistological staining of CD68 (Cluster of Differentiation 68) (Fig. 4.3 – A), which is highly expressed in tissue macrophages, was similar to CD45. CD68 expression together with cell morphology supports differentiation of most monocytes into macrophages.

Cells positive for CD163 (scavenger receptor for the hemoglobin-haptoglobin complex), an M2-like macrophage marker, were detected in 3D-3-cultures (Fig. 4.3 – A). $CD163^+$ cells could also be detected in tumor-immune, but in CAF-immune co-cultures and THP-1 monocultures only residual levels were detected (Fig. 4.3 – A and supplementary Table S4.1). This data strongly suggests that the presence of both NCI-H157 spheroids and CAF are required to promote the differentiation of monocytic cells towards M2-like macrophages and that polarization of THP-1 cells depends on the interaction with other cell types. While most of the $CD45^+$ cells were detected in clusters, on the edges and inside the spheroids, $CD163^+$ cells were mostly infiltrated in tumor spheroids (Fig. 4.3 – A).

We also analyzed the secretory profile of the cultures, screening for the presence of cytokines and chemokines associated with immunosuppressive environment and invasive phenotype (Fig. 4.3 – B). Tumor cells in monoculture secreted IL4, IL13, IL10 and CXCL1 cytokines previously described as associated with macrophage recruitment and induction of an M2-like activation state[44–48]. Moreover, in 3D-3-cultures, there was an increased secretion of metalloproteinase-9 (MMP9) and of cytokines typically expressed by M2-like macrophages, namely CCL22 and CCL24[49–51]. The secretion profile and immunodetection show that M2-like macrophages are present in 3D-3-cultures.

We also established 3D-3-culture models with donor-derived peripheral blood monocytes (PBM), isolated from peripheral blood mononuclear cells (PBMC). PBM maintained high cell viability over 7 days when cultured as 3D-3-cultures. After 4 days, approximately 70 to 80% of $CD45^+$ cells expressed the M2-like markers CD206 and

CD163 while in microencapsulated mono-cultures (Microencapsulated PBM) this percentage was significantly lower, around 2 to 6% (Fig. 4.3 – C). In comparison with the 2D cultures (2D PBM), the differences in percentage of differentiated cells were less evident, although median fluorescence intensity of each marker was higher in 3D-3-culture (Sup. Fig. S4.2). This suggests that the phenotype of the macrophages expressing

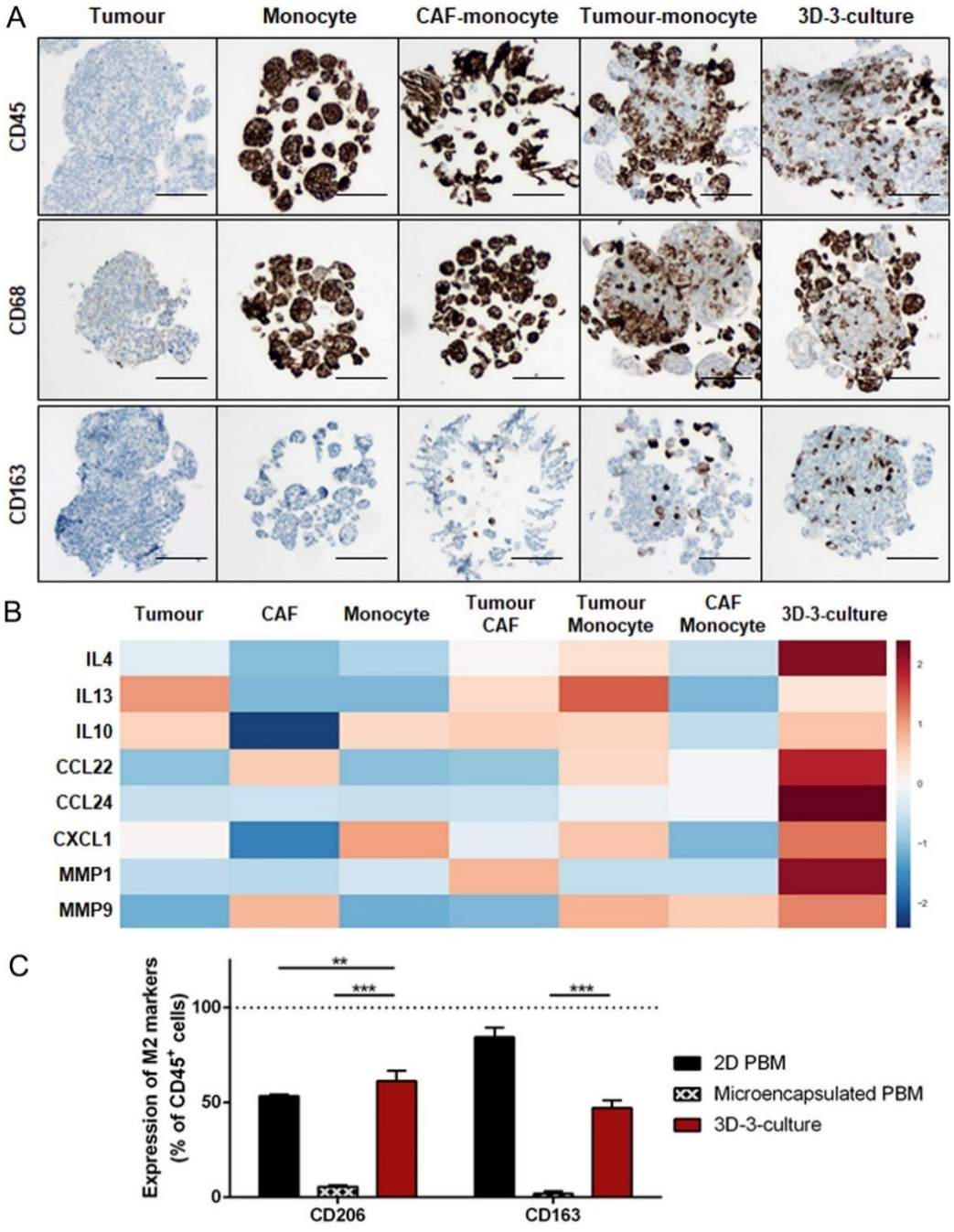

Legend on the next page

Figure 4.3 - Characterization of the immunosuppressive TME in 3D-3-cultures. A) Immunohistochemistry staining of alginate microcapsules in 3 µm thick paraffin sections after 3 weeks of culture with the immune markers CD45, CD68 PG-M1 and CD163. From the left: Tumor and monocyte mono-cultures, CAF-monocyte and tumor-monocyte double co-cultures and 3D-3-culture. Scale bars represent 100 µm. **B)** Heat map of the cytokine profile of IL4, IL13, IL10, CCL22, CCL24, CXCL1, MMP1 and MMP9, represented in z-score. From left: Mono-cultures of tumor, CAF and monocytes, double co-cultures of tumor-CAF, tumor-monocyte, CAF-monocyte and 3D-3-culture. All the proteins presented had a significant differential expression ($p \leq 0.05$) by ANOVA analysis. **C)** Immunodetection of cells double positive for the leucocyte marker CD45 and M2-associated markers CD163 and CD206 of peripheral blood derived macrophages 4 days after isolation in monolayer mono-culture (2D PBM) and microencapsulated mono-culture (Microencapsulated PBM) and in 3D-3-cultures (with tumor cells and CAF). Data are mean ± SEM from up to six independent experiments. * indicate significant differences between different cultures; (***$p < 0.001$; **$p < 0.01$) by an unpaired t-student test.

M2-like markers was different, pointing to a higher maturation in the 3D-3-culture. Altogether, these observations indicate that not only an immortalized monocytic cell line, but also primary monocytes polarize into M2-like macrophages in the 3D-3-culture setup.

3.3 Effects of chemo- and immunotherapies can be assessed in 3D-3-culture

As proof-of-concept that the 3D-3-culture setup allows the study of the effect of drugs in an immunity relevant context, we challenged it with Cisplatin and Paclitaxel, two chemotherapeutic drugs routinely used in the treatment of NSCLC [52,53], as well as BLZ945, an immunomodulatory drug targeting CSF1R (Colony Stimulating Factor 1 Receptor) [16,17,54,55]. This receptor was upregulated over time in 3D-3-culture (data not shown) and previous reports showed that its inhibition leads to decreased proliferation of BM-derived monocytes and promotes repolarization of M2-like macrophages into an M1-like phenotype[16,18].

Dose-response curves for Cisplatin and Paclitaxel were established for tumor monocultures and the IC_{50} value was determined by measuring ATP levels and confirmed through additional readouts (resazurin reduction and DNA quantification) (Sup. Fig. S4.3).

Treatment with Paclitaxel led to a reduction of the ATP levels of tumor, CAF and monocyte monocultures, which ranged from 58 to 37% of the control (Fig. 4.4 – A). The 3D-3-culture and CAF-monocyte co-culture presented a metabolic activity of approximately 80% upon treatment, showing less sensitivity to the drug comparing with the mono-culture (Fig. 4.4 – A and sup. Fig. S4.4 – A). The lower drug response in 3D-3-cultures reflects the lower induction of apoptosis throughout the cultures, as observed by NucView™ fluorescence staining (Fig. 4.4 – C and sup. Fig. S4.4). Nevertheless, proliferating cells could still be detected in 3D-3-cultures, as well as in co-culture controls, in tumor spheroids and in the stromal and immune compartments. These data suggest that there is a subset of tumor and immune cells not affected by the drug (Fig. 4.4 – D).

In contrast to what was observed for Paclitaxel, no significant differences were observed between the metabolic activity of tumor monoculture and the 3D-3-culture upon treatment with Cisplatin (Fig. 4.4 – B). The ATP levels of monocyte and CAF monocultures, as well as monocyte-CAF co-cultures ranged from 7 to 23% of the control, showing that all cell compartments were affected by the treatment (Fig. 4.4 – B). The generalized effect of cisplatin was also evident in the apoptosis fluorescence staining, in which apoptotic cells can be observed throughout the tumor, stromal and immune compartments (Fig. 4.4 – C and sup. Fig. S4.4). Concomitantly, hardly any proliferative cells were detected after treatment in the 3D-3-culture (Fig. 4.4 – D).

Concerning BLZ945 treatment, there were no significant alterations in ATP levels in THP-1 and tumor monocultures relative to the non-treated controls (Fig. 4.5 – A), suggesting that the concentrations employed were not acting through generalized toxicity mechanisms. BLZ945 induced a decrease in CD163 gene expression in 3D-3-cultures after drug treatment and an increase in the expression of the M1-associated gene CCR7

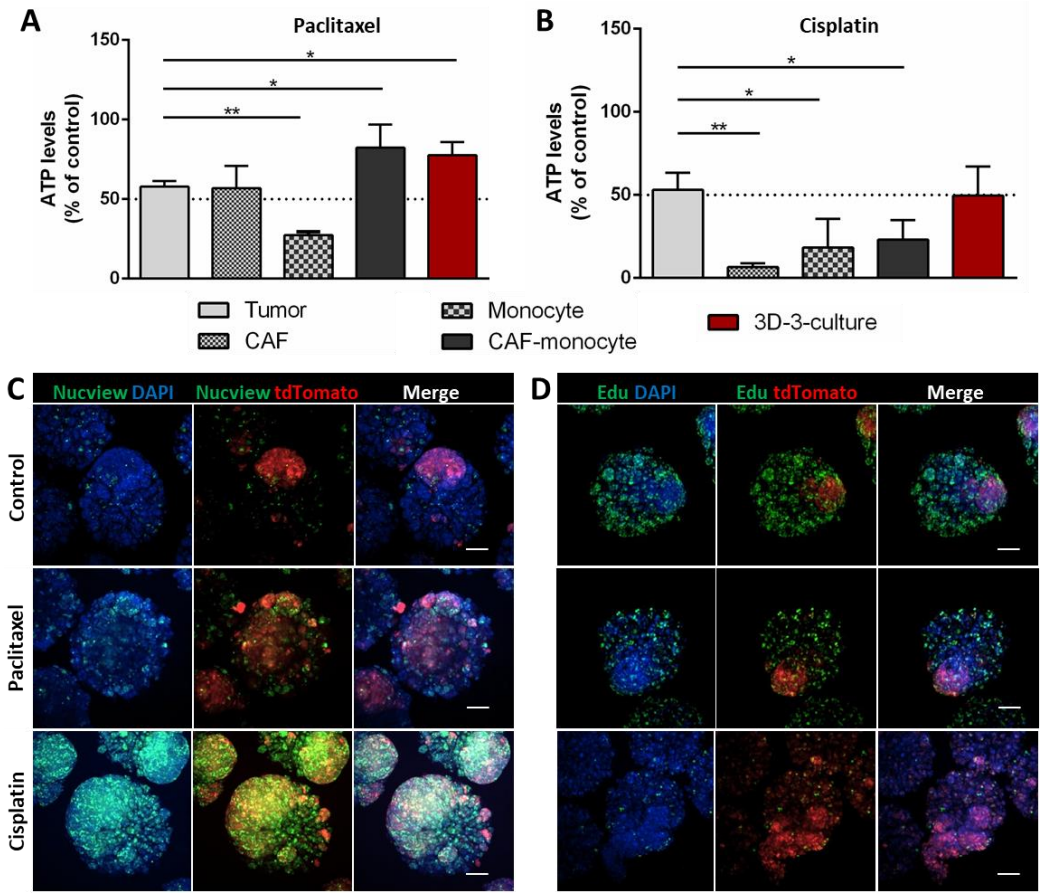

Figure 4.4 - Chemotherapeutic treatment in 3D-3-culture. Metabolic activity (ATP levels) of **A)** Paclitaxel (10^{-8} M) and **B)** Cisplatin (10^{-5} M) treated mono-cultures of tumor, monocyte and CAF, double co-culture of CAF-monocyte and 3D-3-culture. Data are mean ± SEM from three independent experiments. * indicate significant differences between tumor and other cultures by an unpaired t-student test (**p<0.01, *p<0.05). Immunofluorescence images of 3D-3-culture after treatment and respective controls for analysis of **C)** apoptosis: NucView™ (green) - apoptotic cells; tdTomato (red) – NCI-H157; DAPI (blue) - nuclei; and **D)** proliferation: Edu (green) - proliferative cells; tdTomato (red) - NCI-H157; DAPI (blue) - nuclei. Scale bars represent 100 µm.

(C-C chemokine receptor type 7; Fig. 4.5 – B). The expression of PTPRC (CD45) also increased up to 2-fold, although there was no evidence of alteration of the numbers of immune cells either due to apoptosis or proliferation (Fig. 4.5 – B). Gene expression of CSF1R increased up to 1.8-fold (Fig. 4.5 – B), in accordance to what has been previously reported in cultured primary monocytes[18]. CCR7 gene expression also increased after

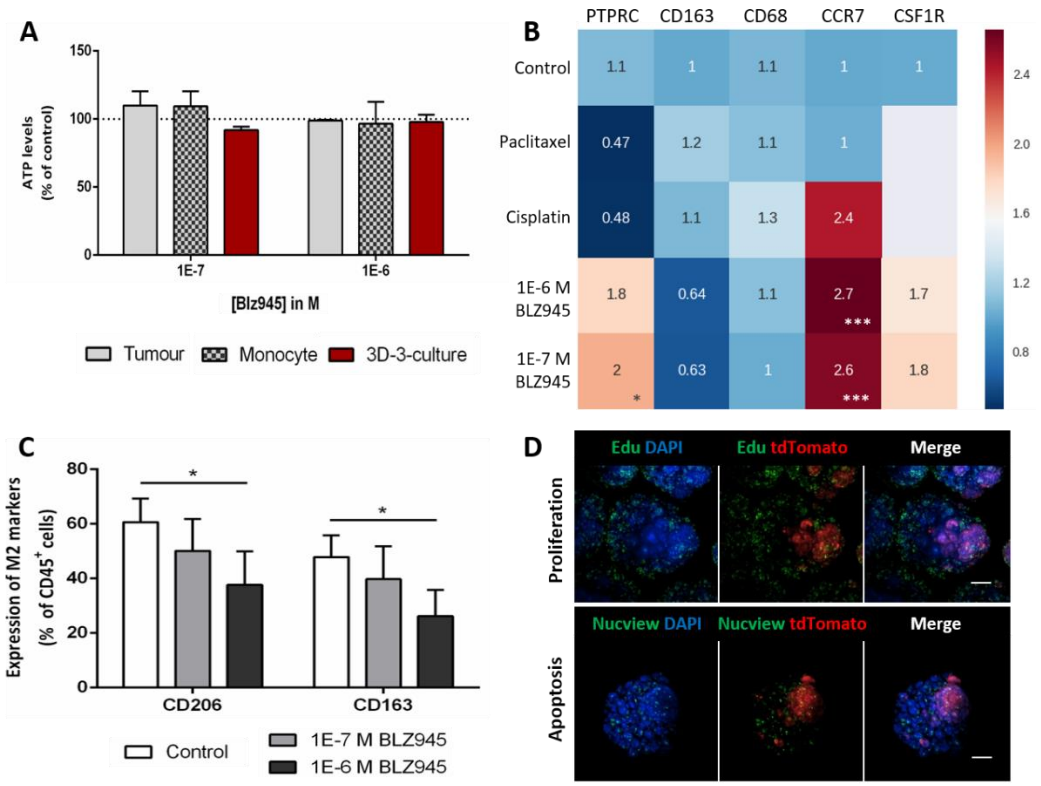

Figure 4.5 - Immunotherapeutic treatment in 3D-3-culture. A) Metabolic activity (ATP levels) of cultures after treatment with 10^{-7} and 10^{-6} M of BLZ945 in tumor and monocyte mono-cultures and 3D-3-culture. Data are mean ± SEM for three independent experiments. **B)** Heat map with fold increase in gene expression of macrophage markers after treatment with chemotherapeutic and immunotherapeutic drugs in 3D-3-culture, relatively to the non-treated controls. Data are mean from three independent experiments. * indicate significant differences of treated conditions to control by a two-way ANOVA and a Sidak's multiple comparison test (***$p < 0.001$, *$p < 0.05$). **C)** Immunodetection of cells double positive for the leucocyte marker CD45 and M2-associated markers CD163 and CD206 of 3D-3-cultures with donor-derived monocytes with and without treatment with BLZ945 (10^{-7} and 10^{-6} M). Data are mean ± SEM from three independent experiments. * indicate significant differences between treated conditions and control by a paired t-student test (*$p < 0.05$). **D)** Immunofluorescence images of (10^{-6} M) BLZ945 treated cultures, showing apoptosis in the upper panel: NucView™ (green) - apoptotic cells; tdTomato (red) – NCI-H157; DAPI (blue) - nuclei; and proliferation in the lower panel: Edu (green) - proliferative cells; tdTomato (red) – NCI-H157; DAPI (blue) – nuclei. Scale bars represent 100 µm.

cisplatin treatment, while expression of CD68 and CD163 remains unchanged (Fig. 4.5 –

B). This may suggest that, in addition to the depletion of immune cells, the phenotype of the surviving macrophage population is also modulated in cisplatin-treated cultures. In fact, several reports have indicated that cisplatin plays a role in immunomodulation, specifically by altering the ratio of M2/M1-like macrophages[56,57].

In PBM-3D-3-cultures treated with $1x10^{-6}$ M of BLZ945, there was a reduction of up to 39% of $CD206^+$ cells and up to 45% reduction in $CD163^+$ cells (Fig. 4.5 – C). These results suggest that the treatment with BLZ945 leads to a decrease in the M2-like macrophage population in 3D-3-cultures both with the THP-1 cell line and with PBM, which may be attributed to a repolarization from M2- to the M1-like macrophage phenotype, as previously reported [16,18]. This repolarization of the macrophage compartment did not have a significant impact on the viability of tumor cells in 3D-3-culture (Fig. 4.5 – A, D). Nevertheless, the results demonstrate that our model is suitable to perform immunomodulation studies *in vitro*, allowing the depiction of specific effects on each cellular component.

4. DISCUSSION

Extensive studies have shown that the tumor microenvironment (TME) is important for disease progression and drug response, however, its integration into drug screening platforms has been difficult due to the lack of cellular models amenable for throughput screening. In this work, we describe the development of a 3D-3-culture system, combining alginate microencapsulation and stirred culture, which incorporates tumor spheroids, cancer-associated fibroblasts and trans-polarized macrophages in an environment where the dynamic interaction between each compartment is recapitulated. Our results demonstrate that the 3D-3-culture allows polarization of a monocytic cell line (THP-1) and peripheral blood-derived monocytes (PBM) into tumor-associated macrophages (TAM) and infiltration in the tumor tissue, which can be modulated upon exposure to chemotherapeutic and immunomodulatory drugs. This system allows the study of monocyte recruitment, as well as, phenotype induction in a robust system, with continuous monitoring and compatible with drug screening platforms.

In the 3D-3-culture, NCI-H157 tumor cells maintained their proliferative state and displayed phenotypic markers typical of aggressive stages of NSCLC, such as expression of N-cadherin and vimentin, coupled with low expression of E-cadherin. This pattern, typical of late-stage epithelial-to-mesenchymal transition, was also described for immunohistochemical analysis of human tissue samples from primary tumors of lung squamous cell carcinoma and correlates with advanced stage tumors[58]. Although no major differences in the proliferation and histological markers of tumor cells were observed upon co-cultivation with CAF and myeloid cells, there was an evident spatial remodeling of the different cell compartments within the alginate microcapsules over the course of the culture. This can be attributed to the ECM accumulation observed within the microcapsules (Col I, IV and FN) and the secretion of metalloproteinases (MMP1 and MMP9) and suggests an increased invasive phenotype in the 3D-3-culture. This secretory profile was previously described for co-cultures of tumor cells, fibroblasts and macrophages, and is associated with the acquisition of higher metastatic potential[34,59].

The 3D-3-culture model allowed for the recapitulation of key hallmarks of lung cancer immune microenvironment. Early reports indicate that spheroids are suitable for tumor-immune interaction studies[60,61], as tumor architecture is important in establishing the immunosuppressive TME found in human tumors[62–65]. In the 3D-3-culture, CD68 and $CD163^+$ cells were detected, pointing to macrophage polarization into an M2-like phenotype, as described for primary tumors of NSCLC[66,67]. Moreover, a high proportion of $CD163^+$ cells was detected within tumor spheroids, demonstrating that the developed model was conducive to cell migration, as occurs with the myeloid infiltrate in human lung cancers. Although the detection of $CD163^+$ cells was also observed in tumor-immune and CAF-immune co-culture controls, however, at a much lower level. This is in line with previous reports suggesting that the stromal compartment is also primarily involved in the recruitment and activation of monocytes in the TME[68], as CAF exhibit an activated fibroblast phenotype, with altered secretory profile and ECM production[23,69]. In fact, in co-culture models of blood monocytes

with breast cancer or CAF spheroids, monocyte migration was higher towards CAF spheroids, a phenotype linked to overexpression of CCL2[70].

A significant feature of the developed 3D-3-culture model for tumor modelling is the use of an inert scaffold, as the introduction of physiologically relevant ECM remains a fundamental challenge for tumor modelling in current *in vitro* settings[22]. Routinely used Matrigel or collagen-based artificial ECM substrates do not represent the predominant ECM proteins found in the target tissue[22]. We demonstrate that the alginate microcapsules allow the accumulation of collagen type I and IV, forming collagen fibers that intercalate cells, and fibronectin, resembling the tissue architecture and contributing to the migration and tissue remodeling within the microcapsules. This cell remodeling allows cell interactions to occur naturally, resulting in a cell distribution within the alginate microcapsules that presents features existent in the human tissue of NSCLC patients, such as macrophage infiltration and extravasation of tumor cells to the surrounding stroma[71].

The accumulation of a cocktail of soluble factors plus the cell-cell interactions observed have a key role in modulating the phenotype of macrophages in the 3D-3-culture model, since the polarization of macrophages was not promoted by the supplementation with cytokines. Analysis of the secretory profile in the 3D-3-culture model evidenced the formation of an immunosuppressive environment. Therefore, the induction of an M2-like phenotype observed may be explained by the accumulation of IL4, IL13, IL10 and CXCL1, cytokines previously described to contribute to the referred phenotype[44–46]. Furthermore, a specific accumulation of CCL22 and CCL24 in week three of the 3D-3-cultures was observed. Both cytokines were previously reported to be produced by TAMs and are involved in the recruitment and differentiation of regulatory T cells to the TME, which correlate with poor prognosis and suppress antitumor-specific immune responses[15,51,72]. MMP9 was also upregulated primarily in 3D-3-cultures. This metalloprotease was reported to be expressed by TAMs from primary lung cancer tissue and its expression is correlated with disease progression in NSCLC patients[73]. Recent reports also highlight the important role of cell-cell interactions. Specifically, binding of tumor-associated mucin O-glycans to lectin receptors on immune cells may promote

immune-tolerance and emergence of immune-resistant cancer cell variants[74–77] These studies were important to help dissect the TAM inducing stimuli, however, these were mainly conducted in models where the TME complexity is not represented (tumor cell monocultures), in a non-human setting (GEMM models) or using targeted approaches towards identifying the partners of previously described tumoral glycoconjugates or lectins. The developed 3D-3 model allows for cell-cell interaction between the different cell compartments. Therefore, it could be used to surpass some of the drawbacks of the above described models, and to allow the dissection of the concerted action of both soluble factors and cell-cell interactions in response to a given stimuli, namely anticancer therapy.

The development of novel and improved therapeutics is an area of intense study in cancer research but still presents huge attrition rates. One of the limitations of current pre-clinical platforms is the lack of integration of multiple TME compartments. The use of platinum-based compounds, such as cisplatin, for chemotherapy has shown clinical efficacy against several solid tumors, including NSCLC[78]. Paclitaxel, a microtubule-stabilizing agent, is another standard-of-care drug that induces cell death through interruption of mitosis[79]. Here we show that challenging our model with each compound led to different results. Although both drugs ultimately lead to cancer cell apoptosis, they present different mechanisms of action that might explain the different results obtained: paclitaxel is a microtubule stabilizer, whereas cisplatin crosslinks DNA. Treatment with cisplatin led to a generalized tumor cell apoptosis, which was not affected by the presence of other cells in the TME. Paclitaxel, on the other hand, leads to a less extensive apoptosis induction in the 3D-3-culture than in mono-cultures, suggesting that the reciprocal interactions occurring between the stromal and immune compartment may alter cell´s sensitivity to the drug. Such discrepancies are often observed when comparing response of *in vitro* drug screening platforms, devoid of TME, and *in vivo* drug sensitivity, highlighting the importance of incorporating the TME components when addressing drug response[80]. This shows that the developed model can aid in deciphering the microenvironmental regulation of therapeutic response. Moreover, the immunomodulatory effects of each chemotherapeutic agent could also

be depicted. Cisplatin treatment led to a significant increase in CCR7 expression in the surviving macrophage population, which was not evident for paclitaxel treatment. In fact, increasing preclinical and clinical evidence has shown that cisplatin can modulate the immune system alone or in combination with immunotherapies[56]. Early studies had already linked cisplatin action to the activation of macrophages into an antitumoral state[81,82]. These findings demonstrated that cisplatin significantly increases antigen-presenting ability of murine macrophages. It also alters the macrophages´ secretory profile. Costimulatory factors such as IL1, IL6, TNFα and NO, enhance autocrinally the antigen presenting and antitumor ability of other immune cells present in the TME[81,82]. More recently, adjuvant cisplatin chemotherapy increased antitumor efficacy through an increase of antigen specific $CD8^+$ cells systemically and intratumorally and by shifting the M1-/M2-like phenotype ratio in mice[83]. On the other hand, paclitaxel tumor reducing effects seem to also involve a direct stimulation of TAM's cytotoxicity[84,85] and cytokine release, namely IL-12, TNFα and iNOS by TAM[84,86]. However, its potential for inducing immunogenic cell death (ICD) by mitosis catastrophe-mediated tumor cell death is not fully understood[84].

Upon challenging the 3D-3-culture with the CSF1R inhibitor BLZ954, a significant decrease in the expression of CD206 and CD163 in the macrophage population was observed. CSF1R activation has been linked with proliferation and survival of macrophages, but also with the expression of M2-like genes[87]. Its inhibition is a promising anticancer strategy showing reduced tumor size and improved survival in a mouse breast tumor model[88] and leading to a significant clinical activity in patients[17]. Several reports have also shown that the effect of CSF1R inhibition in TAM could not only be dependent on macrophage depletion, but rather a repolarization into a more M1-like anti-tumor macrophage phenotype[16,55]. These effects could be recapitulated in our model which indicates that it is able to depict the immunomodulatory effects previously observed for mouse models in a human relevant TME context[16,55].

In conclusion, we have developed a 3D-3-culture model that mimics the dynamic interaction between tumor, stromal and immune compartments, alongside

accumulation of ECM and secreted factors. This contributed to the maintenance of key features of advanced stage lung carcinoma, including the immunosuppressive environment. This model allowed the activation of monocytes into a TAM-associated phenotype without addition of external factors and the macrophage phenotype could be modulated upon treatment with immune-targeting and chemotherapeutic drugs. One of the main features of the 3D-3-culture system is that it is scalable, compatible with drug screening platforms and flexible, combining the use of cell lines with primary immune cells (PBM). This system is also transferable to other pathologies, by using tumor cell lines of other cancer types, such as breast cancer. Establishing *in vitro* models using cell lines enables the labelling of individual cell types. These models can be complemented with single cell imaging for tracking the response of specific cell compartments to a given stimuli, or with gene editing tools, such as CRISPR–Cas9 system, for the development of more translatable *in vitro* models of disease[22]. Nevertheless, this culture system may also be adapted to incorporate patient-derived tumor samples for *ex vivo* assessment of therapeutic efficacy using precision medicine approaches for translational research.

5. SUPPLEMENTARY MATERIAL

Supplementary Table S4.1 - Quantitative analysis of CD68 and CD163 immunohistochemistry staining in the different culture groups. Data is expressed as the percentage of positive staining among the total cell area. Data are mean + SD of a minimum of 7 capsules per condition.

	Tumour	Monocyte	CAF Monocyte	Tumour Monocyte	3D-3-culture
CD68 (%)	-	≥ 99	≥ 95	21.8 ± 9.2	21.4 ± 8.6
CD163 (%)	-	0.11 ± 0.08	2.1 ± 1.3	3.9 ± 1.5	3.2 ± 1.9
Ratio CD163/CD68 (%)	-	≤1	≤3	15-20	15-20

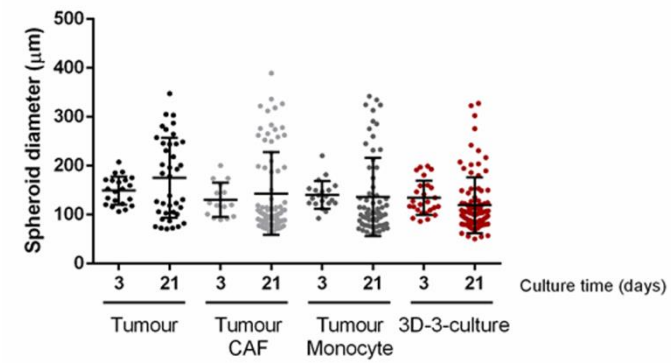

Supplementary Figure S4.1 - Analysis of tumour spheroid diameter over time (day 3 and day 21) for the different culture groups: tumour monocultures, tumour-CAF and tumour-monocyte co-cultures and 3D-3-culture. Data are mean ± SD from 12 capsules from independent experiments. Statistical analysis was performed using an unequal variances t-test.

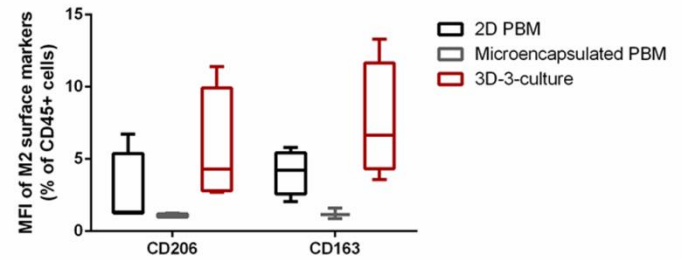

Supplementary Figure S4.2 - Mean fluorescence intensity of cells double positive for the leucocyte marker CD45 and M2-associated markers CD163 and CD206 of peripheral blood derived macrophages 4 days after isolation in monolayer mono-culture (2D PBM) and microencapsulated mono-culture (Microencapsulated PBM) and in 3D-3-cultures (with tumour cells and CAF). Data are mean ± SEM from up to six independent experiments.

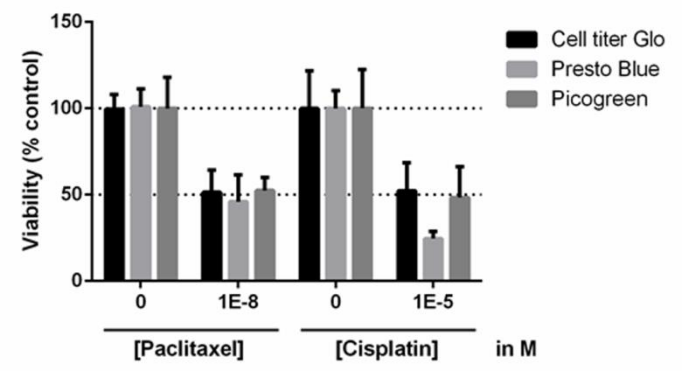

Supplementary Figure S4.3 – Comparison between methods to determine cell viability in tumour monocultures, when exposed to the half maximal inhibitory concentrations (IC50) of Cisplatin and Paclitaxel. Cell titer Glo measures ATP levels, Presto blue measures resazurin reduction capacity and Picogreen measures dsDNA. Data are mean + SEM of up to 3 independent experiments.

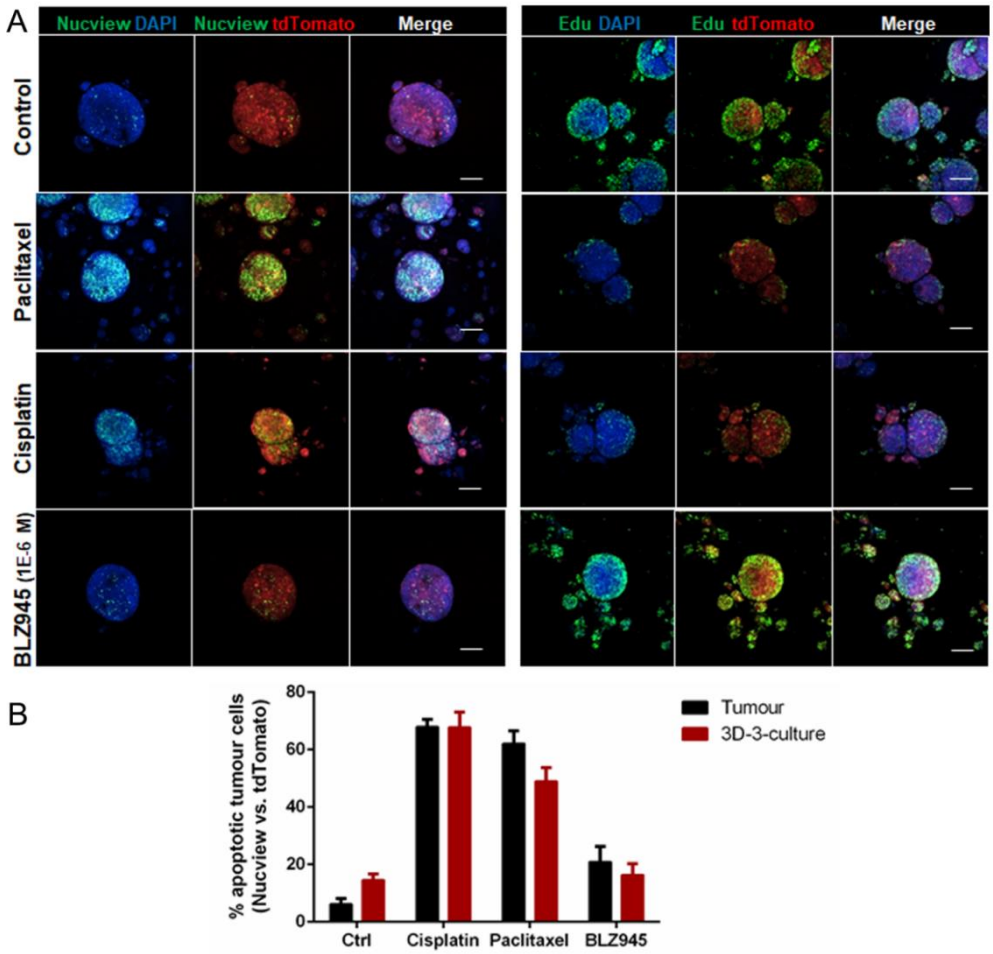

Supplementary Figure S4.4 - Analysis of apoptosis and proliferation of cultures upon drug treatment. Immunofluorescence images of monocultures after treatment and respective controls for analysis of (A) apoptosis: Nucview (green) - apoptotic cells; tdTomato (red) – NCI-H157; DAPI (blue) - nuclei; and (B) proliferation: Edu (green) - proliferative cells; tdTomato (red) – NCI-H157; DAPI (blue) – nuclei. Scale bars represent 100 µm. C) Quantitative analysis of apoptotic cells in the tumour cell subset in mono- and 3D-3-cultures (green vs. red channel). Data are mean + SEM of a minimum of three images per condition.

6. AUTHOR CONTRIBUTION & ACKNOWLEDGEMENTS

The author performed part of the experiments, analyzed the data and wrote the manuscript. The author acknowledges Dr Vítor E. Santo for the discussions in the initial phase of the work. Also, support from the IMI Joint Undertaking (grant agreement no. 115188), MINECO/FEDER (Severo Ochoa SEV-2015-0522, BIO2014-59614-JIN, RYC-2015-17935), Fundación Privada Cellex, Fundación Mig-Puig and CERCA program and FCT (iNOVA4Health—UID/Multi/04462/2013, SFRH/BD/52202/2013, SFRH/BD/52208/2013).

7. REFERENCES

1. Quail, D. F. & Joyce, J. A. Microenvironmental regulation of tumor progression and metastasis. *Nat. Med.* **19,** 1423–37 (2013).
2. Nyga, A. *et al.* The next level of 3D tumour models: immunocompetence. *Drug Discov. Today* **21,** 1421–1428 (2016).
3. Sathyanarayanan, V. & Neelapu, S. S. Cancer immunotherapy: Strategies for personalization and combinatorial approaches. *Mol. Oncol.* **9,** 2043–2053 (2015).
4. Jeanbart, L. & Swartz, M. A. Engineering opportunities in cancer immunotherapy. *Proc. Natl. Acad. Sci.* **112,** 14467–14472 (2015).
5. Feder-Mengus, C., Ghosh, S., Reschner, A., Martin, I. & Spagnoli, G. C. New dimensions in tumor immunology: what does 3D culture reveal? *Trends Mol. Med.* **14,** 333–340 (2008).
6. Reck, M. *et al.* Pembrolizumab versus Chemotherapy for PD-L1–Positive Non–Small-Cell Lung Cancer. *N. Engl. J. Med.* **375,** 1823–1833 (2016).
7. Tang, H., Qiao, J. & Fu, Y.-X. Immunotherapy and tumor microenvironment. *Cancer Lett.* **370,** 85–90 (2016).
8. Bremnes, R. M. *et al.* The Role of Tumor Stroma in Cancer Progression and Prognosis: Emphasis on Carcinoma-Associated Fibroblasts and Non-small Cell Lung Cancer. *J. Thorac. Oncol.* **6,** 209–217 (2011).
9. Domagala-Kulawik, J. The role of the immune system in non-small cell lung carcinoma and potential for therapeutic intervention. *Transl. lung cancer Res.* **4,** 177–190 (2015).
10. Elliott, L. A., Doherty, G. A., Sheahan, K. & Ryan, E. J. Human Tumor-Infiltrating Myeloid Cells: Phenotypic and Functional Diversity. *Front. Immunol.* **8,** (2017).
11. Ostuni, R., Kratochvill, F., Murray, P. J. & Natoli, G. Macrophages and cancer: From mechanisms to therapeutic implications. *Trends Immunol.* **36,** 229–239 (2015).
12. Sica, A., Allavena, P. & Mantovani, A. Cancer related inflammation: The macrophage connection. *Cancer Lett.* **267,** 204–215 (2008).
13. Solinas, G., Germano, G., Mantovani, A. & Allavena, P. Tumor-associated macrophages (TAM) as major players of the cancer-related inflammation. *J. Leukoc. Biol.* **86,** 1065–1073 (2009).
14. Mao, Y., Poschke, I. & Kiessling, R. Tumour-induced immune suppression: role of inflammatory mediators released by myelomonocytic cells. *J. Intern. Med.* **276,** 154–170 (2014).
15. Noy, R. & Pollard, J. W. Tumor-Associated Macrophages: From Mechanisms to Therapy.

Immunity **41,** 49–61 (2014).
16. Pyonteck, S. M. *et al.* CSF-1R inhibition alters macrophage polarization and blocks glioma progression. *Nat. Med.* **19,** 1264–1272 (2013).
17. Ries, C. H. *et al.* Targeting tumor-associated macrophages with anti-CSF-1R antibody reveals a strategy for cancer therapy. *Cancer Cell* **25,** 846–859 (2014).
18. Mao, Y. *et al.* Targeting Suppressive Myeloid Cells Potentiates Checkpoint Inhibitors to Control Spontaneous Neuroblastoma. *Clin. Cancer Res.* **22,** 3849–3859 (2016).
19. Cuccarese, M. F. *et al.* Heterogeneity of macrophage infiltration and therapeutic response in lung carcinoma revealed by 3D organ imaging. *Nat. Commun.* **8,** 14293 (2017).
20. Sharma, S. V., Haber, D. A. & Settleman, J. Cell line-based platforms to evaluate the therapeutic efficacy of candidate anticancer agents. *Nat. Rev. Cancer* **10,** 241–253 (2010).
21. Lovitt, C. J., Shelper, T. B. & Avery, V. M. Cancer drug discovery: recent innovative approaches to tumor modeling. *Expert Opin. Drug Discov.* **11,** 885–894 (2016).
22. Horvath, P. *et al.* Screening out irrelevant cell-based models of disease. *Nat. Rev. Drug Discov.* **15,** 751–769 (2016).
23. Turley, S. J., Cremasco, V. & Astarita, J. L. Immunological hallmarks of stromal cells in the tumour microenvironment. *Nat. Rev. Immunol.* **15,** 669–682 (2015).
24. Hutchinson, L. & Kirk, R. High drug attrition rates—where are we going wrong? *Nat. Rev. Clin. Oncol.* **8,** 189–190 (2011).
25. Liu, Z., Delavan, B., Roberts, R. & Tong, W. Lessons Learned from Two Decades of Anticancer Drugs. *Trends Pharmacol. Sci.* **38,** 852–872 (2017).
26. Santo, V. E. *et al.* Adaptable stirred-tank culture strategies for large scale production of multicellular spheroid-based tumor cell models. *J. Biotechnol.* **221,** 118–129 (2016).
27. Hickman, J. a. *et al.* Three-dimensional models of cancer for pharmacology and cancer cell biology: Capturing tumor complexity in vitro/ex vivo. *Biotechnol. J.* **9,** 1115–1128 (2014).
28. Weiswald, L.-B., Bellet, D. & Dangles-Marie, V. Spherical Cancer Models in Tumor Biology. *Neoplasia* **17,** 1–15 (2015).
29. Estrada, M. F. *et al.* Modelling the tumour microenvironment in long-term microencapsulated 3D co-cultures recapitulates phenotypic features of disease progression. *Biomaterials* **78,** 50–61 (2016).
30. Kuen, J., Darowski, D., Kluge, T. & Majety, M. Pancreatic cancer cell/fibroblast co-culture induces M2 like macrophages that influence therapeutic response in a 3D model. *PLoS One* **12,** e0182039 (2017).
31. Martinez-Marin, D. *et al.* PEDF increases the tumoricidal activity of macrophages towards prostate cancer cells in vitro. *PLoS One* **12,** e0174968 (2017).
32. Linde, N., Gutschalk, C. M., Hoffmann, C., Yilmaz, D. & Mueller, M. M. Integrating macrophages into organotypic co-cultures: A 3D in vitro model to study tumor-associated macrophages. *PLoS One* **7,** (2012).
33. Rama-Esendagli, D., Esendagli, G., Yilmaz, G. & Guc, D. Spheroid formation and invasion capacity are differentially influenced by co-cultures of fibroblast and macrophage cells in breast cancer. *Mol. Biol. Rep.* **41,** 2885–2892 (2014).
34. Liu, X., Kiefl, R., Roskopf, C., Tian, F. & Huber, R. M. Interactions among Lung Cancer Cells, Fibroblasts, and Macrophages in 3D Co-Cultures and the Impact on MMP-1 and VEGF Expression. *PLoS One* **11,** e0156268 (2016).
35. Nakasone, E. S. *et al.* Imaging Tumor-Stroma Interactions during Chemotherapy Reveals Contributions of the Microenvironment to Resistance. *Cancer Cell* **21,** 488–503 (2012).
36. Schambach, A. *et al.* Overcoming promoter competition in packaging cells improves production of self-inactivating retroviral vectors. *Gene Ther.* **13,** 1524–1533 (2006).
37. Haubeiss, S. *et al.* Dasatinib reverses Cancer-associated Fibroblasts (CAFs) from primary Lung Carcinomas to a Phenotype comparable to that of normal Fibroblasts. *Mol. Cancer* **9,**

168 (2010).
38. Madar, S. *et al.* Modulated expression of WFDC1 during carcinogenesis and cellular senescence. *Carcinogenesis* **30,** 20–27 (2009).
39. Rudisch, A. *et al.* High EMT Signature Score of Invasive Non-Small Cell Lung Cancer (NSCLC) Cells Correlates with NFκB Driven Colony-Stimulating Factor 2 (CSF2/GM-CSF) Secretion by Neighboring Stromal Fibroblasts. *PLoS One* **10,** e0124283 (2015).
40. Stock, K. *et al.* Capturing tumor complexity in vitro: Comparative analysis of 2D and 3D tumor models for drug discovery. *Sci. Rep.* **6,** 28951 (2016).
41. Gualda, E. J. *et al.* SPIM-fluid: open source light-sheet based platform for high-throughput imaging. *Biomed. Opt. Express* **6,** 4447 (2015).
42. Egeblad, M., Rasch, M. G. & Weaver, V. M. Dynamic interplay between the collagen scaffold and tumor evolution. *Curr. Opin. Cell Biol.* **22,** 697–706 (2010).
43. Gopal, S. *et al.* Fibronectin-guided migration of carcinoma collectives. *Nat. Commun.* **8,** 14105 (2017).
44. Mantovani, A., Marchesi, F., Malesci, A., Laghi, L. & Allavena, P. Tumour-associated macrophages as treatment targets in oncology. *Nat. Rev. Clin. Oncol.* **14,** 399–416 (2017).
45. Miyake, M. *et al.* CXCL1-Mediated Interaction of Cancer Cells with Tumor-Associated Macrophages and Cancer-Associated Fibroblasts Promotes Tumor Progression in Human Bladder Cancer. *Neoplasia* **18,** 636–646 (2016).
46. Shigdar, S. *et al.* Inflammation and cancer stem cells. *Cancer Lett.* **345,** 271–278 (2014).
47. Kumar, V., Patel, S., Tcyganov, E. & Gabrilovich, D. I. The Nature of Myeloid-Derived Suppressor Cells in the Tumor Microenvironment. *Trends Immunol.* **37,** 208–220 (2016).
48. Gabrilovich, D. I., Ostrand-Rosenberg, S. & Bronte, V. Coordinated regulation of myeloid cells by tumours. *Nat. Rev. Immunol.* **12,** 253–268 (2012).
49. Jaguin, M., Houlbert, N., Fardel, O. & Lecureur, V. Polarization profiles of human M-CSF-generated macrophages and comparison of M1-markers in classically activated macrophages from GM-CSF and M-CSF origin. *Cell. Immunol.* **281,** 51–61 (2013).
50. Guo, Q. *et al.* New Mechanisms of Tumor-Associated Macrophages on Promoting Tumor Progression: Recent Research Advances and Potential Targets for Tumor Immunotherapy. *J. Immunol. Res.* **2016,** 1–12 (2016).
51. Martinez, F. O., Helming, L. & Gordon, S. Alternative Activation of Macrophages: An Immunologic Functional Perspective. *Annu. Rev. Immunol.* **27,** 451–483 (2009).
52. Dasari, S. & Bernard Tchounwou, P. Cisplatin in cancer therapy: Molecular mechanisms of action. *Eur. J. Pharmacol.* **740,** 364–378 (2014).
53. Chang, A. Chemotherapy, chemoresistance and the changing treatment landscape for NSCLC. *Lung Cancer* **71,** 3–10 (2011).
54. Strachan, D. C. *et al.* CSF1R inhibition delays cervical and mammary tumor growth in murine models by attenuating the turnover of tumor-associated macrophages and enhancing infiltration by $CD8^+$ T cells. *Oncoimmunology* **2,** e26968 (2013).
55. Zhu, Y. *et al.* CSF1/CSF1R Blockade Reprograms Tumor-Infiltrating Macrophages and Improves Response to T-cell Checkpoint Immunotherapy in Pancreatic Cancer Models. *Cancer Res.* **74,** 5057–5069 (2014).
56. de Biasi, A. R., Villena-Vargas, J. & Adusumilli, P. S. Cisplatin-Induced Antitumor Immunomodulation: A Review of Preclinical and Clinical Evidence. *Clin. Cancer Res.* **20,** 5384–5391 (2014).
57. Chang, C. L. *et al.* Dose-dense chemotherapy improves mechanisms of antitumor immune response. *Cancer Res.* **73,** 119–127 (2013).
58. Prudkin, L. *et al.* Epithelial-to-mesenchymal transition in the development and progression of adenocarcinoma and squamous cell carcinoma of the lung. *Mod. Pathol.* **22,** 668–678 (2009).

59. Chimal-Ramírez, G. K. *et al.* MMP1, MMP9, and COX2 Expressions in Promonocytes Are Induced by Breast Cancer Cells and Correlate with Collagen Degradation, Transformation-Like Morphological Changes in MCF-10A Acini, and Tumor Aggressiveness. *Biomed Res. Int.* **2013,** 1–15 (2013).
60. Hauptmann, S., Zwadlo-Klarwasser, G., Jansen, M., Klosterhalfen, B. & Kirkpatrick, C. J. Macrophages and multicellular tumor spheroids in co-culture: a three-dimensional model to study tumor-host interactions. Evidence for macrophage-mediated tumor cell proliferation and migration. *Am. J. Pathol.* **143,** 1406–15 (1993).
61. Ochsenbein, A. F. *et al.* Immune surveillance against a solid tumor fails because of immunological ignorance. *Immunology* **96,** 2233–2238 (1999).
62. Feder-Mengus, C. *et al.* Multiple mechanisms underlie defective recognition of melanoma cells cultured in three-dimensional architectures by antigen-specific cytotoxic T lymphocytes. *Br. J. Cancer* **96,** 1072–1082 (2007).
63. Ghosh, S. *et al.* Culture of melanoma cells in 3-dimensional architectures results in impaired immunorecognition by cytotoxic T lymphocytes specific for Melan-A/MART-1 tumor-associated antigen. *Ann. Surg.* **242,** 851–857, discussion 858 (2005).
64. Dangles, V. *et al.* Impact of human bladder cancer cell architecture on autologous T-lymphocyte activation. *Int. J. Cancer* **98,** 51–56 (2002).
65. Dangles-Marie, V. *et al.* A three-dimensional tumor cell defect in activating autologous CTLs is associated with inefficient antigen presentation correlated with heat shock protein-70 down-regulation. *Cancer Res.* **63,** 3682–7 (2003).
66. Lavin, Y. *et al.* Innate Immune Landscape in Early Lung Adenocarcinoma by Paired Single-Cell Analyses. *Cell* **169,** 750–765.e17 (2017).
67. Almatroodi, S. A., McDonald, C. F., Darby, I. A. & Pouniotis, D. S. Characterization of M1/M2 Tumour-Associated Macrophages (TAMs) and Th1/Th2 Cytokine Profiles in Patients with NSCLC. *Cancer Microenviron.* **9,** 1–11 (2016).
68. Silzle, T. *et al.* Tumor-associated fibroblasts recruit blood monocytes into tumor tissue. *Eur. J. Immunol.* **33,** 1311–1320 (2003).
69. Comito, G. *et al.* Cancer-associated fibroblasts and M2-polarized macrophages synergize during prostate carcinoma progression. *Oncogene* **33,** 2423–2431 (2014).
70. Ksiazkiewicz, M. *et al.* Importance of CCL2-CCR2A/2B signaling for monocyte migration into spheroids of breast cancer-derived fibroblasts. *Immunobiology* **215,** 737–747 (2010).
71. Popper, H. H. Progression and metastasis of lung cancer. *Cancer Metastasis Rev.* **35,** 75–91 (2016).
72. Walker, J. M. *Tumor Immunology*. **1393,** (Springer New York, 2016).
73. Wang, R. *et al.* Tumor-associated macrophages provide a suitable microenvironment for non-small lung cancer invasion and progression. *Lung Cancer* **74,** 188–196 (2011).
74. Macauley, M. S., Crocker, P. R. & Paulson, J. C. Siglec-mediated regulation of immune cell function in disease. *Nat. Rev. Immunol.* **14,** 653–666 (2014).
75. Méndez-Huergo, S. P., Blidner, A. G. & Rabinovich, G. A. Galectins: emerging regulatory checkpoints linking tumor immunity and angiogenesis. *Curr. Opin. Immunol.* **45,** 8–15 (2017).
76. Takamiya, R., Ohtsubo, K., Takamatsu, S., Taniguchi, N. & Angata, T. The interaction between Siglec-15 and tumor-associated sialyl-Tn antigen enhances TGF-?? secretion from monocytes/macrophages through the DAP12-Syk pathway. *Glycobiology* **23,** 178–187 (2013).
77. Beatson, R. *et al.* The mucin MUC1 modulates the tumor immunological microenvironment through engagement of the lectin Siglec-9. *Nat. Immunol.* **17,** 1273–1281 (2016).
78. Fennell, D. A. *et al.* Cisplatin in the modern era: The backbone of first-line chemotherapy

for non-small cell lung cancer. *Cancer Treat. Rev.* **44,** 42–50 (2016).
79. Prota, A. E. *et al.* Molecular Mechanism of Action of Microtubule-Stabilizing Anticancer Agents. *Science (80-.).* **339,** 587–590 (2013).
80. Klemm, F. & Joyce, J. A. Microenvironmental regulation of therapeutic response in cancer. *Trends Cell Biol.* **25,** 198–213 (2015).
81. Sodhi, A. Mechanism of NF-κB translocation in macrophages treated in vitro with cisplatin. *Immunol. Lett.* **63,** 9–17 (1998).
82. Singh, R. A. & Sodhi, A. Antigen presentation by cisplatin-activated macrophages: Role of soluble factor(s) and second messengers. *Immunol. Cell Biol.* **76,** 513–519 (1998).
83. Fridlender, Z. G. *et al.* Chemotherapy Delivered After Viral Immunogene Therapy Augments Antitumor Efficacy Via Multiple Immune-mediated Mechanisms. *Mol. Ther.* **18,** 1947–1959 (2010).
84. Bracci, L., Schiavoni, G., Sistigu, A. & Belardelli, F. Immune-based mechanisms of cytotoxic chemotherapy: implications for the design of novel and rationale-based combined treatments against cancer. *Cell Death Differ.* **21,** 15–25 (2014).
85. Park, S. *et al.* Tumor suppression via paclitaxel-loaded drug carriers that target inflammation marker upregulated in tumor vasculature and macrophages. *Biomaterials* **34,** 598–605 (2013).
86. Javeed, A. *et al.* Paclitaxel and immune system. *Eur. J. Pharm. Sci.* **38,** 283–290 (2009).
87. Laoui, D., van Overmeire, E., de Baetselier, P., van Ginderachter, J. A. & Raes, G. Functional relationship between tumor-associated macrophages and macrophage colony-stimulating factor as contributors to cancer progression. *Front. Immunol.* **5,** 1–15 (2014).
88. Ngambenjawong, C., Gustafson, H. H. & Pun, S. H. Progress in tumor-associated macrophage (TAM)-targeted therapeutics. *Adv. Drug Deliv. Rev.* (2017). doi:10.1016/j.addr.2017.04.010

CHAPTER V

DISCUSSION

TABLE OF CONTENTS

1. DISCUSSION AND PERSPECTIVES

Cancer therapies have long evolved from indiscriminately affecting proliferative cells, using untargeted approaches, which invariably result in toxic side effects and often lack of efficacy. Currently, development of antitumor therapeutics can be divided into two main categories, according to the strategy pursued: i) identification of cell-intrinsic genetic drivers of tumorigenesis and cancer cell genetic dependencies that may constitute druggable molecular targets, and ii) identification of tumor microenvironment (TME) drivers of tumor progression, therapeutic resistance and suppression of antitumor immunity that may provide a rational for combination therapies.

The work carried out in this thesis aimed at the development of approaches with potential for clinical translational in both categories: A) implementation of a therapeutic strategy to target Basal-Like Breast Cancer (BLBC) genetic dependencies and B) development of 3D cellular models for preclinical research, incorporating the crosstalk between tumor cells and cells from the TME.

1.1 Strategies to target cancer-intrinsic vulnerabilities

In ***Chapter II***, we explored previously identified molecular targets for their potential for BLBC therapy and evaluated a therapeutic strategy based on rAAV-mediated shRNA delivery for their targeting and preclinical efficacy evaluation. Among the hits identified by Petrocca *el* at., proteasome machinery subunits PSMA2 and PSMB4 and antiapoptotic protein MCL1 were identified as the most promising since BLBC cells presented selective sensitivity to their downregulation[1].

Although these are genes expressed in normal cells and in multiple tissues, we reasoned that the specificity of neoplastic cells dependency on these mechanisms could be exploited therapeutically. The exploitation of molecular targets for cancer has had a profound impact in several malignancies and drastically increased the outcome of genetically defined patient subsets[2]. Examples include targeting BCR-ABL in chronic myeloid leukemia (CML), B-Raf proto-oncogene, serine/threonine kinase (BRAF) or MEK

kinase for melanoma and advanced NSCLC, EGFR and ALK for specific subsets of lung cancer and ERBB2 for HER2-overexpressing breast cancer[3]. However, molecular targets are not an option for every tumor type. Cytotoxic chemotherapy is still the primary treatment for patients with basal-like triple negative breast cancer (BL-TNBC). These tumors present a high response rate to taxane and anthracycline-based chemotherapy; however, overall prognosis for these patients is poor due to the high likelihood of recurrence and metastasis[4]. Potentially actionable molecular alterations in this subtype have been uncovered by the widespread application of different omics technologies, such as protein from the PI3K/MTOR or RAS/RAF/MEK pathways, and targets currently in clinical investigation include poly(ADP-ribose) polymerases (PARP), PI3K and MEK, heat shock protein 90 alpha family class A member 1 (HSP90AA1), and histone deacetylase and androgen receptor inhibitors[5]. However, no driver alteration or genetic dependency has shown clinical benefits so far[5].

There are several factors to contemplate when designing a therapeutic strategy and, since the goal is to develop a viable clinical approach, it is important to consider its translation potential. Our strategy relied on downregulation of previously uncovered hits using small-hairpin RNA (shRNA). These activate RNAi machinery on the target cells and lead to the knockdown of the target gene[6]. While several options have proven effective *in vitro*, such as antisense oligonucleotides[7,8], the clinical translation of these approaches has proven challenging[9]. The use of small molecule inhibitors, on the other hand, can achieve high efficacy without major toxicity[9]. Nevertheless, posttranscriptional regulation of gene expression is prone to adaptation to new molecular targets arising from basic cancer studies and abolishes total protein function, which can be a limitation with small molecule inhibitors[10,11]. Still, efficacious strategies for gene delivery are needed for the full realization of RNAi potential to treat cancer.

Viral vectors are increasingly used as gene delivery agents as they achieve high infection rates *in vivo* and their tropism can be engineered to target a receptor or cell of interest. The specific properties of Adeno-associated Viral (AAV) vectors make them attractive vectors to conduct *in vivo* gene therapy. These are engineered from adeno-associated

virus which are nonpathogenic, naturally replication-deficient and mostly non-integrative, which greatly reduces their oncogenic potential[12]. Although gene replacement strategies have yielded promising results for inherited monogenic disorders, rAAV gene therapy now includes strategies for gene knockdown and gene editing[13]. rAAV vectors have been reported to transduce a wide variety of primary cancer cells and cell lines, and shown positive results as anticancer therapy delivery agents[14]. Moreover, the use of rAAV as a delivery platform for shRNA has been successful in preclinical and clinical trials for hepatitis C virus infection and chronic hepatitis B, α1-antitrypsin deficiency, facioscapulohumeralmuscular dystrophy, age-related macular degeneration and retinitis pigmentosa and neurodegenerative disorders such as Huntington's or Parkinson's disease[15], further highlighting the potential for clinical translation of the developed therapeutic approach.

Therefore, we implemented a platform for production and purification of rAAV vectors expressing shRNA sequences targeting the genes of interest. Production was based on transient transfection of HEK293 producer cells. Production platforms based on transient transfection can supply clinical trials that require limited vector doses, such as targeting the retina or brain, or that require small subset of patients, such as rare diseases[16]. Commercial options for establishing E.coli and HEK293 master cell banks, as well as for plasmid DNA and transfection reagents' production are available, all qualified for preclinical and clinical testing, making this approach easy and fast to implement[16]. Alternatives with higher scalability include baculovirus, adenovirus and herpes virus production systems. These do, however, require more extensive lead time for master cell bank preparation and production vector preparation[16]. The final outcome includes larger vector lots, with doses reaching larger target organs and patient populations[16]. However, once this lead time has passed, the subsequent production of large scale lots is much faster than transient transfection[16]. Thus, at this stage in vector development, production platforms based on transient transfection were chosen for the present study and provided the necessary vector quantities to test our strategy.

One of the challenges in viral vectors encoding shRNA is the activation of the RNAi machinery on the producer cells[17]. This can take a toll on producer cell viability, likely impairing rAAV production. By changing the stoichiometry of the plasmids at transfection and decreasing the proportion of capsid-encoding plasmid on the transfection mix, the production of capsid proteins could be reduced and, consequently, reduce the number of empty capsids in the final preparation. Moreover, decreasing harvesting time to 48h further contributed to decrease the ratio of empty/full capsids, as producer cells presented higher viability at that time point. This strategy enabled the production of high quality rAAV batches, reaching yields comparable to current rAAV production platforms[16,18].

We validated the knockdown efficiency in BLBC cell lines *in vitro* and assessed each vector´s potential for BLBC treatment. While all vectors led to a reduction in overall cell viability, PSMA2 emerged as the most promising target since it induced specific apoptotic induction *in vitro* of up to 2-fold in a BLBC cell line. As the phenotype of cell lines can change when cultured in the 3D configuration, especially in the proliferative status, evaluation of its biological effect on a BLBC xenograft models was conducted. rAAV-mediated delivery of an shRNA targeting *PSMA2* led to a persistent decrease in tumor progression over time. On the other hand, administration of rAAV-PLK1sh vectors showed an impact on tumor progression only at the highest dose tested. Interestingly, this was the only vector, other than rAAV-PSMA2sh, which resulted in a significant induction of apoptosis *in vitro*. However, *PLK1* knockdown efficiency was lower, which could possibly account for the lower efficacy also observed *in vivo*. It is important to note that the lower efficacy of the rAAV2-PLK1sh was not due to a lower infection capability, as all developed rAAV vectors displayed comparable transduction efficiency in the cell lines tested. We cannot exclude the possibility that the tropism, and consequently the infection rate, could be altered in the mouse xenograft model, when compared to the transduction rates observed *in vitro*. However, since the rAAV capsid was maintained within all vectors tested, this effect would be visible in all vectors and, therefore, comparative analysis is still possible. Nevertheless, it is still an important limitation of the present study that we have not been able to identify gene target

knockdown in the analyzed tumors, nor detect *eGFP* expression. We hypothesize that the apoptosis induction in infected cells could be impairing the detection of *eGFP* expression and gene knockdown at the time points analyzed. Another interesting aspect is that rAAV2-PSMA2sh appears to lose its therapeutic effect at later time points. Although it is important to note that by that time point fewer replicates were tested, which decreases statistical power, it is still intriguing. This may reflect the tumor´s evolution along therapy and loss of therapeutic sensibility. In fact, several mechanisms have been linked to resistance to proteasome inhibition, namely overexpression of other proteasomal subunits, activation of the aggresome-autophagy pathway, heat shock protein and growth factor induction, among others[19].

Although gene therapy approaches based on AAV vectors have shown a very safe and efficacious profile in clinical studies, with no major toxicity events reported[20], its inherent biology poses important limitations for gene therapy applications, especially for cancer targeting approaches. In contrast to other frequently used viral vectors, such as retro and lentivirus, rAAV vectors are non-integrative, remaining mostly episomal after gene transfer[21]. While this decreases the risk for insertional mutagenesis, it also decreases the long-term efficacy when targeting proliferative tissues[12]. Therefore, another important limitation of the present study is the fact that multiple doses of rAAV injections were provided over the course of the treatment. Since AAV are ubiquitous and non-pathogenic, the majority of the human population has already come into contact with these viruses and, therefore, has preexisting immunity for the developed vectors[22]. Therefore, the goal has been to achieve a single dose approach, able to provide long-term transgene expression and therapeutic effect, as the neutralizing antibodies developed after the first injection would render further treatments ineffective[22].

Several strategies have been developed in an attempt to overcome these limitations. rAAV engineering for modification of its natural properties and acquisition of characteristics beneficial for gene therapy, such as decreased immunogenicity and increased infection efficiency, are an intense area of research. In the present work, AAV's amenability for capsid engineering was exploited towards the development of

rAAV variants with increased tropism towards BLBC. In ***Chapter III***, we used directed evolution approaches to restrict AAV2 tropism and uncover novel biomarkers for this important medical need. To date, the BLBC subtype is still characterized as a group of heterogeneous diseases that have in common the low or lack of expression of the typical BC biomarkers – ER, PR, Her2. Several attempts were made to try to subdivide this BC subtype into clinically useful categories. Nevertheless, these are still treated as a single entity with the same treatment option – cytotoxic chemotherapy. A vector with restricted tropism would give an additional safety level to the developed gene silencing strategy, adding to the previously established selectivity of the molecular targets, and ensuring that the therapy does not promote unspecific toxicity to normal cells and tissues. Furthermore, by restricting rAAV´s tropism to the tissue of interest, the therapy could be administered systemically, and possibly target BLBC in the metastatic setting.

Since there are no biomarkers for this disease, a rational engineering approach was not possible. Therefore, after an initial depletion step using non-cancerous breast primary cells, sequential rounds of infection using several BLBC cell lines were performed. Unfortunately, a single capsid variant was selected. Upon analysis of its tropism, we were able to demonstrate higher transduction capacity towards BLBC cell lines. However, transduction efficiency was also increased for primary cells derived from mammary tissues, rendering the capsid variant ineffective for BC targeting approaches. Alternative routes for directed evolution include performing the screening for relevant variants using more accurate preclinical models, such as or 3D cellular models or animal systems[23,24]. Due to the lack of time these strategies were not followed within the scope of the present thesis but will be pursued in other projects in the Lab.

1.2 Approaches for the development of 3D cellular models incorporating cues from the TME

The potential of immunotherapies for the treatment of cancer has been shown in the success of checkpoint blockade therapies and adoptive T cell transfer approaches[25,26]. These can mediate complete tumor regression in a subset of patients. However, not all patients respond to the treatment. One of the working

hypotheses emphasizes the role of the TME surrounding the lesion, which can result in the inefficacy of immunotherapy in most cases. Different strategies are emerging to tackle the immunosuppressive nature of the TME and more accurate preclinical models are needed for accurate evaluation of those[3].

Based on an *in vitro* cellular model system developed in the Lab by Estrada *et al.*[27], we constructed a tumor model that incorporated key components found in the tumor microenvironment (TME). This model supported crosstalk between the different components through direct cell-cell contact and through the exchange of soluble factors.

In the work developed within the scope of this thesis, NSCLC tumor spheroids, cancer associated fibroblasts (CAF) and monocytes were co-culture within alginate microcapsules and maintained for long-term in stirred culture systems.

Within the tumoral compartment, H157 spheroids were composed of proliferative cells, positive for markers typical of aggressive stages of NSCLC, such as vimentin and N-cadherin. Upon co-culture with CAF and monocytes, extensive accumulation of extracellular matrix (ECM) components, namely collagen types I and IV, and fibronectin, within the alginate microcapsules was observed. These allowed migration of the cellular components present[28], which enable an extensive spatial remodeling observed along culture time. Furthermore, the cytokine secretory profile of these cultures pointed to the development of an immunosuppressive environment, also reported in the TME of NSCLC patients[29]. It is important to note that there was no addition of exogenous differentiating factors; thus, observed cell phenotypes were a result of spontaneous interactions between the different cellular components.

Upon three weeks of culture, the presence of CD68+ cells – macrophage marker - could be detected across the alginate microcapsules, indicating that the cultured monocytes were differentiated into macrophages. Both macrophages differentiated from THP1 and peripheral blood derived monocytes (PBM) expressed markers associated with M2-like pro-tumoral effects, namely CD163. Macrophages derived from PBM were also positive for the Mannose receptor C-Type 1 (MRC1, also known as CD206) marker, another

marker of M2-like macrophages[31]. These receptors have also been reported in tumor associated macrophages (TAM) present in several solid tumors, including NSCLC[30]. CD68+CD163+ TAM were correlated with poor progression-free survival and overall survival in NSCLC[32] and their presence was an independent prognostic marker for response to EGFR inhibitors[32]. By recapitulating this phenotype *in vitro*, this model could be used to identify key mechanisms inducing TAM differentiation and uncover new therapeutic strategies[33]. Also, identification of key modulators responsible for the differential response to treatment could help select patients that would benefit from combination therapies.

Extensive infiltration of CD163+ macrophages into the tumor spheroids was observed in the triple co-culture, reminiscent of the myeloid infiltration in human NSCLC tumors[34]. This infiltration is crucial for the development of an accurate cellular model incorporating the TME since direct co-culture has been shown to promote M2-like activation states with induction of secretion of pro-tumoral factors such as EGF, and IL10[33]. Furthermore, the soluble factors detected in our model indicated the generation of an immunosuppressive TME, further contributing to M2-like polarization. In fact, even monoculture of NSCLC spheroids in alginate microcapsules had detectable levels of secreted IL4, IL10, IL13 and CXCL1, which increased in the triple co-cultures. IL10, IL4, and IL13 have been described to induce an M2-like polarization state in macrophages[34]. CXCL1, detected in our triple co-cultures, has been reported to be present in high levels at the TME of NCSLC and correlated with lower disease-free progression times; it has also been proposed as an indicator of NSCLC progression, together with other markers[35].

To assess our cellular model´s amenability for drug testing, the effects of two standard-of-care chemotherapeutic drugs – paclitaxel and cisplatin – were tested. Challenging our model with both cisplatin and paclitaxel led to apoptosis induction in the tumoral compartment. However, while the phenotype of NSCLC spheroids was not altered upon co-culture with CAF and TAM, the interaction with these cells did alter their sensitivity to the drugs. NSCLC spheroids presented reduced susceptibility to paclitaxel challenge when in triple co-culture, indicating that interaction with TAM and CAF in culture may

be inducing therapeutic resistance. We hypothesize that this could be a result of the higher cytotoxic effect that cisplatin demonstrated towards CAF-macrophage co-cultures. This co-culture control presented pronounced reduction of viability upon cisplatin challenge when compared to monoculture of tumor spheroids and the triple co-culture, which may have limited their influence on the tumor compartment´s drug response. In fact, co-culture with macrophages has already been shown to mediate breast cancer cell resistance to paclitaxel, as well as other chemotherapeutics[36]. Furthermore, previous reports indicate that IGF produced by stromal cells promote cancer cell survival and resistance to therapy in pancreatic and brain tumors[37,38], and blockage of these growth factors was shown to increase the efficacy of paclitaxel therapy in metastatic breast cancer[39]. Lastly, CXCL1, which was detected at high levels in the triple co-cultures, mediates myeloid infiltration in breast cancer, which produce chemokines, such as S100A8/9, that enhance cancer cell survival[40]. Blocking CXCL1 receptor – CXCR2 – increased the efficacy of chemotherapeutic drugs, including paclitaxel[40]. While additional studies should be conducted to further dissect the stroma-TME axis leading to decreased susceptibility to paclitaxel in the present model, these results indicate that previously described interactions between the different components are being recapitulated in the model, highlighting its potential to test combination approaches and uncover additional targets for combination therapy.

Response to cisplatin, on the other hand, was maintained upon co-culture with CAF and TAM. An increased gene expression of *CCR7* after cisplatin challenge was observed, suggesting that there was a shift in the macrophage surviving population towards an M1-like phenotype. No increased cytotoxic effect in tumor was observed as a consequence of repolarization. Nevertheless, repolarization of macrophages and its effect on tumor cells may be dependent on T cell activation, which is absent in our model[41]. On the other hand, activation of CCR7 signaling was shown to promote survival of cancer cells after EGFR and cisplatin treatments in head and neck squamous carcinoma[42]. Since CCR7 signaling has also been linked to proliferation and decreased apoptosis in NSCLC[43], the increased expression of CCR7 after cisplatin treatment may reflect the decreased sensitivity of these cells to the therapy and consequent increased

proportion in culture. To assess these effects, the expression of CCR7 should be evaluated in FACS-isolated tumor and macrophages, separately.

The plasticity and high response to stimuli characteristic of TAM was also supported in the developed model, as evidenced by immunomodulation upon culture exposure to a CSF1R inhibitor, BLZ945. Several clinical studies are ongoing to investigate the effect of targeting TAM using CSF1R inhibitors[41]. CSF1R inhibition resulted in altered TAM recruitment and repolarization of the macrophages within TME into a pro-tumoral M1-like state, which was shown to contribute to tumor regression in mouse models of brain and breast cancer[44–47]. Upon challenge, the macrophage population expressing M2-like markers decreased, in parallel with an increase of the gene expression of M1-like receptor CCR7. This suggests that the repolarization effect already described for CSF1R inhibition was reproduced in culture. Moreover, there was no decrease in viability observed upon BLZ945 challenge, indicating that the lower proportion of M2-like macrophages in culture was not a result of cell death. Also, gene expression analysis of macrophage marker CD68 showed that it was maintained along drug treatment, further supporting this hypothesis.

Although their translation into clinical trials has shown manageable safety profiles, the use of CSF1R inhibitors as monotherapy has led to disappointing results in solid tumors[48]. The most advanced CSF1R inhibitor in clinical development has showed limited efficacy in glioblastoma patients and no objective responses[48,49]. The attrition rates observed in ongoing clinical trials may reflect intrinsic differences between murine and human responses to CSF1R blocking. The model system here developed could be used to identify factors that are limiting the effect of CSF1R in humans, and to test in a human setting the combinations of CSF1R inhibition with immuno-, chemo- and targeted therapies, currently ongoing[48].

Although few blockers of Th2 cytokines, such as IL4 and IL13, have gone through clinical trials for solid tumors, recent reports suggest that blocking of this crosstalk may be favorable for combination with radiotherapy or paclitaxel-chemotherapy in slowing tumor growth in mammary tumors[50]. In this setting, therapeutic effects were CD8+ T

cell dependent, thus incorporation of T cells in the developed model should be evaluated. Nevertheless, the strong accumulation of these cytokines in culture may merit its use for dissection of the effects of cytokine-targeted therapies.

The pro-tumoral effects of TAM can be mediated by their interaction with other cells. Hence, markers for additional cell populations should be investigated to fully evaluate the potential of the model developed. Monocytic precursors can also give rise to other cells contributing to the immunological state of the TME, such as MSDC and dendritic cells[33]. Clinical significance of these cells has been extensively explored in terms of their effect on tumor progression and response to drugs[51,52]. Thus, their presence and influence within this model should be investigated.

Moreover, several of the effects of TAM discussed previously are mediated through the activation of T cells. Additionally, TAM can directly suppress T cells through the expression of inhibitory receptors, and the cooperation effect of CSF1R inhibition and checkpoint inhibitors or adoptive T cell therapy has been shown[53–56]. Hence, given their overrepresentation in current immunotherapeutic targets, the inclusion of T cells in *in vitro* models should be explored. Using patient-derived tumor samples in combination with peripheral blood-derived mononuclear cells from the same donor could open these possibilities. Finally, the broad application of the developed platform to other pathologies and patient-derived tumour samples could give clinicians an opportunity to perform *ex vivo* assessment of therapeutic efficacy using precision medicine approaches.

2. FINAL REMARKS

The advances in pharmacogenomics over the recent years aim at providing a rational stratification of patients for a given therapy[57]. This could revolutionize precision medicine by uncovering the most relevant genetic drivers and cellular pathways mediating disease progression and therapeutic response in a genetically defined subset of patients[57]. However, the development of therapies for a given tumor indication has proven an often inaccurate and complex process, as have therapeutic biomarker identification, which is often a slow and inefficient[58]. Following *in vitro* observation of

a given mechanism or pathway, standard animal testing follows, using mostly mouse models[59]. Since the majority of these models presents compromised immune systems and offers non-human tumor-stromal interactions, the concurrence rate of clinical translation can be as low as 8%. Moreover, the pain and discomfort these animal undergo are a growing concern[60,61]. Thus, the development of accurate *in vitro* cellular models aims at bridging the gap between traditional *in vitro* and *in* vivo models. By providing tumor phenotypes that better resemble the *in vivo* setting, and by eliminating the interspecies discrepancies of cellular interactions in *in vivo* models, these could allow more accurate disease modeling and drug testing. The development and applications of strategies that could target specifically the cell of interest, within such heterogeneous environments, would facilitate the process and generate safer therapies, with fewer side-effects.

3. AUTHOR CONTRIBUTION & ACKNOWLEDGEMENTS

The author wrote this chapter.

4. REFERENCES

1. Petrocca, F. *et al.* A genome-wide siRNA screen identifies proteasome addiction as a vulnerability of basal-like triple-negative breast cancer cells. *Cancer Cell* **24,** 182–96 (2013).
2. Padma, V. V. An overview of targeted cancer therapy. *BioMedicine* **5,** 19 (2015).
3. Gotwals, P. *et al.* Prospects for combining targeted and conventional cancer therapy with immunotherapy. *Nat. Rev. Cancer* **17,** 286–301 (2017).
4. Foulkes, W. D., Smith, I. E. & Reis-Filho, J. S. Triple-Negative Breast Cancer. *N. Engl. J. Med.* **363,** 1938–1948 (2010).
5. Bianchini, G., Balko, J. M., Mayer, I. A., Sanders, M. E. & Gianni, L. Triple-negative breast cancer: challenges and opportunities of a heterogeneous disease. *Nat. Rev. Clin. Oncol.* **13,** 674–690 (2016).
6. Petrocca, F. & Lieberman, J. Promise and Challenge of RNA Interference–Based Therapy for Cancer. *J. Clin. Oncol.* **29,** 747–754 (2011).
7. Ross, S. J. *et al.* Targeting KRAS-dependent tumors with AZD4785, a high-affinity therapeutic antisense oligonucleotide inhibitor of KRAS. *Sci. Transl. Med.* **9,** eaal5253 (2017).
8. Aartsma-Rus, A. New Momentum for the Field of Oligonucleotide Therapeutics. *Mol. Ther.* **24,** 193–194 (2016).
9. Quinn, B. A. *et al.* Targeting Mcl-1 for the therapy of cancer. *Expert Opin. Investig. Drugs* **20,** 1397–1411 (2011).
10. Weihua, Z. *et al.* Survival of Cancer Cells Is Maintained by EGFR Independent of Its Kinase Activity. *Cancer Cell* **13,** 385–393 (2008).

11. Kikani, C. K., Dong, L. Q. & Liu, F. “New”-clear functions of PDK1: Beyond a master kinase? *J. Cell. Biochem.* **96,** 1157–1162 (2005).
12. Luo, J. *et al.* Adeno-associated virus-mediated cancer gene therapy: Current status. *Cancer Lett.* **356,** 347–356 (2015).
13. Berns, K. I. & Muzyczka, N. AAV: An Overview of Unanswered Questions. *Hum. Gene Ther.* **28,** 308–313 (2017).
14. Santiago-Ortiz, J. L. & Schaffer, D. V. Adeno-associated virus (AAV) vectors in cancer gene therapy. *J. Control. Release* **240,** 287–301 (2016).
15. Valdmanis, P. N. & Kay, M. A. Future of rAAV Gene Therapy: Platform for RNAi, Gene Editing, and Beyond. *Hum. Gene Ther.* **28,** 361–372 (2017).
16. Snyder, R. O. An Overview of rAAV Vector Product Development for Gene Therapy. in (ed. Childers, M. K.) 21–37 (Springer New York, 2016). doi:10.1007/978-1-4939-3228-3_2
17. Maunder, H. E. *et al.* Enhancing titres of therapeutic viral vectors using the transgene repression in vector production (TRiP) system. *Nat. Commun.* **8,** 14834 (2017).
18. Kotin, R. M. Large-scale recombinant adeno-associated virus production. *Hum. Mol. Genet.* **20,** R2–R6 (2011).
19. Manasanch, E. E. & Orlowski, R. Z. Proteasome inhibitors in cancer therapy. *Nat. Rev. Clin. Oncol.* **5,** 101–110 (2017).
20. Samulski, R. J. & Muzyczka, N. AAV-Mediated Gene Therapy for Research and Therapeutic Purposes. *Annu. Rev. Virol.* **1,** 427–451 (2014).
21. *Viral Vectors for Gene Therapy*. *Methods in Molecular Biology* **737,** (Humana Press, 2011).
22. Mingozzi, F. & High, K. A. Immune responses to AAV vectors: overcoming barriers to successful gene therapy. *Blood* **122,** 23–36 (2013).
23. Michelfelder, S. *et al.* Successful Expansion but Not Complete Restriction of Tropism of Adeno-Associated Virus by In Vivo Biopanning of Random Virus Display Peptide Libraries. *PLoS One* **4,** e5122 (2009).
24. Dalkara, D. *et al.* In Vivo-Directed Evolution of a New Adeno-Associated Virus for Therapeutic Outer Retinal Gene Delivery from the Vitreous. *Sci. Transl. Med.* **5,** 189ra76-189ra76 (2013).
25. June, C. H., Riddell, S. R. & Schumacher, T. N. Adoptive cellular therapy: A race to the finish line. *Sci. Transl. Med.* **7,** 280ps7-280ps7 (2015).
26. Topalian, S. L. *et al.* Safety, Activity, and Immune Correlates of Anti–PD-1 Antibody in Cancer. *N. Engl. J. Med.* **366,** 2443–2454 (2012).
27. Estrada, M. F. *et al.* Modelling the tumour microenvironment in long-term microencapsulated 3D co-cultures recapitulates phenotypic features of disease progression. *Biomaterials* **78,** 50–61 (2016).
28. Egeblad, M., Rasch, M. G. & Weaver, V. M. Dynamic interplay between the collagen scaffold and tumor evolution. *Curr. Opin. Cell Biol.* **22,** 697–706 (2010).
29. Almatroodi, S. A., McDonald, C. F., Darby, I. A. & Pouniotis, D. S. Characterization of M1/M2 Tumour-Associated Macrophages (TAMs) and Th1/Th2 Cytokine Profiles in Patients with NSCLC. *Cancer Microenviron.* **9,** 1–11 (2016).
30. Aras, S. & Raza Zaidi, M. TAMeless traitors: Macrophages in cancer progression and metastasis. *Br. J. Cancer* **117,** 1583–1591 (2017).
31. Yuan, A. *et al.* Opposite Effects of M1 and M2 Macrophage Subtypes on Lung Cancer Progression. *Sci. Rep.* **5,** 14273 (2015).
32. Chung, F.-T. *et al.* Tumor-associated macrophages correlate with response to epidermal growth factor receptor-tyrosine kinase inhibitors in advanced non-small cell lung cancer. *Int. J. Cancer* **131,** E227–E235 (2012).
33. Komohara, Y., Jinushi, M. & Takeya, M. Clinical significance of macrophage heterogeneity in human malignant tumors. *Cancer Sci.* **105,** 1–8 (2014).

34. Popper, H. H. Progression and metastasis of lung cancer. *Cancer Metastasis Rev.* **35,** 75–91 (2016).
35. Cao, Y., Huang, H., Wang, Z. & Zhang, G. The Inflammatory CXC Chemokines, GROα high , IP-10 low , and MIG low , in Tumor Microenvironment Can Be Used as New Indicators for Non-small Cell Lung Cancer Progression. *Immunol. Invest.* **46,** 361–374 (2017).
36. Shree, T. *et al.* Macrophages and cathepsin proteases blunt chemotherapeutic response in breast cancer. *Genes Dev.* **25,** 2465–2479 (2011).
37. Ireland, L. *et al.* Chemoresistance in Pancreatic Cancer Is Driven by Stroma-Derived Insulin-Like Growth Factors. *Cancer Res.* **76,** 6851–6863 (2016).
38. Quail, D. F. *et al.* The tumor microenvironment underlies acquired resistance to CSF-1R inhibition in gliomas. *Science (80-.).* **352,** aad3018-aad3018 (2016).
39. Ireland, L. *et al.* Blockade of insulin-like growth factors increases efficacy of paclitaxel in metastatic breast cancer. *Oncogene* **37,** 2022–2036 (2018).
40. Acharyya, S. *et al.* A CXCL1 paracrine network links cancer chemoresistance and metastasis. *Cell* **150,** 165–178 (2012).
41. Ruffell, B. & Coussens, L. M. Macrophages and Therapeutic Resistance in Cancer. *Cancer Cell* **27,** 462–472 (2015).
42. Wang, J. *et al.* Autocrine and Paracrine Chemokine Receptor 7 Activation in Head and Neck Cancer: Implications for Therapy. *JNCI J. Natl. Cancer Inst.* **100,** 502–512 (2008).
43. Xu, Y. *et al.* CCL21/CCR7 Prevents Apoptosis via the ERK Pathway in Human Non-Small Cell Lung Cancer Cells. *PLoS One* **7,** e33262 (2012).
44. Pyonteck, S. M. *et al.* CSF-1R inhibition alters macrophage polarization and blocks glioma progression. *Nat. Med.* **19,** 1264–1272 (2013).
45. Strachan, D. C. *et al.* CSF1R inhibition delays cervical and mammary tumor growth in murine models by attenuating the turnover of tumor-associated macrophages and enhancing infiltration by CD8 $^{+}$ T cells. *Oncoimmunology* **2,** e26968 (2013).
46. Ries, C. H. *et al.* Targeting tumor-associated macrophages with anti-CSF-1R antibody reveals a strategy for cancer therapy. *Cancer Cell* **25,** 846–859 (2014).
47. Tap, W. D. *et al.* Structure-Guided Blockade of CSF1R Kinase in Tenosynovial Giant-Cell Tumor. *N. Engl. J. Med.* **373,** 428–437 (2015).
48. Peyraud, F., Cousin, S. & Italiano, A. CSF-1R Inhibitor Development: Current Clinical Status. *Curr. Oncol. Rep.* **19,** 70 (2017).
49. Butowski, N. *et al.* Orally administered colony stimulating factor 1 receptor inhibitor PLX3397 in recurrent glioblastoma: an Ivy Foundation Early Phase Clinical Trials Consortium phase II study. *Neuro. Oncol.* **18,** 557–564 (2016).
50. Shiao, S. L. *et al.* T H 2-Polarized CD4 + T Cells and Macrophages Limit Efficacy of Radiotherapy. *Cancer Immunol. Res.* **3,** 518–525 (2015).
51. Kumar, V., Patel, S., Tcyganov, E. & Gabrilovich, D. I. The Nature of Myeloid-Derived Suppressor Cells in the Tumor Microenvironment. *Trends Immunol.* **37,** 208–220 (2016).
52. De Vlaeminck, Y., González-Rascón, A., Goyvaerts, C. & Breckpot, K. Cancer-Associated Myeloid Regulatory Cells. *Front. Immunol.* **7,** 1–9 (2016).
53. Zhu, Y. *et al.* CSF1/CSF1R Blockade Reprograms Tumor-Infiltrating Macrophages and Improves Response to T-cell Checkpoint Immunotherapy in Pancreatic Cancer Models. *Cancer Res.* **74,** 5057–5069 (2014).
54. Mao, Y. *et al.* Targeting Suppressive Myeloid Cells Potentiates Checkpoint Inhibitors to Control Spontaneous Neuroblastoma. *Clin. Cancer Res.* **22,** 3849–3859 (2016).
55. Holmgaard, R. B. *et al.* Timing of CSF-1/CSF-1R signaling blockade is critical to improving responses to CTLA-4 based immunotherapy. *Oncoimmunology* **5,** (2016).
56. Mok, S. *et al.* Inhibition of CSF-1 Receptor Improves the Antitumor Efficacy of Adoptive Cell Transfer Immunotherapy. *Cancer Res.* **74,** 153–161 (2014).

57. Nieto, M. A., Huang, R. Y.-J., Jackson, R. A. & Thiery, J. P. EMT: 2016. *Cell* **166,** 21–45 (2016).
58. Sun, Y. Translational Horizons in the Tumor Microenvironment: Harnessing Breakthroughs and Targeting Cures. *Med. Res. Rev.* **35,** n/a-n/a (2015).
59. Hoarau-Véchot, J., Rafii, A., Touboul, C. & Pasquier, J. Halfway between 2D and Animal Models: Are 3D Cultures the Ideal Tool to Study Cancer-Microenvironment Interactions? *Int. J. Mol. Sci.* **19,** 181 (2018).
60. Voskoglou-Nomikos, T., Pater, J. L. & Seymour, L. Clinical predictive value of the in vitro cell line, human xenograft, and mouse allograft preclinical cancer models. *Clin. cancer Res.* **9,** 4227–39 (2003).
61. Mak, I. W. Y., Evaniew, N. & Ghert, M. Lost in translation: animal models and clinical trials in cancer treatment. *Am. J. Transl. Res.* **6,** 114–8 (2014).

ITQB-UNL | Av. da República, 2780-157 Oeiras, Portugal
Tel (+351) 214 469 100 | Fax (+351) 214 411 277

www.itqb.unl.pt